Response to reviewer 2:

General comments This paper reports the results of source apportionment based on a 1-year campaign in China. Besides the specific results, the paper presents an interesting methodology, based on the synergic use of radioactive and stable carbon isotopes. The paper ends with an open question, but this may be the trigger to foster new research. Therefore, I think the paper is worth the publication.

Response: We appreciate the reviewer's thoughtful and valuable comments, which are very helpful for revising and improving our manuscript. We have carefully addressed the reviewer's comments. Below are point-to-point responses.

Specific comments

1) Introduction, page 2 lines 16-18: "The ^{14}C content of an aerosol sample is usually reported relative to an oxalic acid standard and expressed as fraction modern ($F^{14}C$). ^{14}C content of the standard is related to the unperturbed atmosphere in the reference year of 1950 (Mook and van der Plicht, 1999; Reimer et al., 2004)"; please change to "The ^{14}C content of an aerosol sample is usually reported relative to an oxalic acid standard and expressed as fraction modern ($F^{14}C$). ^{14}C content of the standard is related to the unperturbed atmosphere in the reference year of 1950 (Mook and van der Plicht, 1999; Reimer et al., 2004), and this is usually done with/by means of/similar a standard"; this sentence is more correct and actually describes much better the definition formula in the following line.

Response: We agree with the reviewer, that this formulation is not entirely clear. Text and Eq. (1) is revised to clarify the definition of $F^{14}C$ as shown in the revised manuscript (marked-up copy, page 2, line 26–31; page 3, line 1–3). We tried to be even more specific and refer now concretely to OxII standard multiplied by 0.7459.

2) Introduction, page 2 lines 21-22: the assumptions on $F^{14}C$ are reported in a far too simplistic in several points (later on they become simple "conversion factors"). I suggest the authors to better introduce these quantities to facilitate the reader and also the writing of the following sections. The same for $\delta^{13}C$: it is introduced in the following sections, it is true, but at this stage there are already some sentences maybe not clear to readers not too familiar with stable carbon isotopes (e.g. "signature depleted", but it is not clear with respect with which reference.)

Response: We introduce the $F^{14}C$ of contemporary sources in details as follows (page 3 line 5–14):

> "However, $F^{14}C$ values of the contemporary (or non-fossil) carbon sources are bigger than 1 due to the nuclear bomb tests that nearly doubled the $^{14}CO_2$ in the atmosphere in the 1960s and 1970s. Currently, $F^{14}C$ of the atmospheric CO_2 is approximately 1.04 (Levin et al., 2010).This value is decreasing every year, because the $^{14}CO_2$ produced by bomb testing is taken up by oceans and the biosphere and diluted by ^{14}C-free CO_2 produced by fossil fuel burning . For biogenic aerosols, aerosols emitted from cooking as well as annual crop, the $F^{14}C$ is close to the value of current atmospheric CO_2. $F^{14}C$ of

wood burning is higher than that, because a significant fraction of carbon in the wood burned today was fixed during times when atmospheric $^{14}C/^{12}C$ ratios were substantially higher than today. Estimates of $F^{14}C$ for wood burning are based on tree-growth models (e.g., Lewis et al., 2004; Mohn et al., 2008) and found to range from 1.08 to 1.30 (Szidat et al., 2006; Genberg et al., 2011; Gilardoni et al., 2011; Minguillón et al., 2011; Dusek et al., 2013)."

The new citations are included in the revised reference list.

Text in the method section is revised to clarify the "conversion factor" by adding their physical meanings, as follows (page 7 line 11–13; line 18–22):

"$F^{14}C$ of EC ($F^{14}C_{(EC)}$) was converted to the fraction of biomass burning (f_{bb}(EC)) by dividing with $F^{14}C$ of biomass burning ($F^{14}C_{bb}$= 1.10 ± 0.05; Lewis et al., 2004; Mohn et al., 2008; Palstra and Meijer, 2014) given that biomass burning is the only non-fossil source of EC, to eliminate the effect from nuclear bomb tests in the 1960s." (page 7 line 11–13)

"$F^{14}C$ of OC ($F^{14}C_{(OC)}$) was converted to the fraction of non-fossil (f_{nf}(OC)) by dividing the $F^{14}C$ of non-fossil sources including both biogenic and biomass burning ($F^{14}C_{nf}$ =1.09 ± 0.05; Lewis et al., 2004; Levin et al., 2010; Y. Zhang et al., 2014a). The lower limit of 1.04 corresponds to current biospheric sources as the source of OC, the upper limit corresponds to burning of wood as the main source of OC, with only little input from annual crops." (page 7 line 18–22)

$F^{14}C_{bb}$ (1.10 ± 0.05) for EC is slightly smaller than $F^{14}C_{nf}$ (1.09 ± 0.05) for OC, because except biomass burning, biogenic emissions also contribute to OC, but have a smaller $F^{14}C$ than that of biomass burning.

For stable carbon isotopes, we change "the stable carbon isotope (^{13}C, expressed as $\delta^{13}C$)" to "the stable carbon isotope composition (namely the $^{13}C/^{12}C$ ratio, expressed as $\delta^{13}C$ in Eq. (2))" in the revised text (page 3 line 19–20). $\delta^{13}C$ is useful to distinguish sources of aerosols. The distinction is possible because for example, $\delta^{13}C$ values of carbon from coal combustion are less depleted (or enriched, i.e., enrichment in $^{13}C/^{12}C$ ratio) compared to the aerosol carbon emitted by other sources, for example, liquid fossil fuel combustion (-28 ‰ to -24 ‰) and C3 plants burning (-35 ‰ to -24 ‰) (Andersson et al. (2015) and references therein). The "signature depleted" is based on the comparison between different emission sources. To clarify, we explain the term "enriched" and "depleted" $\delta^{13}C$ as follows:

"Different emission sources have their own source signature: carbonaceous aerosol from coal combustion is enriched in ^{13}C (i.e., has higher $\delta^{13}C$ values of ~ -25 ‰ to -21 ‰) compared to aerosol from liquid fossil fuel combustion ($\delta^{13}C$ ~ -28 ‰ to -24 ‰) and from burning of C3 plants ($\delta^{13}C$ ~ -35 ‰ to -24 ‰) (Andersson et al. (2015) and references therein)." (page 3 line 21–25)

3) Introduction, page 3 line 7 and table S1: actually, source signatures are not that well distinct, as they have overlaps: may the authors discuss deeper this point?

Response: We appreciate this point. If it is ok with the reviewer, we will put the deeper discussion into the methods section 2.6, where we introduce the use of ^{13}C data for source apportionment and can further elaborate on the consequences of the overlapping signatures.

Though with some overlaps, different emission sources have their own source signature. To avoid misunderstanding, we change "Different emission sources have their ***distinct*** source signature" in the introduction section to "Different emission sources have their ***own*** source signature" (page 3 line 22).

Source signatures of $\delta^{13}C$ presented in Table S1 (shown as mean ± standard deviation) are established for the purpose of the source apportionment for EC (see revised Sect. 2.6). For burning C3 plants, coal and liquid fossil fuel, their $\delta^{13}C$ source signatures for EC are fully complied and established in Andersson et al. (2015) by a thorough literature search. In brief, the mean and standard deviation for $\delta^{13}C$ endmembers for the different sources are estimated as the average and standard deviation of the different data sets, respectively. For burning corn stalk residues in the study area, our $\delta^{13}C$ values of aerosols from corn stalk burning were complied in Fig. S6 and its source signatures are established as -16.4 ± 1.4 ‰ (mean ± standard deviation), as described in Sect 4.3.1 (Sect. 3.4.1 in the draft manuscript) and as addressed in Question 14. To clarify, we add ranges of source signatures of $\delta^{13}C$ into Supplemental Table S1, besides the established mean ± standard deviation for source apportionment of EC.

The source endmembers for $\delta^{13}C$ are less well-constrained than for $F^{14}C$, as $\delta^{13}C$ varies with fuel types and combustion conditions. For example, $\delta^{13}C$ values for liquid fossil fuel combustion overlaps with $\delta^{13}C$ values for both coal and C3 plant combustion. In this study, to account for the variability of the isotope signatures of $\delta^{13}C$ and $F^{14}C$ from the different sources, the Bayesian Markov chain Monte Carlo techniques (MCMC) were used as explained in the Method section. Uncertainties of both source endmembers for each source and the measured ambient $\delta^{13}C_{EC}$ and $F^{14}C_{(EC)}$ are propagated. These serve as input of MCMC to estimate the source contributions to EC. The MCMC results are the posterior probability density functions (PDF) for the relative contributions from the sources (Fig. S7, Fig. S8). The PDF of the relative source contributions of liquid fossil fuel combustion (vehicle) and coal combustion is skewed. By contrast, the PDF of the relative source contributions of biomass burning is symmetric as it is well-constrained by $F^{14}C$ (Fig. S8(a)). In this study, the median with its interquartile range was used to give the estimates of the contribution of any particular source to EC throughout the manuscript (e.g., Table 1, Sect. 4.3.2).

This point is clarified in the Method Sect. 2.6 by adding the following (page 8 line 14-22):

> "$\delta^{13}C_{bb}$, $\delta^{13}C_{liq.fossil}$ and $\delta^{13}C_{coal}$ are the $\delta^{13}C$ signature emitted from biomass burning, liquid fossil fuel combustion and coal combustion, respectively. The means and the standard deviations for $\delta^{13}C_{bb}$ (-26.7 ± 1.8 ‰ for C3 plants, and -16.4 ± 1.4 ‰ for corn stalk), $\delta^{13}C_{liq.fossil}$ (-25.5 ± 1.3 ‰) and $\delta^{13}C_{coal}$ (-23.4 ± 1.3 ‰) are presented in Table S1

(Andersson et al., 2015 and reference therein; Sect. 4.3.1), and serves as input of MCMC. The source endmembers for $\delta^{13}C$ are less well-constrained than for $F^{14}C$, as $\delta^{13}C$ varies with fuel types and combustion conditions. For example, the range of possible $\delta^{13}C$ values for liquid fossil fuel combustion overlaps to a small extent with the range for coal combustion, although liquid fossil fuels are usually more depleted than coal. The MCMC technique takes into account the variability in the source-signatures of $F^{14}C$ and $\delta^{13}C$ (Table S1), where $\delta^{13}C$ introduces a larger uncertainty than $F^{14}C$. Uncertainties of both source endmembers for each source and the measured ambient $\delta^{13}C_{EC}$ and $F^{14}C_{(EC)}$ are propagated."

Further, to give the readers an idea of this point, we also changed the sentence in the Introduction section "Further, $\delta^{13}C$ of EC allows separation of fossil sources into coal and liquid fossil fuel burning (Andersson et al., 2015; Winiger et al., 2015, 2016), as they have their distinct source signatures" to:

"Further, $\delta^{13}C$ of EC allows separation of fossil sources into coal and liquid fossil fuel burning (Andersson et al., 2015; Winiger et al., 2015, 2016), due to their different source signatures. Typical $\delta^{13}C$ values for EC from previous studies are summarized in Table S1." (page 3 line 30–32).

4) Sampling, page 3 line 28: why was the sampling time chosen to be 10 am to 10 am next day? Due to manual change? How long were the samples kept inside the sampler after sampling?

Response: The sampling time was long chosen to be 10:00 a.m. to 10:00 a.m. the next day (e.g., Cao et al., 2009; Han et al., 2016) due to manual change and safety reasons in accessing the site at midnight.

Only one filter can be loaded into the sampler, so we took the filter out of the sampler after 24 hr sampling and did not keep it in the sampler. The revised text (page 5 line 1) shows that:

"After sampling, we immediately removed the filter from the sampler. All filters were packed in pre-baked aluminum foils, sealed in polyethylene bags and stored at -18 °C in a freezer"

5) Sampling, page 4 line 4: citations missing ("previous studies" are not cited)

Response: Citations are added on page 5 line 2–3.

6) Stable carbon isotope ($\delta^{13}C$) analysis of OC and EC, page 4: some more details on the analysis would be welcome. Further, the title is maybe misleading, as it suggests that only ^{13}C is measured, while I guess that also ^{12}C is assessed for determining $^{13}C/^{12}C$ ratios.

Response: More details on the $\delta^{13}C$ analysis are added as shown in the revised manuscript (page 5 line 21–30; page 6 line 1–7).

The title is changed to "2.3 Stable carbon isotopic composition of OC and EC", to indicate that $^{13}C/^{12}C$ ratios are determined, not only ^{13}C. (page 5 line 20)

7) Radiocarbon (^{14}C) measurement of OC and EC, page 5, line 9: "Two standards with known ^{14}C content are analyzed as quality control: an oxalic acid standard and a graphite standard.": maybe I did not understand, but I believe these standards are respectively for normalization and blank evaluation; if this is correct, they cannot be defined as "for quality control". In case further standards are measured as unknown, these can be defined "for quality control".

Response: Two standards with known ^{14}C content that extracted using our aerosol combustion system (ACS) are analyzed to assess the contamination introduced by the combustion process, and they are treated exactly like the samples (e.g., normalized to the oxalic acid OXII calibration material). The measured deviation in $F^{14}C$ from the nominal values is caused by contamination introduced by the combustion process. The contamination is assessed but not used for further data correction, because the contamination is relatively small (typically below 1.5 µgC per combustion) compared the sample sizes (ranging between 50 and 270 µgC). To clarify, the revised texts show:

> "Two standards with known ^{14}C content are combusted as quality control for the combustion process: an oxalic acid standard and a graphite standard. Small amounts of solid standard material are directly put on the filter holder of the combustion tube and heated at 650 °C for 10 min. In the further ^{14}C analysis, the CO_2 derived from combustion of the standards is treated exactly like the samples. Therefore, the contamination introduced by the combustion process can be estimated from the deviation of measured values (Table S9) from the nominal values of the standards. The contamination is below 1.5 µgC per combustion, which is relatively small compared the samples ranging between 50 and 270 µgC in this study." (page 6, line 19–24)

8) Radiocarbon (^{14}C) measurement of OC and EC, page 5, lines 11-13 and 24-25: there is a repetition of the information, and actually not completely in the same way: please correct it. Further, is this contamination modern or fossil?

Response: ^{14}C measurements of aerosol samples are subject to contaminations, which can be introduced during the combustion process using ACS, or during the graphitization and AMS measurements. For contamination caused by the combustion process, it is already explained in the response to Question 7. Here we addressed the contamination during the graphitization and AMS measurement, thus it is not a repetition of the information.

$F^{14}C$ of aerosols samples was corrected for contamination that occurred during graphitization and AMS measurement. For AMS measurements, samples are usually analyzed together with varying amounts of reference material covering the range of sample mass. Two such materials with known ^{14}C content are used: the oxalic acid OXII calibration material ($F^{14}C = 1.3406$) and a ^{14}C-free CO_2 gas ($F^{14}C = 0$). Contamination during the graphitization and AMS measurement results into the differences between measured and nominal $F^{14}C$ values. The magnitude of these deviations can be used to quantify the contamination with fossil carbon ($F^{14}C_F = 0$) and modern carbon ($F^{14}C_M = 1$), which in turn are used for correcting the sample values (de Rooij et al., 2010; Dusek et al., 2014).

The contamination with fossil carbon and modern carbon is quantified using isotope mass balance (Dusek et al., 2014):

$$F^{14}C_m \cdot M_m = F^{14}C_{st} \cdot M_{st} + F^{14}C_F \cdot M_F + F^{14}C_M \cdot M_M. \quad (S1)$$

M_m and M_{st} stand for the experimentally determined mass and the mass of reference materials either the oxalic acid OXII calibration material ($F^{14}C$ = 1.3406) or a ^{14}C-free CO_2 gas ($F^{14}C$ = 0) with a unit of µgC, respectively. $F^{14}C_m$ and $F^{14}C_{st}$ represent the experimentally determined $F^{14}C$ measured by AMS and nominal $F^{14}C$ of reference materials (Table S9).

The relationships among all masses are described as Eq. (S2):

$$M_m = M_{st} + M_F + M_M, \quad (S2)$$

where M_M is calculated using Eq. (S1) by substituting $F^{14}C_{st} = 0$ for a ^{14}C-free CO_2 gas as:

$$M_M = F^{14}C_m \cdot M_m. \quad (S3)$$

Substitute $F^{14}C_{st} = 1.3406$ for OXII and the derived M_M from Eq. (S3), M_F is derived by combining Eq. (S1) and Eq. (S2) as:

$$M_F = ((1.3406 - F^{14}C_m) \cdot M_m - (1.3406 - 1) \cdot M_M)/1.3406. \quad (S4)$$

M_M and M_F is calculated by applying Eq. (S3) and Eq. (S4), and they are mass dependent. The modern carbon contamination (M_M) is between 0.35 and 0.50 µg C, and the fossil carbon contamination (M_F) is around 2 µg C for sample bigger than 100 µgC.

In the revised manuscript, we add the detailed calculation of modern and fossil contamination in the supplemental material (Supplemental S3). The revised manuscript adds:

> "The differences between measured and nominal $F^{14}C$ values are used to correct the sample values (de Rooij et al., 2010; Dusek et al., 2014) for contamination during graphitization and AMS measurement (Supplemental S3). The modern carbon contamination is between 0.35 and 0.50 µg C, and the fossil carbon contamination is around 2 µg C for sample bigger than 100 µgC." (page 7 line 5–9)

9) Source apportionment methodology using ^{14}C: as already aforementioned, the use of the definition "conversion factors" is misleading, as they have a physical meaning (as it is clear at page 6, line 24). Authors should introduce this concept earlier in the text, so that they can also explain the use of different values for their "conversion factors". This would definitely make the paper easier to read.

Response: As addressed in the response to Question 2, the revised manuscript uses the physical meanings (i.e., $F^{14}C$ of biomass burning ($F^{14}C_{bb}$) for EC, $F^{14}C$ of non-fossil sources ($F^{14}C_{nf}$) for OC) instead of "conversion factors" (page 7 line 11–13, line 18–22). This concept is added in the revised Introduction section (page 3 line 5–13).

10) Temporal variation of fossil and non-fossil fractions of OC and EC, page 7: levoglucosan, hopanes and picene are cited for the first time, with no reference to S2, where the measurements

are described. The existence of ancillary/additional measurements deserves to be introduced as part of the methodology.

Response: We add briefly the measurement of source markers in the Sect. 2.2 as part of the methodology and change the title to "2.2 Organic carbon (OC), elemental carbon (EC) and source markers measurement". S2 is kept in the supplemental material for details on the measurements.

Further, S2 is mentioned (page 9 line 17) when organic markers (levoglucosan, hopanes and picene) are cited in the main text for the first time.

11) ^{13}C signature of OC and EC, page 9, line 12: "$\delta^{13}C_{OC}$ was in general similar to $\delta^{13}C_{EC}$": this means that the biogenic source is roughly negligible: can the author comment with finding also in relation to the radiocarbon measurement results?

Response: $\delta^{13}C_{OC}$ was in general similar to $\delta^{13}C_{EC}$: it suggests that biogenic OC is probably not very important, as could be expected from the high TC concentrations and strong anthropogenic sources. This can be true, as we would expect a bit different $\delta^{13}C_{OC}$ from $\delta^{13}C_{EC}$ if biogenic sources play an important role on OC.

In light of ^{14}C, we still measure a considerable fraction of non-fossil OC, and it would seem that this is more related to the biomass burning. Or, if there is biogenic OC, but by chance their $\delta^{13}C$ signatures are relatively similar with those for the source mixture of EC, which is not very likely.

The following statements were added to the revised manuscript:

> "$\delta^{13}C_{OC}$ was in general similar to $\delta^{13}C_{EC}$. This suggests that biogenic OC is probably not very important, as could be expected from the high TC concentrations. ^{14}C analysis indicates a considerable fraction of non-fossil OC than non-fossil EC, and it would seem that this is mainly related to the biomass burning, which has higher OC/EC ratios than fossil fuel burning. If the contribution of biogenic OC plays an important role, then the biogenic $\delta^{13}C$ signatures should be relatively similar to the source mixture of EC, which is rather unlikely, especially as this source mixture is not constant" (page 11 line 5–9)

12) I suggest moving section 4.4 straight after 4.2, as this discussion follows directly from the last sentences of 4.2.

Response: The order of the two sections has been changed. The order of Fig. 7 and Fig. 8 is also changed accordingly.

13) Changes in emission sources in Xi'an, China (2008/2009 vs. 2012/2013), pages 15-16: the cited papers taken for comparison focus, respectively, on a big haze episode and on an intensive campaign (2 winter months), and not on a campaign aiming at being representative for a year, therefore I think this comparison is not very useful. Further, contributions are roughly the same within the uncertainties.

Response: We did the whole year measurement in Xi'an for the year 2008/2009. In this study, we selected samples with varying $PM_{2.5}$ mass and carbonaceous aerosols for ^{14}C analysis. The

selected samples cover periods of low, medium and high $PM_{2.5}$ concentrations to get samples representative of the various pollution conditions that did occur in each season. Here we only compare the winter season due to the limited source apportionment results for EC in Xi'an. For Xi'an, we see from this study (see Fig. 1(a), except the Chinese New Year eve, which is not included in the comparison) but also some studies in preparation that the ^{14}C values do not change very much between polluted days and clean days. In addition, two months (the intensive campaign by Wang et al. (2016)) almost cover the whole winter (in total, 3 months). Thus, we think that it makes sense to compare the results from this study with the two cited paper.

For EC source apportionment, it is noted that the quartile ranges for 2008/2009 values (this study) overlaps ranges for 2012/2013 values (average ± SD). Compared to the uncertainties of radiocarbon measurements, the uncertainties of PMF results are always larger, making the overlapped ranges very likely. However, comparing the probability distribution functions for both cases give a more complete picture. Figure S14 and Figure S15 shows the probability density functions (PDF) of the relative source contributions to EC from coal combustion and vehicle emissions, respectively. Results from this study for the year 2008/2009 are shown in grey (this is also shown in the original Fig. S8), and from Wang et al. (2016) for the year 2012/2014 shown in yellow. For the PDF by Wang et al. (2016), we assume normal distribution as their source apportionment results are not known and given in the form of average ± SD. As shown in Fig. S14 and Fig. S15, though with some overlaps, the PDF of the relative source contribution of coal combustion (vehicle emissions) does clearly shift to the lower side (higher side) from the year 2008/2009 to 2012/2013. With the current inherent uncertainties in these two states of the art source apportionment methods it will not be possible to draw more firm conclusions than that these probability distributions show a certain trend, despite some possible overlap.

We also have some additional observation data to support the conclusion as discussed in Sect. 4.6. The decreased contributions of coal combustion are also evidenced from the declined enrichment factor of As and Pb, indicators of coal combustion. Increasing vehicular emissions is supported by the increasing level of NO_2, an indicator for the contribution of vehicular emissions.

In the revised manuscript, the above discussion is added in the section of Changes in emission sources in Xi'an, China (2008/2009 vs. 2012/2013) (page 18 line 25–27; page 19, line 7–14). The Fig. S14 and Fig. S15 is added to the supplemental material.

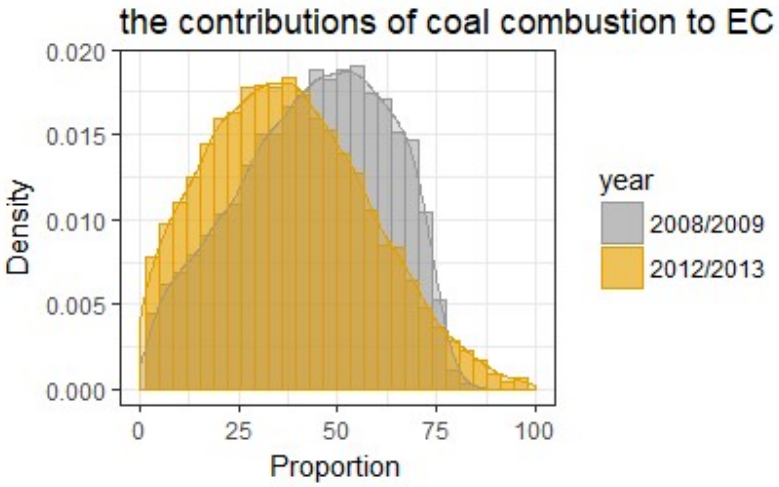

Figure S14. Probability density functions (PDF) of the relative source contributions of coal combustion to EC in winter in the year 2008/2009 (this study, shown in grey; this is also shown in Fig. S8) and 2012/2013 by Wang et al. (2016), shown in yellow.

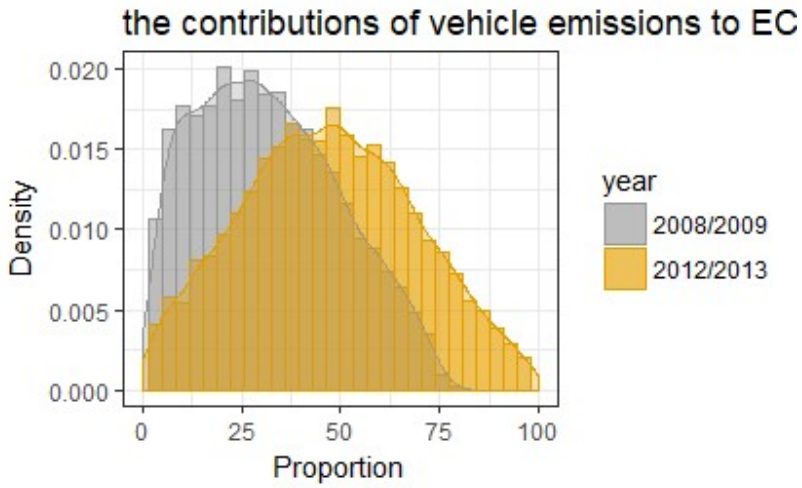

Figure S15. Probability density functions (PDF) of the relative source contributions of vehicle emissions to EC in winter in the year 2008/2009 (this study, shown in grey; this is also shown in Fig. S8.) and 2012/2013 by Wang et al. (2016), shown in yellow

14) Supplement, table S1: far as I get, the reported interval for C4 plants is wide as different plants (corn, sugar cane, grass and maybe more) have different signatures: why do the authors "decrease" this range to -16.4 ± 1.4 per mil? (Further, please pay attention to number of digits, e.g. -23.4 ±1.3 and not -23.38 ±1.3)

Response: In this study, $\delta^{13}C$ for corn stalk is used as it is the dominant C4 plant in Xi'an and its surrounding areas (Sun et al., 2017; Zhu et al., 2017), with little sugarcane and other C4 plants as explained in Sect. 4.3.1 where details on selection of $\delta^{13}C$ endmembers for C4 plants in the study area are described. $\delta^{13}C$ values of aerosols from corn stalk burning were compiled from literature, ranging from -19.3 ‰ to -13.6 ‰ (Fig. S6). $\delta^{13}C$ source signatures for emissions from burning corn stalk were determined as -16.4 ± 1.4 ‰ (mean ± standard deviation): the mean (-16.4 ‰) was computed as the average of the different data sets, and standard deviation (1.4 ‰) analogously calculated.

In the revised manuscript, we change the title of Sect. 4.3.1 to "4.3.1 Selection of $\delta^{13}C$ endmembers for aerosols from corn stalk burning in the study area", to clarify that the $\delta^{13}C$=-16.4 ± 1.4 ‰ is specific for burning corn stalk, which is a subtype of C4 plant. Further, in the notation of Table S1, we add the following as a reminder:

> "In this study, $\delta^{13}C$ for corn stalk is used as it is the dominant C4 plant in Xi'an and its surrounding areas (Sun et al., 2017; Zhu et al., 2017), with little sugarcane and other C4 plants."

Number of digits are all corrected for $\delta^{13}C$ values throughout the manuscript, according the reviewer's comments.

References:

Cao, J. J., Zhu, C. S., Chow, J. C., Watson, J. G., Han, Y. M., Wang, G.H., Shen, Z. X., and An, Z. S.: Black carbon relationships with emissions and meteorology in Xi'an, China, Atmos. Res., 94, 194–202, 2009.

de Rooij, M., van der Plicht, J., and Meijer, H.: Porous iron pellets for AMS ^{14}C analysis of small samples down to ultra-microscale size (10–25μgC), Nucl. Instrum. Meth. B: Beam Interactions with Materials and Atoms, 268, 947-951, 2010.

Dusek, U., Ten Brink, H., Meijer, H., Kos, G., Mrozek, D., Röckmann, T., Holzinger, R., and Weijers, E.: The contribution of fossil sources to the organic aerosol in the Netherlands, Atmos. Environ., 74, 169-176, 2013.

Dusek, U., Monaco, M., Prokopiou, M., Gongriep, F., Hitzenberger, R., Meijer, H.A.J. and Röckmann, T.: Evaluation of a two-step thermal method for separating organic and elemental carbon for radiocarbon analysis, Atmos. Meas. Tech., 7(7), 1943–1955, https://doi.org/10.5194/amt-7-1943-2014, 2014.

Genberg, J., Hyder, M., Stenström, K., Bergström, R., Simpson, D., Fors, E., Jönsson, J. Å., and Swietlicki, E.: Source apportionment of carbonaceous aerosol in southern Sweden, Atmospheric Chemistry and Physics, 11, 11387-11400, 2011.

Gilardoni, S., Vignati, E., Cavalli, F., Putaud, J. P., Larsen, B. R., Karl, M., Stenström, K., Genberg, J., Henne, S., and Dentener, F.: Better constraints on sources of carbonaceous aerosols using a combined ^{14}C – macro tracer analysis in a European rural background site, Atmos. Chem. Phys., 11, 5685-5700, https://doi.org/10.5194/acp-11-5685-2011, 2011.

Han, Y. M., Chen, L.W., Huang, R.J., Chow, J. C., Watson, J. G., Ni, H. Y., Liu, S. X., Fung, K.

K., Shen, Z. X, Wei, C., Wang, Q. Y., Tian, J., Zhao, Z. Z., Prévôt, A. S. H., and Cao, J. J.: Carbonaceous aerosols in megacity Xi'an, China: implications of thermal/optical protocols comparison, Atmos. Environ., 132, 58–68, 2016.

Minguillón, M. C., Perron, N., Querol, X., Szidat, S., Fahrni, S. M., Alastuey, A., Jimenez, J. L., Mohr, C., Ortega, A. M., Day, D. A., Lanz, V. A., Wacker, L., Reche, C., Cusack, M., Amato, F., Kiss, G., Hoffer, A., Decesari, S., Moretti, F., Hillamo, R., Teinilä, K., Seco, R., Peñuelas, J., Metzger, A., Schallhart, S., Müller, M., Hansel, A., Burkhart, J. F., Baltensperger, U., and Prévôt, A. S. H.: Fossil versus contemporary sources of fine elemental and organic carbonaceous particulate matter during the DAURE campaign in Northeast Spain, Atmos. Chem. Phys., 11, 12067-12084, https://doi.org/10.5194/acp-11-12067-2011, 2011.

Sun, J., Shen, Z., Cao, J., Zhang, L., Wu, T., Zhang, Q., Yin, X., Lei, Y., Huang, Y., Huang, R., Liu, S., Han, Y., Xu, H., Zheng, C., and Liu, P.: Particulate matters emitted from maize straw burning for winter heating in rural areas in Guanzhong Plain, China: current emission and future reduction, Atmos. Res., 184, 66–76, 2017.

Szidat, S., Jenk, T. M., Synal, H. A., Kalberer, M., Wacker, L., Hajdas, I., Kasper-Giebl, A., and Baltensperger, U.: Contributions of fossil fuel, biomass-burning, and biogenic emissions to carbonaceous aerosols in Zurich as traced by ^{14}C, J.Geophys. Res.-Atmos., 111, 2006.

Zhu, C. S., Cao, J. J., Tsai, C. J., Zhang, Z. S., and Tao, J.: Biomass burning tracers in rural and urban ultrafine particles in Xi'an, China, Atmos. Pollut. Res., 8, 614–618, http://dx.doi.org/10.1016/j.apr.2016.12.011, 2017.

Response to reviewer 3:

General comments:

This manuscript reported datasets of carbon isotopes (^{13}C and ^{14}C) of OC and EC in a major inland city of China, Xi'an, during one-year sampling, which were used to study the source apportionment of carbonaceous aerosols by combining ^{13}C and ^{14}C with Bayesian Markov chain Monte Carlo (MCMC) scheme. The data and methodology are reliable and novel. This paper shed some new light on the source apportionment of carbonaceous aerosols by distinguishing coal and liquid fossil fuel contributions to EC, C3 and C4 plant to biomass burning. The paper is relatively well-written, and it should be acceptable for publication after some moderate to major revision.

Response: We appreciate the constructive suggestion. We carefully considered all the comments of the reviewer in the revised manuscript.

Major points: 1. Be clear re mean or median values of source contribution, E.g., P1/L23, the 45% and 31% are median values in Figure 4. Need to be consistent in the manuscript.

Response: We agree with the reviewers that the mean or median values of source contribution is not clear enough to readers. Throughout the manuscript, the average with one standard deviation is used to represent the best estimate and uncertainties of radiocarbon results, respectively, as stated in Sect. 2.5: Source apportionment methodology using ^{14}C (page 8 line 1–2). Thus, we used the average and one standard deviation for f_{bb}(EC), f_{fossil}(EC), f_{nf}(OC), f_{fossil}(OC), EC_{bb}, EC_{fossil}, OC_{nf} and OC_{fossil} throughout the manuscript.

For EC source apportionment results derived from the MCMC model (Sect 2.6), the median was used to represent the best estimate of the contribution of any particular source to EC. Uncertainties of this best estimate are expressed as inter-quartile range and 95 % range of corresponding PDF, as stated on page 14 line 19–20: "The median was used to represent the best estimate of the contribution of any particular source to EC. Uncertainties of this best estimate are expressed as inter-quartile range and 95 % range of corresponding PDF."

The revision in the abstract lines (page 1, line 22):

> "relative contributions from coal combustion and liquid fossil fuel combustion are estimated as 45 % (<u>median;</u> 29–58 %, interquartile range) and 31 % (18–46 %) in winter"

The revised texts show that (page 14 line 21–23):

> "For both MCMC4 and MCMC3, the MCMC-derived fraction of biomass burning EC (f_{bb}, <u>median with interquartile range calculated by Eq. (7)</u>) is similar to that obtained from radiocarbon data (<u>f_{bb}(EC), average with one standard deviation by Eq. (3)</u>) as both of them are well-constrained by $F^{14}C$. "

The revised caption of Fig. S9:

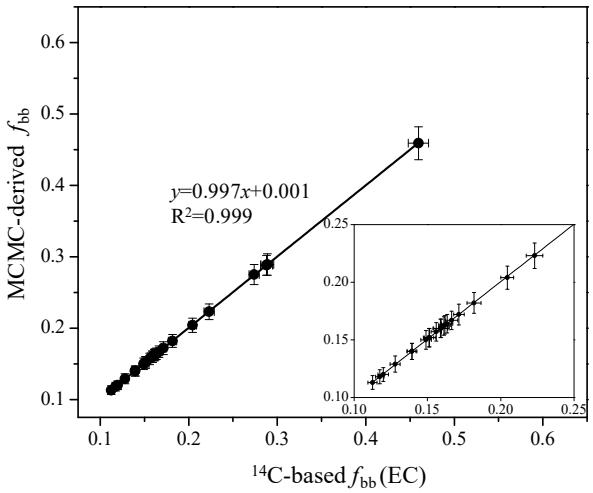

Figure S9. Comparison between the MCMC-derived fraction of biomass burning EC (f_{bb} derived from MCMC4) and that obtained from radiocarbon data (^{14}C-based f_{bb}(EC)). Average and one standard deviation is shown for f_{bb}(EC), median with interquartile range is shown for f_{bb} . f_{bb} derived from MCMC3 is also very similar to f_{bb}(EC)."

Also, we checked the rest of the manuscript with care. When the MCMC results are discussed, the median with the interquartile range is clearly stated (e.g., page 15, line 4–5; page 18, line 25; Table 2; Fig. 5). We believe that after revision, the mean and median of the source apportion results is clear.

2. The flow of introduction is not well organized, and some part of the ^{14}C introduction should be moved to the method part. I suggest re-organization and strengthening of the scientific objectives of this study in the introduction. In addition, you need to explain why we need to further distinguish the coal and fuel combustion in EC but not OC? Fossil sources contribute averagely 46% to OC based on your results, so it is important.

Response: We improved the introduction according to the comments and suggestions by the reviewer (page 2, line 2–23). The question regarding the ^{14}C introduction is addressed in the response of question 8. The objectives of this study are re-organized in the introduction (page 4, line 14–20).

We did not further distinguish the coal and liquid fossil fuel combustion in fossil OC, because OC is chemically reactive, and δ^{13}C of OC can be affected by atmospheric processing (Kirillova et al., 2013). The revised texts show (page 4, line 1–3):

"The interpretation of the stable carbon isotope signature for OC source apportionment is more difficult, because OC is chemically reactive and δ^{13}C signatures of OC are not only determined by the source signatures but also influenced by atmospheric processing."

3. Provide more clear details of blank/contamination evaluation for ^{14}C analysis, instrumental analytical precision and mention of source markers (S2) in the method part.

Response: The revised manuscript adds the following (page 7, line 5–9) in the method part:

> "The differences between measured and nominal $F^{14}C$ values are used to correct the sample values (de Rooij et al., 2010; Dusek et al., 2014) for contamination during graphitization and AMS measurement (Supplemental S3). The modern carbon contamination is between 0.35 and 0.50 µg C, and the fossil carbon contamination is around 2 µg C for sample bigger than 100 µgC"

The detailed calculation of modern and fossil contamination is added in the supplemental material (Supplemental S3):

> **"S3 Determination of modern and fossil contamination for radiocarbon measurement**
>
> $F^{14}C$ of aerosols samples was corrected for contamination that occurred during graphitization and AMS measurement. For AMS measurements, samples are usually analyzed together with varying amounts of reference material covering the range of sample mass. Two such materials with known ^{14}C content are used: the oxalic acid OXII calibration material ($F^{14}C$ = 1.3406) and a ^{14}C-free CO_2 gas ($F^{14}C$ = 0). Contamination during the graphitization and AMS measurement results into the differences between measured and nominal $F^{14}C$ values. The magnitude of these deviations can be used to quantify the contamination with fossil carbon ($F^{14}C_F$ = 0) and modern carbon ($F^{14}C_M$ = 1), which in turn are used for correcting the sample values (de Rooij et al., 2010).
>
> The contamination with fossil carbon and modern carbon is quantified using isotope mass balance (Dusek et al., 2014):
>
> $$F^{14}C_m \cdot M_m = F^{14}C_{st} \cdot M_{st} + F^{14}C_F \cdot M_F + F^{14}C_M \cdot M_M. \quad (S1)$$
>
> M_m and M_{st} stand for the experimentally determined mass and the mass of reference materials either the oxalic acid OXII calibration material ($F^{14}C$ = 1.3406) or a ^{14}C-free CO_2 gas ($F^{14}C$ = 0) with a unit of µgC, respectively. $F^{14}C_m$ and $F^{14}C_{st}$ represent the experimentally determined $F^{14}C$ measured by AMS and nominal $F^{14}C$ of reference materials (Table S9).
>
> The relationships among all masses are described as Eq. (S2):
>
> $$M_m = M_{st} + M_F + M_M, \quad (S2)$$
>
> where M_M is calculated using Eq. (S1) by substituting $F^{14}C_{st} = 0$ for a ^{14}C-free CO_2 gas as:
>
> $$M_M = F^{14}C_m \cdot M_m. \quad (S3)$$
>
> Substitute $F^{14}C_{st} = 1.3406$ for OXII and the derived M_M from Eq. (S3), M_F is derived by combining Eq. (S1) and Eq. (S2) as:
>
> $$M_F = ((1.3406 - F^{14}C_m) \cdot M_m - (1.3406 - 1) \cdot M_M)/1.3406. \quad (S4)$$

M_M and M_F is calculated by applying Eq. (S3) and Eq. (S4), and they are mass dependent. The modern carbon contamination (M_M) is between 0.35 and 0.50 µg C, and the fossil carbon contamination (M_F) is around 2 µg C for sample bigger than 100 µgC."

For OC and EC analysis the precision is determined as follows:

We repeat the analysis of samples, and the differences between the replicated analysis for the same sample (n=10) are smaller than 5% for TC, 5% for OC, and 10% for EC, respectively. This description is added in the Sect. 2.2 (page 5, line 15–16).

Following the reviewer's suggestion, we add briefly the measurement of source markers in the Sect. 2.2 as part of the methodology (page 5, line 17–19) and change the title to "2.2 Organic carbon (OC), elemental carbon (EC) and source markers measurement". S2 is kept in the supplemental material for details on the measurements.

4. The result section needs to be better structured and written. There are many parts, specially, sections 3.4 and 3.5, should be moved to discussion; and formulas could be moved to methods part.

Response: We have moved the sections 3.4 and 3.5 to the discussion following the reviewer's suggestion. In the revised manuscript, they are Sect. 4.3 and Sect. 4.4, respectively. The order of figures in the main text and supplemental material is adapted accordingly.

However, if the reviewer allows, we prefer to leave the formulas in the result and discussion section. In the Sect 4.3 (the original Sect. 3.4) and Sect 4.4 (the original Sect. 3.5), we detailed the way to model concentrations and sources of primary OC using those formulas and tried to explain the differences between the observed and modelled OC concentrations and sources. We hope that it would enhance the clarity and flow of this manuscript by leaving the equations in the part where they are need to know. This can also save the readers some time by avoiding going back to the method part, because those equations to model concentrations and sources of primary OC are not familiar to everyone. Further, there are equations used for illustrating the concept but not for calculation, for example:

$$\text{Observed OC conentrations} - \text{OC}_{\text{pri,e}} = \text{OC}_{\text{o,nf}} + \text{SOC}_{\text{coal}} + \text{SOC}_{\text{liq.fossil}}, \quad (12)$$

PS: we think the section of "**Sect. 3.4 $\delta^{13}C/F^{14}C$-based statistical source apportionment of EC**" and "**Sect. 3.5 Estimating mass concentrations and sources of primary OC**" (Sect. 4.3 and 4.4 of the revised manuscript) are results of this study. If we move these two sections to the discussion part, then the result section is very short and the discussion section is very long. If the reviewer agrees, we would like to move the two sections back the the result section.

5. There are many comparisons without in depth discussion in the discussion section. And comparison among different methods and different climate event seems not reasonable in 4.3.

Response: We did the whole year measurement in Xi'an for the year 2008/2009. In this study, we selected samples with varying $PM_{2.5}$ mass and carbonaceous aerosols for ^{14}C analysis. The selected samples cover periods of low, medium and high $PM_{2.5}$ concentrations to get samples

representative of the various pollution conditions that did occur in each season (see details in Sect. 2.1 and Supplemental S1 for sample selection). Here we only compare the winter season due to the limited source apportionment results for EC in Xi'an. For Xi'an, we see from this study (Fig. 1(a), except the Chinese New Year eve, which is not included in the comparison) but also some studies in preparation that the ^{14}C values do not change very much between polluted days and clean days. In addition, two months (the intensive campaign by Wang et al. (2016)) almost cover the whole winter (in total, 3 months). Thus, we think that it makes sense to compare the results from this study with the two cited paper.

Further, we address this question by answering the following questions 32 and 33 from the reviewer.

(a) **32.** P15/L16-20 I don't think it's reasonable to directly compare results of different methods, e.g., you got contribution of biomass burning to EC by MCMC4 with 4 sources while Zhang et al. (2015) got the fraction by 2 sources. Furthermore, taking into account of the error bar, the fraction fossil (76%)/ biomass (24%) of this study are the same to Zhang et al. (2015). Finally, Zhang et al. (2015) studied samples during the extreme winter haze episode of 2013.

Response: For the 4 sources solved by MCMC4, we did a posteriori combination of PDF of burning C3 and C3 plant, and named the combined PDF as biomass burning and denote the biomass burning contribution to EC as f_{bb} (Sect. 4.3.2). As addressed in Question 1, we compared the MCMC-derived f_{bb} with the ^{14}C-derived f_{bb}(EC) i.e. two sources similar to Zhang et al. (2015), and found they were very similar to each other (Fig. S9), as both of them are well-constrained by $F^{14}C_{(EC)}$ (page 14, line 21–23 in the revised text):

> "For both MCMC4 and MCMC3, the MCMC-derived fraction of biomass burning EC (f_{bb}, median with interquartile range calculated by Eq. (7)) is similar to that obtained from radiocarbon data (f_{bb}(EC), median with one standard deviation by Eq. (3)) as both of them are well-constrained by $F^{14}C$ (Table 2, Table S5, Table S7, Fig. S9)."

Thus, we think it is reasonable to compare the f_{bb} derived by MCMC4 with that from ^{14}C-derived fraction of biomass burning and fossil fuel burning in EC by Zhang et al. (2015).

We agree with the reviewer that taking into account of the error bar, the fraction fossil (76%) and biomass burning (24%) in EC of this study are the same to Zhang et al. (2015). The revised text shows that (page 18, line 27–29):

> "Taken into account of the uncertainties, comparable contributions were also reported at the same sampling site for winter 2012/2013 based on ^{14}C measurements (22 ± 3 %, Zhang et al., 2015a) and positive matrix factorization (PMF) receptor model simulation (20.1 ± 7.9 %, Wang et al., 2016) (Fig. 8)."

We noted that this study and Zhang et al. (2015) with different sampling focus. We conducted the campaign aiming at being representative for a year, and Zhang et al. (2015a) focus on the extreme winter haze. In this study, we selected samples with varying $PM_{2.5}$ mass and carbonaceous aerosols for ^{14}C analysis. The selected samples cover periods of low, medium and high $PM_{2.5}$ concentrations to get samples representative of the various pollution conditions that did occur in each season. And we compare the sources of EC in winter from this study with Zhang et al.

(2015a). We think that this comparison is reasonable, because for Xi'an, we see from this study (see Fig. 1(a), except the Chinese New Year eve, which is not included in the comparison) but also some studies in preparation that the ^{14}C values do not change very much between polluted days and clean days. We add the following clarification to the manuscript:

> "The contributions from biomass burning to EC was 24 % (median; interquartile range 22–26 %) in winter 2008/2009 (Fig. 8, Table 2) with no considerable change in ^{14}C values between polluted days and clean days (Fig. 1(a), except the Chinese New Year eve)." (page 18, line 25–27)

(b) **33.** P15/L23-28 The same question as above. Because the PMF model didn't use ^{14}C, is this reasonable for comparison?

Response: In our opinion it is reasonable to compare two different state of the art methods, provided that the uncertainty analysis for each is carefully done. If this was not possible, we would not be able, or justified to draw general conclusions from either method.

For EC source apportionment, it is noted that the quartile ranges for 2008/2009 values from MCMC4 (this study) overlaps ranges for 2012/2013 values (average ± SD) from the PMF model by Wang et al. (2016). Compared to the uncertainties of radiocarbon measurements, the uncertainties of PMF results are always larger, making the overlapped ranges very likely. But this will not change our conclusion that the source contributions of fossil EC are likely to have changed from 2008/2009 to 2013/2014, with decreasing contributions from coal burning and increasing contributions from motor vehicles. Figure S14 and Figure S15 shows the probability density functions (PDF) of the relative source contributions to EC from coal combustion and vehicle emissions, respectively. Results from this study for the year 2008/2009 are shown in grey (this is also shown in the original Fig. S8), and from Wang et al. (2016) for the year 2012/2014 shown in yellow. For the PDF by Wang et al. (2016), we assume normal distribution as their source apportionment results are not known and given in the form of average ± SD. As shown in Fig. S14 and Fig. S15, though with some overlaps, the PDF of the relative source contribution of coal combustion (vehicle emissions) does clearly shift to the lower side (higher side) from the year 2008/2009 to 2012/2013. Those discussions are added to the revised manuscript ((page 18 line 25–27; page 19, line 7–14).). Figure S14 and Figure S15 is added to the supplemental material.

We also have some additional observation data to support the conclusion as discussed in Sect. 4.6. The decreased contributions of coal combustion are also evidenced from the declined enrichment factor of As and Pb, indicators of coal combustion. Increasing vehicular emissions is supported by the increasing level of NO_2, an indicator for the contribution of vehicular emissions. (page 19, line 25–28; 29–31)

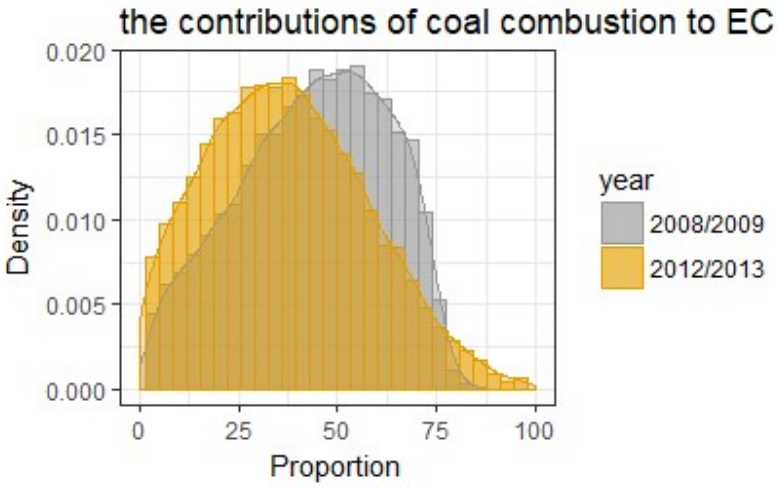

Figure S14. Probability density functions (PDF) of the relative source contributions of coal combustion to EC in winter in the year 2008/2009 (this study, shown in grey; this is also shown in Fig. S8) and 2012/2013 by Wang et al. (2016), shown in yellow.

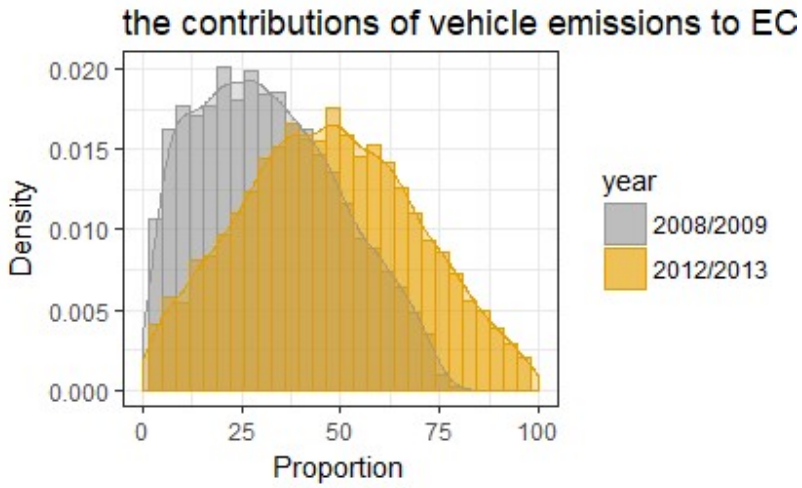

Figure S15. Probability density functions (PDF) of the relative source contributions of vehicle emissions to EC in winter in the year 2008/2009 (this study, shown in grey; this is also shown in Fig. S8) and 2012/2013 by Wang et al. (2016), shown in yellow.

6. The Conclusion part was too long. I suggest summarizing the key points.

Response: thank you for this comment. The conclusion was shortened and the key points were summarized in the revision of the manuscript (page 20, page 21)

Minor points and suggestions:

7. Introduction: P2/L1-10 This part didn't emphasize the importance of carbonaceous aerosol very well. And the structure and description are very similar to the second paragraph of the introduction from Zhang et al., (2015a, Atmos. Chem. Phys). Need to revise.

Response: Thank you for spotting this. We re-write this part in the revised manuscript (page 2, line 2–23).

8. P2/L16: The definition and expression of fraction modern is not explicit. "The ^{14}C content" is not a ratio as "fraction modern". I don't think the standard need normalize for fractionation to ^{13}C=-25‰. You can refer to Stuiver and Polach (1977) and modify this sentence. I also suggest move this "^{14}C result report" part to the Methods part.

Response: Thank you for pointing this out. The revised manuscript shows that "The $^{14}C/^{12}C$ ratio of an aerosol sample is reported as fraction modern ($F^{14}C$)" (page 2, line 26).
Isotope fractionations occurs for ^{13}C and ^{14}C during the sample pre-treatment and measurements. To correct the isotope fractionations, samples are normalized to $\delta^{13}C$ = -25 ‰ with respect to VPDB, and the standards are normalized in the same way (Mook and van der Plicht, 1999; Reimer et al., 2004). $\delta^{13}C$ = -25 ‰ is chosen for normalization for isotope fractionations because it is a representative average of the majority of organic samples in nature. The only exception is that, due to the historical reasons, the old Oxalic Acid standard (OX1) is normalized to its own $\delta^{13}C$= -19‰.
We report the ^{14}C results of our aerosol samples as fraction modern ($F^{14}C$), following the nomenclature of Reimer et al. (2004). We read the Stuiver and Polach (1977) very carefully and find that $F^{14}C$ is referred to as A_{SN}/A_{ON} in Stuiver and Polach (1977), where the subscript "$_N$" denotes normalization for isotope fractionation for samples and standards as shown in Table 1 in Stuiver and Polach (1977). We also note that A_{SN}/A_{ON} in Stuiver and Polach (1977) are normalized to $\delta^{13}C$= -19‰ of OX1. We think this citation is very helpful for readers to understand the ^{14}C data reporting, and we add the new citation in the revised text (page 2, line 28).

We moved the "^{14}C result part" from the method part to the introduction part, following one reivewer's comment in the preliminary review. In the revised manuscript, we clarify the definition of $F^{14}C$ by explaining it in more detail (page 2 line 26–31; page 3 line 1–3). Further, we introduce the assumptions on $F^{14}C$ for contemporary sources (page 3, line 5–13) to facilitate the reader and also the writing of the following sections, following the comments by the reviewer 2. We think it probably better to leave the $F^{14}C$ definition and assumptions on $F^{14}C$ for contemporary sources in the introduction, if possible. We believe by doing this, the readers can better understand why ^{14}C is a very useful tool in the aerosol source apportionment and how.

9. P2/L25 Clarify which kind of ^{14}C studies only have two datasets: seasonal variations? TC or other? For example, Zhang et al. (2015b, EST) also reported annual and seasonal variations of EC in Beijing.
Response: This is an oversight. The revised manuscript adds the Y. Zhang et al.(2015b) and shows that:

"Despite a fair number of ^{14}C studies in China in recent years, only a few ^{14}C datasets so far reported annual results and seasonal variations of OC and EC (Y. Zhang et al., 2014a, 2015b, 2017)" (page 3 line 17–18)

10. P2/L27-30 It's better to introduce ^{13}C first and introduce ^{14}C as a novel tool. The ^{13}C values of distinct sources you listed overlap with each other.

Response: We agree with the reviewer than the ^{14}C is a novel tool and can constrain fossil and biomass burning contribution to EC very well. But in this study, we can only separate fossil EC into EC from coal combustion and EC from vehicular emission by complementing ^{14}C with ^{13}C. Using ^{14}C alone can not separate the fossil EC into EC from coal combustion and liquid fossil fuel combustion.

In the introduction session, we introduce how the dual-carbon isotope-based (14C&13C) constrains on EC sources:

"EC from fossil sources (e.g., coal combustion, liquid fossil fuel burning) can be first separated from biomass burning by $F^{14}C$ of EC. Further, $\delta^{13}C$ of EC allows separation of fossil sources into coal and liquid fossil fuel burning (Andersson et al., 2015; Winiger et al., 2015, 2016), due to their different source signatures." (page 3 line 29–32)

The order of this description is the same of Eq. (7)–(9) for MCMC model in Sect. 2.6. Thus, we prefer to introduce $F^{14}C$ first followed by ^{13}C, if the reviewer allows.

It is noted that ^{13}C source signatures are not that well distinct and they have some overlaps. If it is ok with the reviewer, we will put the deeper discussion into the methods section 2.6, where we introduce the use of ^{13}C data for source apportionment and can further elaborate on the consequences of the overlapping signatures.

The source endmembers for $\delta^{13}C$ are less well-constrained than for $F^{14}C$, as $\delta^{13}C$ varies with fuel types and combustion conditions. For example, $\delta^{13}C$ values for liquid fossil fuel combustion overlaps with $\delta^{13}C$ values for both coal and C3 plant combustion. In this study, to account for the variability of the isotope signatures of $\delta^{13}C$ and $F^{14}C$ from the different sources, the Bayesian Markov chain Monte Carlo techniques (MCMC) were used as explained in the Method section. Uncertainties of both source endmembers for each source and the measured ambient $\delta^{13}C_{EC}$ and $F^{14}C_{(EC)}$ are propagated. These serve as input of MCMC to estimate the source contributions to EC. The MCMC results are the posterior probability density functions (PDF) for the relative contributions from the sources (Fig. S7, Fig. S8). The PDF of the relative source contributions of liquid fossil fuel combustion (vehicle) and coal combustion is skewed. By contrast, the PDF of the relative source contributions of biomass burning is symmetric as it is well-constrained by $F^{14}C$ (Fig. S8(a)). In this study, the median with its interquartile range was used to give the estimates of the contribution of any particular source to EC throughout the manuscript (e.g., Table 2, Sect. 4.3.2).

This point is clarified in the Method Sect. 2.6 by adding the following (page 8 line 14-22):

"$\delta^{13}C_{bb}$, $\delta^{13}C_{liq.fossil}$ and $\delta^{13}C_{coal}$ are the $\delta^{13}C$ signature emitted from biomass burning, liquid fossil fuel combustion and coal combustion, respectively. The means and the standard deviations for $\delta^{13}C_{bb}$ (-26.7 ± 1.8 ‰ for C3 plants, and -16.4 ± 1.4 ‰ for corn stalk), $\delta^{13}C_{liq.fossil}$ (-25.5 ± 1.3 ‰) and $\delta^{13}C_{coal}$ (-23.4 ± 1.3 ‰) are presented in Table S1 (Andersson et al., 2015 and reference therein; Sect. 4.3.1), and serves as input of MCMC. The source endmembers for $\delta^{13}C$ are less well-constrained than for $F^{14}C$, as $\delta^{13}C$ varies with fuel types and combustion conditions. For example, the range of possible $\delta^{13}C$ values for liquid fossil fuel combustion overlaps to a small extent with the range for coal combustion, although liquid fossil fuels are usually more depleted than coal. The MCMC technique takes into account the variability in the source-signatures of $F^{14}C$ and $\delta^{13}C$ (Table S1), where $\delta^{13}C$ introduces a larger uncertainty than $F^{14}C$. Uncertainties of both source endmembers for each source and the measured ambient $\delta^{13}C_{EC}$ and $F^{14}C_{(EC)}$ are propagated."

11. P3/L7: same question as above.

Response: This is addressed as above. We also changed the sentence in the Introduction section "Further, $\delta^{13}C$ of EC allows separation of fossil sources into coal and liquid fossil fuel burning (Andersson et al., 2015; Winiger et al., 2015, 2016), as they have their distinct source signatures" to:

"Further, $\delta^{13}C$ of EC allows separation of fossil sources into coal and liquid fossil fuel burning (Andersson et al., 2015; Winiger et al., 2015, 2016), due to their different source signatures. Typical $\delta^{13}C$ values for EC from previous studies are summarized in Table S1." (page 3 line 30-32).

12. P3/L9-13 You need to provide ^{13}C numbers for example to make readers to remember the trend between different processes.

Response: How depleted the SOA is dependent on the extent of how much the precursors is reacted. As stated in the draft manuscript: "During formation of secondary organic aerosol (SOA), molecules depleted in heavy isotopes are expected to react faster, leading to SOA depleted in ^{13}C compared to its gaseous precursors, if the precursor is only partially reacted (Anderson et al., 2004; Irei et al., 2006; Fisseha et al., 2009)."
To the best of our knowledge, the $\delta^{13}C$ values for the SOA from different processes have not been well studied. So, we can not really give the exact ^{13}C numbers for the different processes. But we agree with the reviewer that some examples of $\delta^{13}C$ values for the SOA would be useful to readers. We add:

"For example, Irei et al. (2006) found that the $\delta^{13}C$ values of particulate SOA formed by OH radical-induced reactions of toluene ranged from -32.2‰ to -32.9 ‰, on average 5.8‰ lighter than those of parent toluene, when 7–29% toluene was reacted." (page 4 line 5–7)

"For example, Bosch et al. (2014) observed the more enriched $\delta^{13}C$ signature of water-soluble OC (-20.8 ± 0.7 ‰) than EC (-25.8 ± 0.3 ‰) at a receptor station for the South

Asian outflow, due to aging of OC during the long-range transport of aerosols." (page 4 line 9–11)

Methods:

13. P4/L1 replace "pre-fired" with "pre-baked"

Response: Done (page 4 line 30)

14. P4/L3 what's the standard for season's classification? Reference? How can you classify autumn to middle day?

Response: We classify the seasons based on the meteorological characteristics and the residential heating period in Xi'an, China. The official residential heating period starts from 15 November to 14 March next year and can be slightly changed with the temperature. The autumn is classified to the middle day of November as it was the last day before the winter heating.

The classification of seasons in this study is also consistent with earlier studies in Xi'an, China (Han et al., 2016; T. Zhang et al., 2014). The citations are added in the revised manuscript (page 5 line 2–3).

15. P4/L15 instrumental analytical precision? Do you have field blank?

Response: The question on the instrumental analytical precision is addressed in the response of Question 3.

Unfortunately, no field blank was collected during this sampling campaign. From more recent sampling campaigns we know that the typical TC on the field blank is usually smaller than 1μg cm^{-2} with little EC, which is often below the detection level. This is much smaller than the TC loading on the collected samples ranging 20 μg cm^{-2} to 300 μg cm^{-2} with an average of 113 μg cm^{-2}. We can not conduct the blank correction, but this will only change the concentrations of OC slightly and even less for EC.

16. P5/L9-13 and L21-25 The whole blank/contamination should include all blank produced during experimental process and it is very important to know if the contamination is modern or fossil for ^{14}C analysis. For combustion process, are the stds modern and fossil? Give the mass and $F^{14}C$ value of the stds. Also, provide the $F^{14}C$ value of combustion contamination. For ^{14}C analysis, give the mass and $F^{14}C$ value of contamination you got in this study. Did you have $F^{14}C$ value of blank filter? Provide which blank you used to correct your ^{14}C data.

Response: Thank you for this comment.

(a). the contamination introduced by the combustion process

For combustion processes, two sets of standard material: the oxalic acid HOxII and anthracite with known ^{14}C contents ($F^{14}C$ = 1.3406 and $F^{14}C$ = 0, respectively) were combusted using ACS and used for quality control. The standard materials were put on the filter holder directly before heating in the oven in O_2 at 650°C for 10 minutes.
The $F^{14}C$ deviations between the nominal values and measured values are attributed to the contamination introduced by the combustion process. The deviations are used to estimate the

contamination by applying Eq. (S1)–(S4) where the actual contamination can be divided into two components: fossil contamination (M_F in µg C) with $F^{14}C_F = 0$ and modern contamination (M_M in µg C) with $F^{14}C_M = 1$ (Dusek et al. 2014). The measured $F^{14}C$ and mass of the standards for quality control of the combustion process is shown in Table S9 in the revised manuscript. Measurements of the anthracite standard ($F^{14}C=0$) yield modern contamination M_M of 0.2–1.2 µg C per extraction. Measurements of OX II standard yield fossil contamination M_F of 0.62–1.47 µg C per extraction.

We can conclude that the ACS system in fact introduced some contamination to the extracted samples but the contamination is not very large: (1) the measured $F^{14}C$ of the standards are deviating the nominal value only by less than 0.02 (the absolute values); (2). compared with our sampling size of 117 µg C (57–157 µg C; mean (min-max)) OC per extraction, 131 µg C (58–267 µg C) EC per extraction, the modern and fossil contamination is relatively small.

In this study, we did not correct the contamination introduced during the combustion process, because the contamination introduced from the combustion processes is small compared with our sample size. ~~and the combined $F^{14}C$ lies around 0.3 to 0.4 close to the range of the values for EC an somewhat below the values for OC, which cause relatively small correction in $F^{14}C$.~~ To determine the actual contamination introduced during the combustion process, a series of blanks and standards made by ACS system covering the mass range of our sample size must be used for the mass-dependent correction.

(b) contamination introduced by graphitization and AMS measurements

The method to estimate contamination is detailed in Supplemental S3 in the revised manuscript. The measure $F^{14}C$ and mass of standards are given in Table S9 in the revised manuscript. In the main text, we add:

> **"**The differences between measured and nominal $F^{14}C$ values are used to correct the sample values (de Rooij et al., 2010; Dusek et al., 2014) for contamination during graphitization and AMS measurement (Supplemental S3). The modern carbon contamination is between 0.35 and 0.50 µg C, and the fossil carbon contamination is around 2 µg C for sample bigger than 100 µgC.**"**

Table S9. The measured $F^{14}C$ values and masses of the standards with their nominal $F^{14}C$ values.

Standards		nominal $F^{14}C$	measured $F^{14}C$ ($F^{14}C_m$)	measured mass (M_m, μgC)
Combustion processes[a]	OXII	1.3406	1.327 ± 0.022	65
	OXII	1.3406	1.321 ± 0.012	117
	anthracite	0	0.020 ± 0.001	51
	anthracite	0	0.002 ± 0.001	75
	anthracite	0	0.004 ± 0.001	219
	anthracite	0	0.005 ± 0.001	254
Graphitization and ^{14}C measurements[b]	^{14}C-free CO_2 gas	0	0.008 ± 0.001	42
	^{14}C-free CO_2 gas	0	0.004 ± 0.000	81
	^{14}C-free CO_2 gas	0	0.005 ± 0.000	91
	^{14}C-free CO_2 gas	0	0.004 ± 0.000	123
	^{14}C-free CO_2 gas	0	0.003 ± 0.000	162
	^{14}C-free CO_2 gas	0	0.002 ± 0.000	186
	^{14}C-free CO_2 gas	0	0.003 ± 0.000	287
	OXII	1.3406	1.268 ± 0.013	45
	OXII	1.3406	1.270 ± 0.012	81
	OXII	1.3406	1.280 ± 0.011	96
	OXII	1.3406	1.305 ± 0.010	128
	OXII	1.3406	1.337 ± 0.010	162
	OXII	1.3406	1.306 ± 0.006	214
	OXII	1.3406	1.311 ± 0.005	321

[a] For combustion processes, two sets of standard material: the oxalic acid HOxII and anthracite with known ^{14}C contents ($F^{14}C$ = 1.3406 and $F^{14}C$ = 0, respectively) were combusted using ACS and used for quality control;
[b] Varying amounts of reference materials covering the range of sample mass are graphitized and analyzed together with samples in the same wheel of AMS, to correct contamination during graphitization and AMS measurement.

(c) blank filter

As addressed in the question 15, unfortunately, no field blank was collected during this sampling campaign. Typical TC on the field blank is usually smaller than 1μg cm^{-2} with little EC. This is much smaller than the TC loading on the collected samples ranging 20 μg cm^{-2} to 300 μg cm^{-2} with an average of 113 μg cm^{-2}. We can not conduct the blank correction, but this will only change the concentrations and $F^{14}C$ of OC slightly and even less for EC.

We measured the OC of one field blank filter for another sampling campaign in Xi'an, China. This OC field blank was analyzed by pooling several extracts of the same filter. The $F^{14}C$ of the OC on the field blank filter ($F^{14}C_{OC,blank}$) was 0.553 ± 0.003. The $F^{14}C_{OC,blank}$ is close to the ambient $F^{14}C$ of OC ($F^{14}C_{OC}$) values for this study, with an average of 0.567 ranging from 0.330

to 0.696. The blank correction will therefore not shift the ambient $F^{14}C_{OC}$ in this study strongly. It is relatively common in the literature that ^{14}C measurements of aerosol filter samples are not blank corrected, either because the blank values are too small to be measured for ^{14}C, or because the correction would be very small compared to the relatively larger carbon amounts that need to be sampled for ^{14}C analysis (e.g., Szudat et al., 2004; 2006). A recent study of Dusek et al. (2017) found that the blank correction for $F^{14}C$ was very small and only slightly change $F^{14}C$ values of ambient samples.

In summary, both the measurements of the blank filter (from a different campaign, but conducted by the same group in the same location, with similar sampling setup) and the combustion standards show that the blank correction would shift the measured ^{14}C only by an insignificant amount, the correction was therefore omitted.

17. P6/L18 Is the "f_{bb}" the same as "f_{bb}" at L1?

Response: Thank you for this comment. Eq. (7) at L18 can be formulated as: $F^{14}C_{(EC)}=F^{14}C_{bb} \times f_{bb}$, because $F^{14}C_{liq.fossil}$ and $F^{14}C_{coal}$ is zero due to the long-time decay. The "f_{bb}" in Eq. (7) at L18 is by definition the same as ^{14}C-based "f_{bb}(EC)" in Eq. (3) at L1, as both of them are calculated by dividing $F^{14}C_{(EC)}$ with $F^{14}C$ of biomass burning ($F^{14}C_{bb}$). However, we use different symbols, because in the first case, f_{bb}(EC) is estimated by a Monte Carlo simulation, based on ^{14}C measurements alone, and in the second case f_{bb} is estimated by the full 4 source MCMC model.

The main difference is that the we use average to represent the best estimate for ^{14}C-derived "f_{bb}(EC)" in Eq. (3), and use median to represent the best estimate for f_{bb} (Eq. (7) at L18) derived from the MCMC. The median is used to represent the best estimate of the contribution of any particular source to EC derived from the MCMC, because the probability density functions (PDF) of the relative source contributions of liquid fossil fuel combustion (vehicle) and coal combustion is skewed. By contrast, the PDF of the relative source contributions of biomass burning is symmetric as it is well-constrained by $F^{14}C$ (Fig. S8(a)). Thus the MCMC-derived f_{bb} (median) is very similar to that f_{bb}(EC) (median), as shown in Fig. S9. This is clarified in the manuscript and the revised text shows that:

> "For both MCMC4 and MCMC3, the MCMC-derived fraction of biomass burning EC (f_{bb}, median with interquartile range calculated by Eq. (7)) is similar to that obtained from radiocarbon data (f_{bb}(EC), median with one standard deviation by Eq. (3)) as both of them are well-constrained by $F^{14}C$ (Table 2, Table S5, Table S6, Fig. S9)." (page 14 line 21–23)

In addition, the caption of Figure S9 is revised to clarify the similarity between f_{bb} and f_{bb}(EC):

> "Figure S9. Comparison between the MCMC-derived fraction of biomass burning EC (f_{bb} derived from MCMC4) and that obtained from radiocarbon data (^{14}C-based f_{bb}(EC)). Average and one standard deviation is shown for f_{bb}(EC), median with interquartile range is shown for f_{bb} . f_{bb} derived from MCMC3 is also very similar to f_{bb}(EC)."

Results:

18. P7/L10 The number of seasonal samples in Table S2 is not the same as in the sampling part, need to clarify this inconsistency.

Response: Thank you for pointing this out. This is a mistake in the number of the samples. The sampling campaign in Xi'an was conducted for 13 months from 5 July 2008 to 8 August 2009 following every-sixth-day sampling schedule. In total, 65 $PM_{2.5}$ samples were collected during the 13 months as shown in the Table S2 in the draft manuscript.
However, this study focuses on the yearly cycle, and it will be confusing that there are two "July" and two "August" in a year cycle if we use the 65 samples collected the 13 months. Thus, at the end, we decide to use the 58 $PM_{2.5}$ samples collected from 5 July 2008 to 27 June 2009 to represent the one-year cycle.

The revised Table S1 shows there are 58 $PM_{2.5}$ samples in total, with 13 in spring, 15 in summer, 12 in autumn, and 18 in winter. We also check the mass concentrations in Table S2, and the mass concentrations of $PM_{2.5}$, OC and EC are the average and standard deviation calculated from the 58 samples collected from 5 July 2008 to 27 June 2009 with the season classification rules stated in the method Sect. 2.1.

19. P8/L20 unify the decimal place to one in the whole manuscript.

Response: Thank you for this comment. The decimal place is unified to one for $\delta^{13}C$ values throughout the manuscript.

20. P8/L30 Is it possible that combustion of a mixture of C4 and C3 plants or liquid fuel will results in the $^{13}C_{EC}$ values of around -24‰.

Response: To investigate if the mixture of C4 and C3 plants or liquid fossil fuel combustion can result in the $\delta^{13}C_{EC}$ values in winter (around -24‰), we run an additional adjusted simulation. In this simulation we assume that coal combustion does not contribute to EC at all in winter, even though coal combustion for heating is known as an important contributor to EC in winter (contributing around 45% to EC, see Sect. 4.3 and Fig. 5). That is, liquid fossil fuel combustion is the only fossil source of EC:

$$f_{\text{fossil}}(\text{EC}) = f_{\text{liq.fossil}} \quad \text{(R1)}$$

where $f_{\text{fossil}}(\text{EC})$ is the relative contribution of fossil fuel to EC. Biomass burning contribution to EC ($f_{\text{bb}}(\text{EC})$) includes contribution from burning C3 ($f_{\text{bb\_C3}}$) and C4 plant ($f_{\text{bb\_C4}}$):

$$f_{\text{bb}}(\text{EC}) = f_{\text{bb\_C3}} + f_{\text{bb\_C4}} \quad \text{(R2)}$$

Further, from the results of MCMC4, we know that C4 plant burning contribute more than that of C3 plant to EC in winter (Fig. S10b; Table S8), that is,

$$f_{\text{bb\_C4}} > f_{\text{bb\_C3}} \quad \text{(R3)}$$

Based on the $\delta^{13}C$ source signature for EC from burning C4 plant ($\delta^{13}C_{\text{bb\_C4}}$ = -16.4 ± 1.4 ‰; mean ± standard deviation), C3 plant ($\delta^{13}C_{\text{bb\_C3}}$ =-26.7 ± 1.8 ‰) and liquid fossil fuel ($\delta^{13}C_{\text{liq.fossil}}$ = -25.5 ± 1.3 ‰), the Eq.(R1)–(R2) and the constraints of Eq.(R3), $\delta^{13}C$ of EC due to burning C4

plant, C3 plant and liquid fossil fuel can be estimated ($\delta^{13}C_{EC,e}$; the subscript "$_e$" denotes "estimated") by Eq.(R4):

$$\delta^{13}C_{EC,e} = \delta^{13}C_{bb\_C3} \times f_{bb\_C3} + \delta^{13}C_{bb\_C4} \times f_{bb\_C4} + \delta^{13}C_{liq.fossil} \times f_{liq.fossil} \quad (R4)$$

A Monte Carlo simulation with 10,000 individual calculations was conducted to estimate propagated uncertainties. For each individual calculation, $\delta^{13}C_{bb\_C4}$, $\delta^{13}C_{bb\_C3}$, $\delta^{13}C_{liq.fossil}$, $f_{liq.fossil}$(=f_{fossil}(EC)) and f_{bb}(EC) are randomly chosen from a normal distribution symmetric around the mean with the standard deviation. Mean and standard deviation of $f_{liq.fossil}$(=f_{fossil}(EC)) and f_{bb}(EC) are derived from the radiocarbon measurements and $F^{14}C$ of biomass burning, and are given in Table S4. In this way 10,000 different estimation of $\delta^{13}C_{EC,e}$ can be calculated. The median was used to represent the best estimate of the contribution of any particular source to EC. Uncertainties of this best estimate are expressed as inter-quartile range (25^{th}-75^{th}) of the 10,000 estimated $\delta^{13}C_{EC,e}$.

Figure R1(A) shows the observed $\delta^{13}C_{EC}$ and the estimated $\delta^{13}C_{EC,e}$ values in winter. The observed $\delta^{13}C_{EC}$ in winter is shown as the filled black squares. The modelled $\delta^{13}C_{EC.e}$ is shown as the median (blue squares) with interquartile range (25^{th}-75^{th} percentile, blue horizontal bars). Five from six observed $\delta^{13}C_{EC}$ values in winter are either outside the interquartile range of the estimated $\delta^{13}C_{EC,e}$ or on the higher/lower end of the range. This makes the assumption of no coal combustion contribution to EC very unlikely, at least for the 3 sample with high f_{fossil}(EC).

Further, the conclusion will not change if no constraint of $f_{bb\_C4} > f_{bb\_C3}$ applys (Fig. R1(B)).

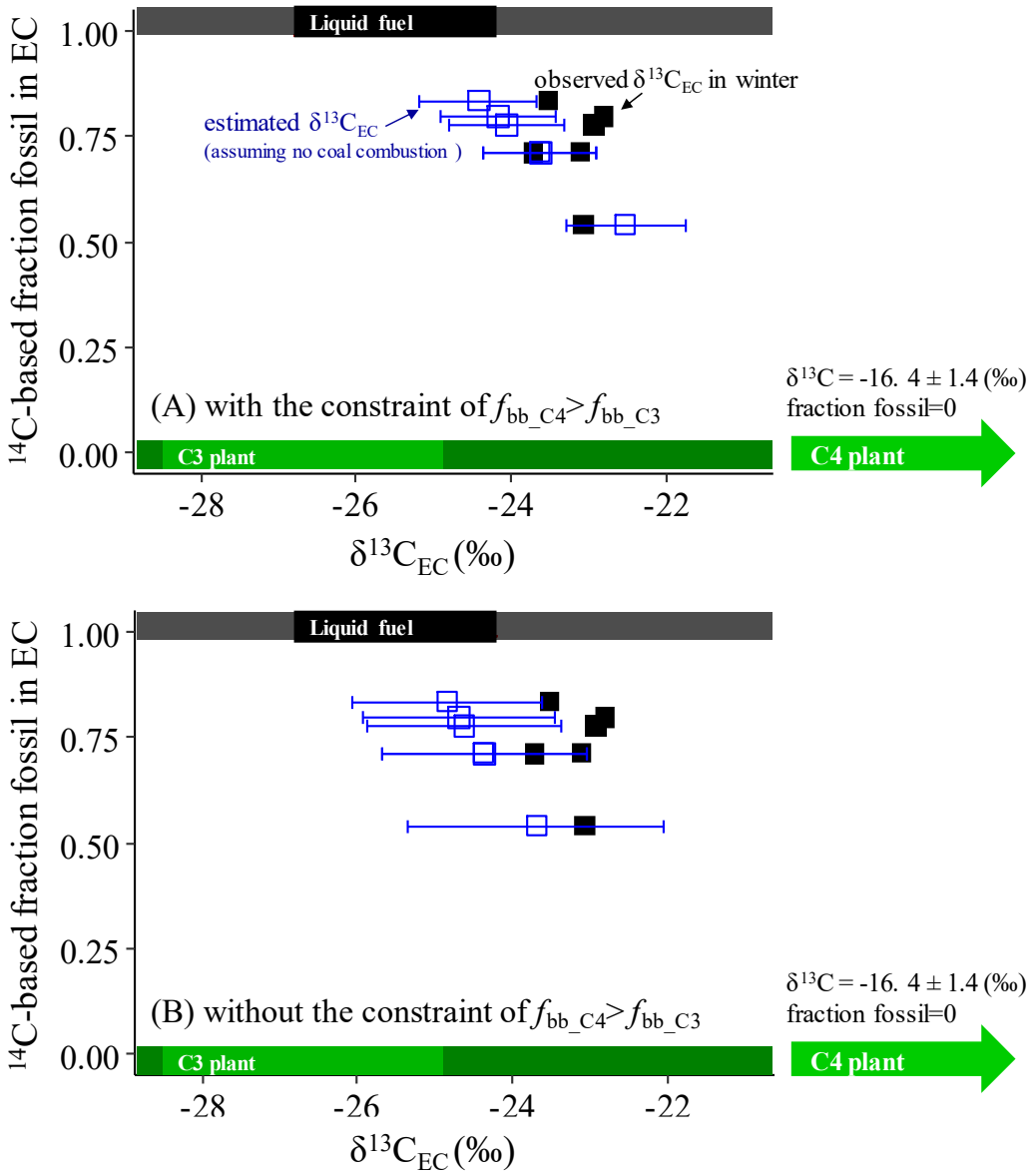

Figure R1. Two-dimensional isotope-based source characterization plot of EC in winter, with the assumption that no coal burning in winter contributed to EC. The observed $\delta^{13}C_{EC}$ in winter is shown as the filled black squares. The estimated $\delta^{13}C_{EC.e}$ with (A) and without (B) the constraint of $f_{bb\_C4} > f_{bb\_C3}$ is shown as the median (blue squares) with interquartile range (25^{th}-75^{th} percentile, blue horizontal bars). The fraction fossil in EC (f_{fossil}(EC)) was calculated using radiocarbon data. The expected $\delta^{13}C$ and ^{14}C endmember ranges for C3 plant burning, and liquid fossil fuel combustion are shown as green and black bars, respectively, within the ^{14}C-based endmember ranges for non-fossil (dark green rectangle, bottom) and fossil fuel combustion (grey rectangle, top). The $\delta^{13}C$ signatures of C4 plants burning is -16.4 ± 1.4 ‰ (mean ± standard deviation) is indicated in the plot but not shown on x-axis. The $\delta^{13}C$ signatures of C3 plants (green rectangle) and liquid fossil (e.g., oil, diesel, and gasoline, black rectangle) are indicated as mean ± standard deviation in Table S1.

21. P9/L26 what do the grey and dark green rectangle mean in Figure 3?

Response: we add the description of the grey and dark green rectangle in the caption of the Fig. 4 (the Fig. 3 in the draft manuscript):

> **"**The expected $\delta^{13}C$ and ^{14}C endmember ranges for biomass burning emissions, liquid fossil fuel combustion, and coal combustion are shown as green, black and brown bars, respectively, within the ^{14}C-based endmember ranges for non-fossil (dark green rectangle, bottom) and fossil fuel combustion (grey rectangle, top).**"**

22. P10/L1 Sections 3.4.1 is not real results of this study

Response: In the revised manuscript, we move the Sect. 3.4 to the discussion section following the reviewer's suggestion. The original Sect. 3.4.1 is Sect. 4.3.1 in the revised manuscript. We think the Sect. 4.3.1 is not a problem now in the discussion section.

23. P10/L10 Provide the four-source calculation formula in 3.4.2 section and change the name MCMC3" in 2.6 section.

Response: Sect 2.6 provides the principle of the MCMC, where f_{bb} in Eq. (7)–(9) represents the relative contributions of biomass burning to EC. f_{bb} represents the relative contributions of C3 plant burning for MCMC3 and represented the sum contribution of C3 and C4 plant burning to EC for MCMC4, respectively.

This is explained as follows:

> **"**Results from a four-source (C3 biomass, C4 biomass, coal and liquid fossil fuel) MCMC4 model and a three-source (C3 biomass, coal and liquid fossil fuel) MCMC3 model were compared to underscore the influence of C4 biomass on source apportionment. The results of the Bayesian calculations are the posterior probability density functions (PDF) for the relative contributions from the sources (Fig. S7, Fig. S8). For MCMC4, we did a posteriori combination of PDF for C3 biomass and C4 biomass, and named the combined PDF as biomass burning, to better compare results with MCMC3. **"** (page 14 line 11–16 in the revised manuscript).

In the main text, we would prefer not to separate the "biomass" into "biomass from C3 plants" and "biomass from C4 plants" to avoid distracting the readers, if possible. Because we tried to say that including C4 plants in calculation (MCMC4) does not affect the contribution of biomass burning to EC but affect the separation between contributions from coal burning and liquid fossil fuel combustion. Further, the relative fraction of C3 and C4 plants in biomass burning is not the main purpose of this study. If we separate f_{bb} into f_{bb}_C3 (contribution of C3 plant burning to EC) and f_{bb}_C4 (contribution of C4 plant burning to EC) in the formulas for MCMC4, then there will be two more symbols but they are not used in the manuscript later on.

In addition, the MCMC3 does not include C4 plant burning, thus does not represent the real-world conditions in Xi'an, China and leads to biased EC source apportionment as discussed on page 14 line 25–32, page 15 line 1–3. So, we would prefer to leave the title of Sect. 2.6 and not to change the title of Sect. 2.6 to "MCMC3".

24. P10/L28 "5 times less than in summer" should use "lower than"

Response: Corrected (page 14 line 29).

25. P10/L29-32 The proportion of liquid fossil fuel combustion in winter (more coal burning) lower than summer (more traffic emission) make sense, why is not your expectation?

Response: Yes, the proportions are still according to expectations, but not the absolute values of EC. We expect that the absolute EC concentrations (μg m^{-3}) from liquid fossil fuel combustion ($EC_{liq.fossil}$) should be roughly constant all over the year, or even higher in winter due to unfavorable meteorological conditions.

The total EC concentrations in winter were only 1.5 times higher than that in summer. To meet our expectation, that is, $EC_{liq.fossil}$ in winter should be roughly equal to or a bit higher than that in summer, the relative contributions of liquid fossil fuel combustion to EC ($f_{liq.fossil}$) in winter should be 1.5 times (or less) lower than that in summer. But the MCMC3-derived contributions of liquid fossil fuel combustion to EC was only 14 % in winter, 5 times lower than in summer. This implies the absolute EC concentrations (μg m^{-3}) from liquid fossil fuel combustion were much smaller in winter than in summer, which is inconsistent with our expectation that absolute EC concentrations from liquid fossil fuel combustion should be roughly constant all over the year, or even higher in winter due to unfavorable meteorological conditions (page 14 line 28–32; page 15 line 1).

26. P11/L16 mean or median?

Response: It is mean values. EC_{bb} (μg m^{-3}) and EC_{fossil} (μg m^{-3}) of individual samples are calculated using Eq. (3) and Eq. (4), respectively. As stated in the method Sect 2.5, the average of EC_{bb} (μg m^{-3}) and EC_{fossil} (μg m^{-3}) derived from 10,000 individual calculations of a Monte Carlo simulation is used to represent the best estimate.

The mean EC_{bb} and EC_{fossil} in the winter is calculated by averaging the EC_{bb} and EC_{fossil} of the selected winter samples for ^{14}C analysis, respectively. The mean EC_{bb} and EC_{fossil} in the warm period is also calculated like this.

27. P12/L14 Does the $OC_{o,nf}$ mean observed non-fossil OC?

Response: The $OC_{o,nf}$ denotes other non-fossil OC except primary OC from biomass burning. We make this definition of $OC_{o,nf}$ more clear in the revised text:

> "Observed OC mass concentrations that exceed $OC_{pri,e}$ can be explained by contribution from secondary OC from coal combustion (SOC_{coal}), and liquid fossil fuel usage ($SOC_{liq.fossil}$) and by other non-fossil OC ($OC_{o,nf}$). $OC_{o,nf}$ includes secondary OC from biomass burning and biogenic sources (SOC_{nf}; SOC non-fossil), and primary OC from vegetative detritus, bioaerosols, resuspended soil organic matter, or cooking." (page 16 line 12–**16**)

28. Discussion P13/L16 Add "Characteristics" in front of 4.1 title.

Response: Thank you for this comment. Done (page 11 line 24).

29. P13/L17 Clarify which f_{fossil} (EC) you used in comparison, the MCMC4 or $F^{14}C$? Because others use the $F^{14}C$ deduced values.

Response: Thank you for this comment. The f_{fossil}(EC) used in comparison is calculated from $F^{14}C_{(EC)}$. To clarify, the revised text shows:

"The annual average f_{fossil}(EC) derived from ^{14}C data in Xi'an is 83 %." (page 11 line 25)

In addition, we try to make this more clear by adding the following note to Table 1 (page 29):

"[a] f_{fossil} (OC) and f_{fossil} (EC) in this study is calculated from the $F^{14}C$ data (see details in Sect. 2.5)."

30. P13/L25 should be 76% as shown in Figure 4.

Response: As addressed in Question 29, the f_{fossil}(EC) is calculated from $F^{14}C_{(EC)}$. The averaged f_{fossil}(EC) in winter is 76.6 % ± 5.4% as shown in Table S5, and round to 77% at P13/L25 in the draft manuscript.

Due to the asymmetrical PDFs (Fig. S8), the individual median contributions of coal and liquid fossil fuel combustion (f_{coal} and $f_{liq.fossil}$) do not add up to the median of the combined PDF for fossil fuel burning (slight difference) and we would like to avoid a discussion on that in the main manuscript, if possible. The f_{fossil}(EC) (average) deduced from ^{14}C data and from MCMC (the sum of $f_{liq.fossil}$ and f_{coal}, median) can be a slight difference from each other, but still very similar as the f_{bb}(EC) and f_{fossil}(EC) is well-constrained by $F^{14}C_{(EC)}$.

31. P15/L4-8 Discussion here is not very convincing. The contribution of biomass burning to EC is the lowest in summer, but the highest contribution of biomass burning to EC occurred in winter (most corn stalk burning in winter, Figures 4 and S5), why no significant correlation was found in winter?

Response: Yes, no significant correlation was found in winter between $F^{14}C_{(EC)}$ and K^+/EC ratios and also not for $F^{14}C_{(EC)}$ and levoglucosan/EC ratios (Fig. S5).

In winter, the biomass burned in the studied area are mixture of crop residues (e.g., wheat straw, corn stalk) and wood. The levoglucosan/K^+ ratio for corn stalk burning and wheat straw burning is 0.21 ± 0.08 and 0.1 ± 0.0, respectively, much lower than those for wood burning (24.0 ± 1.8). No significant correlations between $F^{14}C_{(EC)}$ and K^+/EC ratios or between $F^{14}C_{(EC)}$ and levoglucosan/EC ratios suggest a changing mixture of biomass subtype (e.g., C3 plant (wheat straw and wood), C4 plant (corn stalk)) with different levoglucosan/K^+ ratios. A good correlation can only be expected, if one main type of biomass is burned. The revised manuscript shows:

"No significant correlations of $F^{14}C_{(EC)}$ with K^+/EC or levoglucosan/EC were found in other seasons (Fig. S5), suggesting a changing mixture of biomass subtypes with different levoglucosan/K^+ ratios. In this case the same amount of modern carbon contribution in EC (i.e., same $F^{14}C_{(EC)}$) can be associated with very different K^+/EC and levoglucosan/EC ratios, depending on which type of biomass is dominating at a given time" (page 13 line 19–23)

The correlations between $F^{14}C_{(EC)}$ with K^+ /EC ratios and $F^{14}C_{(EC)}$ with levoglucosan/EC ratios are used to infer the reason for the variability of EC, rather the absolute EC. Because $F^{14}C_{(EC)}$, K^+ /EC

ratios and levoglucosan/EC ratios are all relative term. Discussion on P15/L4-8 in the draft manuscript was discussing the variability of EC in summer, not absolute EC concentrations.

32. P15/L16-20 I don't think it's reasonable to directly compare results of different methods, e.g., you got contribution of biomass burning to EC by MCMC4 with 4 sources while Zhang et al. (2015) got the fraction by 2 sources. Furthermore, taking into account of the error bar, the fraction fossil (76%)/ biomass (24%) of this study are the same to Zhang et al. (2015). Finally, Zhang et al. (2015) studied samples during the extreme winter haze episode of 2013.

Response: This is addressed in Question 5(a).

33. P15/L23-28 The same question as above. Because the PMF model didn't use ^{14}C, is this reasonable for comparison?

Response: This is addressed in Question 5(b).

34. P16/L7 and Figure 7 clarify the relationship between vehicular emissions and liquid fossil fuel combustion somewhere before discussion.

Response: In this study, liquid fossil fuel combustion and vehicular emission is used interchangeably. Because the $\delta^{13}C_{EC}$ signature of liquid fossil fuel combustion was compiled from literature where EC emitted from vehicles were collected and $\delta^{13}C_{EC}$ was measured. We add the following clarification in the revised manuscript where the liquid fossil fuel combustion is mentioned for the first time in the result section:

> "Major EC sources in Xi'an include biomass burning, coal combustion, and liquid fossil fuel (e.g., diesel and gasoline) combustion (i.e., vehicular emissions) …" (page 10 line 15–16)

We repeat this clarification with notes in parentheses several times, for example:

> "This is also evident from our observation that $\delta^{13}C$ values of the ambient aerosol fall within the range of C3 plants, coal and liquid fossil fuel combustion (i.e., vehicular emissions) (Fig. 2)." (page 10 line 20–21)

35. P17/L3 Will the biogenic emission to OC result in lower ^{13}C values than EC?

Response: Thank you for this comment. We agree with the reviewer that if biogenic emissions play an important role on OC, we can expect a bit different $\delta^{13}C_{OC}$ from $\delta^{13}C_{EC}$.. Typically, biogenic OC concentrations are estimated on the order of a few microgram per cubic meter (μg /m^3), which is small compared to the observed TC in this study (Fig. 1 and Table S2). So probably primary and secondary biomass OC is responsible for most of the modern OC. And secondary OC in general might be responsible for more depleted $\delta^{13}C_{OC}$ (e.g., Irei et al., 2006; Fisseha et al., 2009). However, results on $\delta^{13}C$ of biogenic OC are sparse in the literature, and are so far inconclusive weather $\delta^{13}C$ is enriched or depleted. From our data we cannot make a firm conclusion that biogenic OC (mainly secondary) is the main cause.

36. Conclusions condense and summarize the key points of this study in this part.

Response: This is addressed in the Question 5.

37. References Check carefully the papers of the same author, e.g., you have two Zhang et al. (2015a) and where is Zhang et al. (2014a)? I think in section 4.3, you refer to Zhang et al., (2015a, Atmos. Chem. Phys.,)

Response: We check the references very carefully. There is one "Zhang and Cao, 2015a" and one "Zhang and Cao, 2015b" cited. And We find there is one "Zhang et al., 2015a" and one "Zhang et al., 2015b)" as follows:

"**Zhang, Y. L. and Cao, F.**: Fine particulate matter ($PM_{2.5}$) in China at a city level, Sci. Rep., 5, 14884, **2015a**. (page 28 line 3)

Zhang, Y. L. and Cao, F.: Is it time to tackle $PM_{2.5}$ air pollutions in China from biomass-burning emissions?, Environ. Pollut. , 202, 217–219, **2015b**. (page 28line 4–5)

Zhang, Y. L., Huang, R. J., El Haddad, I., Ho, K. F., Cao, J. J., Han, Y., Zotter, P., Bozzetti, C., Daellenbach, K. R., Canonaco, F., Slowik, J. G., Salazar, G., Schwikowski, M., Schnelle-Kreis, J., Abbaszade, G., Zimmermann, R., Baltensperger, U., Prévôt, A. S. H., and Szidat, S.: Fossil vs. non-fossil sources of fine carbonaceous aerosols in four Chinese cities during the extreme winter haze episode of 2013, Atmos. Chem. Phys., 15, 1299–1312, https://doi.org/10.5194/acp-15-1299-2015, **2015a**. (page 28 line 12–16)

Zhang, Y. L., Schnelle-Kreis, J., Abbaszade, G., Zimmermann, R., Zotter, P., Shen, R. R., Schäefer, K., Shao, L., Prévôt, A , and Szidat, S.: Source apportionment of elemental carbon in Beijing, China: insights from radiocarbon and organic marker measurements, Environ. Sci. Technol., 49, 8408–8415, **2015b**." (page 28 line 17–19)"

Zhang et al. (2014a) is cited in the Sect. 2.1 and it is revised to "T. Zhang et al., 2014" to differentiate "Y. Zhang et al., 2014a" and "Y. Zhang et al., 2014b":

"Details about the sampling site can be found elsewhere (Bandowe et al., 2014; T. Zhang et al., 2014)." (page 4 line 26)

And in the reference list:

"Zhang, T., Cao, J.-J., Chow, J. C., Shen, Z.-X., Ho, K.-F., Ho, S. S. H., Liu, S.-X., Han, Y.-M., Watson, J. G., Wang, G.-H., and Huang, R.-J.: Characterization and seasonal variations of levoglucosan in fine particulate matter in Xi'an, China, J. Air Waste Manage., 64, 1317–1327, 10.1080/10962247.2014.944959, 2014.**"** (page 27 line 41; page 28 line 1–2)

In Sect. 4.6 (original Sect. 4.3), we refer to Zhang et al. (2015a, Atmos. Chem. Phys.)

Except the citations pointed out by the reviewer, we find out more mistakes, and correct them all thoughtout the manuscript:

(1) Zhang et al., 2014b (revised to "Y. Zhang et al., 2014a")
(2) Zhang et al., 2014c (revised to "Y. Zhang et al., 2014b")
(3) Liu et al., 2014a (revised to "G. Liu et al., 2014")
(4) Liu et al., 2014b (revised to "J. Liu et al., 2014")
(5) Huang et al., 2014a (revised to "R. Huang et al., 2014")
(6) Huang et al., 2014b (revised to "X. Huang et al., 2014")

References:

de Rooij, M., van der Plicht, J., and Meijer, H.: Porous iron pellets for AMS ^{14}C analysis of small samples down to ultra-microscale size (10–25μgC), Nucl. Instrum. Meth. B: Beam Interactions with Materials and Atoms, 268, 947-951, 2010.

Dusek, U., Monaco, M., Prokopiou, M., Gongriep, F., Hitzenberger, R., Meijer, H.A.J. and Röckmann, T.: Evaluation of a two-step thermal method for separating organic and elemental carbon for radiocarbon analysis, Atmos. Meas. Tech., 7(7), 1943–1955, https://doi.org/10.5194/amt-7-1943-2014, 2014.

Dusek, U., Hitzenberger, R., Kasper-Giebl, A., Kistler, M., Meijer, H. A., Szidat, S., Wacker, L., Holzinger, R., and Röckmann, T.: Sources and formation mechanisms of carbonaceous aerosol at a regional background site in the Netherlands: insights from a year-long radiocarbon study, Atmospheric Chemistry and Physics, 17, 3233-3251, 2017.

Fisseha, R., Saurer, M., Jäggi, M., Siegwolf, R. T. W., Dommen, J., Szidat, S., Samburova, V., and Baltensperger, U.: Determination of primary and secondary sources of organic acids and carbonaceous aerosols using stable carbon isotopes, Atmos. Environ., 43, 431–437, http://dx.doi.org/10.1016/j.atmosenv.2008.08.041, 2009.

Irei, S., Huang, L., Collin, F., Zhang, W., Hastie, D., and Rudolph, J.: Flow reactor studies of the stable carbon isotope composition of secondary particulate organic matter generated by OH-radical-induced reactions of toluene, Atmos. Environ., 40, 5858–5867, 2006.

Mook, W. G. and van der Plicht, J.: Reporting ^{14}C activities and concentrations, Radiocarbon, 41, 227–239, 1999.

Prokopiou, M.: Characterization of a thermal method for separating organic and elemental carbon from aerosol samples using 14-C analysis, MS thesis, University of Groningen, the Netherlands, 2010.

Reimer, P. J., Brown, T. A., and Reimer, R. W.: Discussion: reporting and calibration of post-bomb ^{14}C data, Radiocarbon, 46, 1299–1304, 2004.

Szidat, S., Jenk, T. M., Gäggeler, H. W., Synal, H. A., Hajdas, I., Bonani, G., and Saurer, M.: THEODORE, a two-step heating system for the EC/OC determination of radiocarbon (14C) in the environment, Nuclear Instruments and Methods in Physics Research Section B: Beam Interactions with Materials and Atoms, 223–224, 829-836, http://dx.doi.org/10.1016/j.nimb.2004.04.153, 2004.

Szidat, S., Jenk, T. M., Synal, H. A., Kalberer, M., Wacker, L., Hajdas, I., Kasper‐Giebl, A., and Baltensperger, U.: Contributions of fossil fuel, biomass‐burning, and biogenic emissions to carbonaceous aerosols in Zurich as traced by 14C, Journal of Geophysical Research: Atmospheres (1984–2012), 111, 2006.

Source apportionment of carbonaceous aerosols in Xi'an, China: insights from a full year of measurements of radiocarbon and the stable isotope ^{13}C

Haiyan Ni[1,2,3,4], Ru-Jin Huang[2,3*], Junji Cao[3,5*], Weiguo Liu[2], Ting Zhang[3], Meng Wang[3], Harro A.J. Meijer[1], Ulrike Dusek[1]

[1]Centre for Isotope Research (CIO), Energy and Sustainability Research Institute Groningen (ESRIG), University of Groningen, Groningen, 9747 AG, the Netherlands
[2]State Key Laboratory of Loess and Quaternary Geology (SKLLQG), Institute of Earth Environment, Chinese Academy of Sciences, Xi'an, 710061, China
[3]Key Laboratory of Aerosol Chemistry & Physics (KLACP), Institute of Earth Environment, Chinese Academy of Sciences, Xi'an, 710061, China
[4]University of Chinese Academy of Sciences, Beijing, 100049, China
[5]Institute of Global Environmental Change, Xi'an Jiaotong University, Xi'an 710049, China

Correspondence to: Ru-Jin Huang (rujin.huang@ieecas.cn); Junji Cao (cao@loess.llqg.ac.cn)

Abstract. Sources of organic carbon (OC) and elemental carbon (EC) in Xi'an, China are investigated based on one-year radiocarbon and stable carbon isotope measurements. The radiocarbon results demonstrate that EC is dominated by fossil sources throughout the year, with a mean contribution of 83 ± 5 % (7 ± 2 μg m^{-3}). The remaining 17 ± 5 % (1.5 ± 1 μg m^{-3}) is attributed to biomass burning, with higher contribution in the winter (~24 %) compared to the summer (~14 %). Stable carbon isotopes of EC ($\delta^{13}C_{EC}$) are enriched in winter (-23.20 ± 0.35 4 ‰) and depleted in summer (-25.94 ± 0.46 5 ‰), indicating the influence of coal combustion in winter and liquid fossil fuel combustion in summer. By combining radiocarbon and stable carbon signatures, relative contributions from coal combustion and liquid fossil fuel combustion are estimated as 45 % (median; 29–58 %, interquartile range) and 31 % (18–46 %) in winter, respectively, whereas in other seasons more than one half of EC are from liquid fossil combustion. In contrast with EC, the contribution of non-fossil sources to OC is much larger, with an annual average of 54 ± 8 % (12 ± 10 μg m^{-3}). Clear seasonal variations are seen in OC concentrations both from fossil and non-fossil sources, with maxima in winter and minima in summer, because of unfavourable meteorological conditions coupled with enhanced fossil and non-fossil activities in winter, mainly biomass burning and domestic coal burning. $\delta^{13}C_{OC}$ exhibited similar values with $\delta^{13}C_{EC}$, and showed strong correlations (r^2 = 0.90) in summer and autumn, indicating similar source mixtures with EC. In spring, $\delta^{13}C_{OC}$ is depleted (1.1–2.4 ‰) compared to $\delta^{13}C_{EC}$, indicating the importance of secondary formation of OC (e.g., from volatile organic compound precursors) in addition to primary sources. Modelled mass concentrations and source contributions of primary OC are compared to the measured mass and source contributions. There is strong evidence that both secondary formation and photochemical loss processes influence the final OC concentrations.

1 Introduction

Carbonaceous aerosols ~~are,~~ an important component of fine particulate matter ($PM_{2.5}$, particles with aerodynamic diameter <2.5 μm) in almost all environments, have been identified as critical contributors to severe air pollution events (Cao et al., 2003; R. Huang et al., 2014; Elser et al., 2016; Liu et al., 2016a). In urban areas in China, they typically ~~constituting~~ constitute 20–50 % of $PM_{2.5}$ mass ~~in many urban areas in China~~ (Cao et al., 2007; R. Huang et al., 2014~~a~~; Tao et al., 2017). ~~They~~ Carbonaceous aerosols are of importance because they have adverse impacts on ~~air quality (Watson, 2002),~~ human health (Nel, 2005; Cao et al., 2012; Lelieveld et al., 2015), and climate (Chung and Seinfeld, 2002; Bond et al., 2013), in addition to~~.~~ air quality (Watson, 2002). Carbonaceous aerosols contain a large number of organic ~~–~~species and are operationally divided into organic carbon (OC) and elemental carbon (EC) (Pöschl, 2005). EC can significantly absorb incoming solar radiation and is the most important light-absorbing aerosol component (Bond et al., 2013). On the other hand, OC mainly scatters light, but there is also OC found with light absorbing properties, referred to as brown carbon (Pöschl, 2005; Laskin et al., 2015). Carbonaceous aerosols are believed to contribute large uncertainties in climate radiative forcing (IPCC, 2013). EC and OC are mainly ~~is exclusively~~ emitted ~~as primary aerosols~~ from incomplete combustion of biomass (e.g., wood, crop residues, and grass) and fossil fuels (e.g., coal, gasoline, and diesel). Biomass burning is the only non-fossil sources for EC, but OC also has other non-fossil sources, for example, biogenic emissions and cooking. Unlike EC that exclusively emitted as ~~includes both~~ primary ~~and secondary OC~~aerosols, OC includes both primary and secondary OC, where ~~from non-fossil (e.g., biomass burning, biogenic emissions, and cooking) and fossil sources, where primary OC is emitted directly and~~ secondary OC is formed in the atmosphere via atmospheric oxidation of volatile organic compounds from non-fossil (e.g., biomass burning, biogenic emissions, and cooking) and fossil sources (Jacobson et al., 2000; Pöschl, 2005; Hallquist et al., 2009). ~~Carbonaceous aerosols in $PM_{2.5}$ have been identified as critical contributors to severe air pollution events (Cao et al., 2003; Huang et al., 2014a; Elser et al., 2016; Liu et al., 2016a), but~~So far, ~~their~~ sources and evolution of carbonaceous aerosols remain poorly characterized. A better understanding of OC and EC sources is important for the mitigation of particulate air pollution and improving our ~~-~~understanding of their role in climate radiative forcing.

Radiocarbon (^{14}C) analyses of OC and EC allow a quantitative and unambiguous measurement of their fossil and non-fossil contributions, based on the fact that emissions from fossil sources are ^{14}C-free, whereas non-fossil emissions contain the contemporary ^{14}C content (e.g., Szidat, 2009; Dusek et al., 2013, 2017). The $^{14}C/^{12}C$ ratio ~~content~~ of an aerosol sample is usually reported as fraction modern ($F^{14}C$). $F^{14}C$ relates the $^{14}C/^{12}C$ ratio of the sample ~~relative~~ to the ratio of the unperturbed atmosphere in the reference year of 1950 (Stuiver and Polach, 1977; Mook and van der Plicht, 1999; Reimer et al., 2004). ~~an oxalic acid standard, and expressed as fraction modern ($F^{14}C$).~~ In practice, this is usually done by relating $^{14}C/^{12}C$ ratio of the sample to the ratio of ~~-~~oxalic acid OXII calibration material multiplied by a factor of 0.7459 ~~-^{14}C content of the standard is related to the unperturbed atmosphere in the reference year of 1950 (Mook and van der Plicht, 1999; Reimer et al., 2004),~~:

$$F^{14}C = \frac{(^{14}C/^{12}C)_{sample,[-25]}}{(^{14}C/^{12}C)_{1950,[-25]}} = \frac{(^{14}C/^{12}C)_{sample,[-25]}}{0.7459\times(^{14}C/^{12}C)_{OXII,[-25]}}, \quad (1)$$

where the $^{14}C/^{12}C$ ratio of the sample and standard are both corrected for machine background and normalized for fractionation to $\delta^{13}C$ = -25 ‰ to correct for isotopic fractionation during sample pre-treatment and measurements. Aerosol carbon from living material should have $F^{14}C$ ~1 in an undisturbed atmosphere, and carbon from fossil sources has $F^{14}C$ = 0. However, $F^{14}C$ values of the contemporary (or non-fossil) carbon sources are bigger than 1 due to the nuclear bomb tests that nearly doubled the $^{14}CO_2$ in the atmosphere in the 1960s and 1970s. Currently, $F^{14}C$ of the atmospheric CO_2 is approximately 1.04 (Levin et al., 2010). This value is decreasing every year, because the $^{14}CO_2$ produced by bomb testing is taken up by oceans and the biosphere and diluted by ^{14}C-free CO_2 produced by fossil fuel burning. For biogenic aerosols, aerosols emitted from cooking as well as annual crop, ~~the~~ $F^{14}C$ is close to the value of current atmospheric CO_2. $F^{14}C$ of wood burning is higher than that, because a significant fraction of carbon in the wood burned today was fixed during times when atmospheric $^{14}C/^{12}C$ ratios were substantially higher than today. Estimates of $F^{14}C$ for wood burning are based on tree-growth models (e.g., Lewis et al., 2004; Mohn et al., 2008) and found to range from 1.08 to 1.30 (Szidat et al., 2006; Genberg et al., 2011; Gilardoni et al., 2011; Minguillón et al., 2011; Dusek et al., 2013). When $F^{14}C$ is measured on OC and EC separately, contributions from non-fossil and fossil sources to carbonaceous aerosols can be separated. Previous ^{14}C measurements of carbonaceous aerosols in China found that EC in urban areas is dominated by fossil sources, which account for 66–87 % of EC mass, whereas OC is more influenced by non-fossil sources with fossil sources accounting for only 35–67 % (Table 1). Despite a fair number of ^{14}C studies in China in recent years, only ~~two~~a few ^{14}C datasets so far reported annual results and seasonal variations of OC and EC (Y. Zhang et al., ~~2014b~~2014a, 2015b, 2017).

In addition to ^{14}C source apportionment, analysis of the stable carbon isotope composition (namely the $^{13}C/^{12}C$ ratio, expressed as $\delta^{13}C$ in Eq. (2)) can provide further information regarding sources and atmospheric processing of carbonaceous aerosol (Bosch et al., 2014; Kirillova et al., 2014b; Andersson et al., 2015; Masalaite et al., 2017). Different emission sources have their ~~distinct~~ own source signature: ~~the $\delta^{13}C$ signature of~~ carbonaceous aerosol~~s~~ from coal combustion is ~~less depleted~~ enriched in ^{13}C (i.e., has higher $\delta^{13}C$ values of ~~$\delta^{13}C$~~~ -25 ‰ to -21 ‰) ~~than~~ compared to aerosol~~those~~ from liquid fossil fuel combustion ~~sources~~ ($\delta^{13}C$ ~ -28 ‰ to -24 ‰) and from burning of C3 plants ~~burning~~ ($\delta^{13}C$ ~ -35 ‰ to -24 ‰) (Andersson et al. (2015) and references therein). Complementing ^{14}C source apportionment with ^{13}C measurements allows a better constraint of the contribution of different emission sources to carbonaceous aerosols (Kirillova et al., 2013, 2014a; Bosch et al., 2014; Andersson et al., 2015; Winiger et al., 2015, 2016; Bikkina et al., 2016, 2017; Yan et al., 2017). For example, EC is inert to chemical or physical transformations, thus the $\delta^{13}C_{EC}$ preserves the signature of emission sources (Huang et al., 2006; Andersson et al., 2015; Winiger et al., 2015, 2016). EC from fossil sources (e.g., coal combustion, liquid fossil fuel burning) can be first separated from biomass burning by $F^{14}C$ of EC. Further, $\delta^{13}C$ of EC allows separation of fossil sources into coal and liquid fossil fuel burning (Andersson et al., 2015; Winiger et al., 2015, 2016), due to their differen~~as they have their own distinct~~ source signatures. Typical $\delta^{13}C$ values for EC from previous studies are summarized in ~~(~~Table S1~~)~~. The

interpretation of the stable carbon isotope signature for OC source apportionment is more difficult, because OC is chemically reactive and $\delta^{13}C$ signatures of OC are not only determined by the source signatures but also influenced by atmospheric processing. During formation of secondary organic aerosol (SOA), molecules depleted in heavy isotopes are expected to react faster, leading to SOA depleted in $\delta^{13}C$ compared to its gaseous precursors, if the precursor is only partially reacted (Anderson et al., 2004; Irei et al., 2006; Fisseha et al., 2009). For example, Irei et al. (2006) found that the $\delta^{13}C$ values of particulate SOA formed by OH radical-induced reactions of toluene ranged from -32.2 ‰ to -32.9 ‰, on average 5.8 ‰ lighter than those of parent toluene, when the 7–29 % toluene was reacted. On the other hand, photochemical aging of particulate organics leads to $\delta^{13}C$ enrichment in the remaining aerosols due to a faster loss of the lighter carbon isotope ^{12}C~~fractionation in the aerosol ^{13}C~~ (Irei et al., 2011; Pavuluri and Kawamura, 2016). For example, Bosch et al. (2014) observed the more enriched $\delta^{13}C$ signature of water-soluble OC (-20.8 ± 0.7 ‰) than EC (-25.8 ± 0.3 ‰) at a receptor station for the South Asian outflow, due to aging of OC during the long-range transport of aerosols.

We present, to the best of our knowledge, the first one-year radiocarbon and stable carbon isotopic measurements to constrain OC and EC sources in China. $PM_{2.5}$ samples were collected at Xi'an (33°29'–34°44' N, 107°40'–109°49' E), one of the most polluted megacities in the world (Zhang and Cao, 2015a). The aims of ~~In this~~this study are: (1) to ~~,~~quantify the contributions from fossil and non-fossil sources to OC and EC ~~are quantified~~ by radiocarbon measurements~~.~~; (2) to further distinguish the ~~Fossil~~ fossil sources of EC ~~are further distinguished~~ into coal and liquid fossil fuel combustion by complementing radiocarbon with stable carbon signature~~.~~; (3) to assess the ~~Sources~~ sources and atmospheric processing of OC ~~are~~ qualitatively ~~assessed by~~ using its stable carbon signature. Further, mass concentrations and source contributions of primary OC are estimated based on the apportioned EC and compared with measured OC mass concentrations and source contributions to give insights into OC sources and formation mechanisms (4).

2 Methods

2.1 Sampling

Sampling was carried out at Xi'an High-Tech Zone (34.23° N, 108.88° E, ~10 m above the ground), on a building rooftop of the Institute of Earth Environment, Chinese Academy of Sciences. The sampling site is surrounded by a residential area ~15 km south of downtown and has no major industrial activities. Details about the sampling site can be found elsewhere (Bandowe et al., 2014; T. Zhang et al., 2014~~a~~).

24 h (from 10:00 a.m. to 10:00 a.m. the next day, local standard time [LST]) $PM_{2.5}$ samples were collected every sixth day from 5 July 2008 to 27 June 2009 using a high-volume sampler (TE-6070 MFC, Tisch Inc., Cleveland, OH, USA) operating at 1.0 m^3 min^{-1}. $PM_{2.5}$ samples were collected on Whatman quartz fiber filters (20.3 cm × 25.4 cm, Whatman QM/A, Clifton, NJ, USA) that were ~~pre-fired~~ pre-baked at 900 °C for 3 h to remove absorbed organic vapors (Watson et al., 2009; Chow et

al., 2010). After sampling, we immediately removed the filter from the sampler. All filters were packed in pre-baked aluminium foils, sealed in polyethylene bags and stored at -18 ºC in a freezer. To be consistent with previous studies (Han et al., 2016; T. Zhang et al., 2014), we designated 15 November to 14 March as winter, 15 March to 31 May as spring, 1 June to 31 August as summer, and 1 September to 14 November as autumn, based on the meteorological characteristics and the typical residential heating period. Fifty-eight $PM_{2.5}$ samples were collected in total, with 13 in spring, 15 in summer, 12 in autumn, and 18 in winter. Six samples with varying $PM_{2.5}$ mass and carbonaceous aerosols loading were selected per season for ^{14}C analysis. We selected the samples carefully to cover periods of low, medium and high $PM_{2.5}$ concentrations to get samples representative of the various pollution conditions that did occur in each season. The 24 selected samples are highlighted in Fig. S1 with their OC and EC concentrations. In total, there are 48 radiocarbon data, including 24 for OC and 24 for EC. Details on sample selection for ^{14}C analysis are presented in Supplemental S1.

2.2 Organic carbon (OC), elemental carbon (EC) and source markers measurement

Filter pieces of 0.5 cm^2 were used to measure OC and EC by a Desert Research Institute (DRI) Model 2001 Thermal/Optical Carbon Analyzer (Atmoslytic Inc., Calabasas, CA, USA) following the IMPROVE_A (Interagency Monitoring of Protected Visual Environments) thermal/optical reflectance (TOR) protocol (Chow et al., 1993, 2007, 2011). Details of the OC/EC measurement were described in Cao et al. (2005). The differences between the replicated analysis for the same sample (n=10) are smaller than 5% for TC, 5% for OC, and 10% for EC, respectively.

Organic makers including levoglucosan, picene and hopanes were quantified using Gas chromatography–mass spectrometry (GC/MS). Water-soluble potassium (K^+) was measured in water extracts using Ion Chromatography (Dionex 600, Thermal Scientific-Dionex, Sunnyvale, CA, USA). Details on the measurements are described in Supplemental S2.

2.3 Stable carbon isotopic ~~isotope (^{13}C) analysis~~ composition of OC and EC

The stable carbon isotopic composition of OC and EC was determined using a Finnigan MAT 251 mass spectrometer with a dual inlet system (Bremen, Germany) at the Stable Isotope Laboratory at the Institute of Earth Environment, Chinese Academy of Sciences. For OC, filter pieces were heated at 375 °C for 3 h in a vacuum-sealed quartz tube in the presence of CuO catalyst grains. The evolved CO_2 from OC was ~~collected~~ isolated by a series of cold traps and quantified manometrically. The stable carbon isotopic composition of the CO_2 was determined as $\delta^{13}C_{OC}$ by offline analysis with a Finnigan MAT-251 mass spectrometer. Extraction of EC was done by heating ~~The~~ the carbon that remained on the filters ~~was combusted~~ at 850 °C for 5 h. The resulting CO_2 was purified in cold traps and then ~~and~~ quantified as the EC fraction. The isotopic ratios of the purified CO_2 of EC were measured and determined as $\delta^{13}C_{EC}$. A routine laboratory work standard with a known $\delta^{13}C$ value was measured every day. The quantitative levels of ^{13}C and ^{12}C isotopes were characterized using a ratio of peak intensities of m/z 45 ($^{13}C^{16}O_2$) and 44 ($^{12}C^{16}O_2$) in the mass spectrum of CO_2. Samples were analysed at least in

duplicate, and all replicates showed differences less than 0.3 ‰. $\delta^{13}C$ values are reported in the delta notation as per mil (‰) differences with respect to the international standard Vienna Pee Dee Belemnite (V-PDB):

$$\delta^{13}C\ (‰) = \left[\frac{(^{13}C/^{12}C)_{sample}}{(^{13}C/^{12}C)_{V-PDB}} - 1\right] \times 1000, \quad (2)$$

V-PDB is the primary reference material for measuring natural variations of ^{13}C isotopic content. It is composed of calcium carbonate from a Cretaceous belemnite rostrum of the Pee Dee Formation in South Carolina, USA. Its absolute isotope ratio $^{13}C/^{12}C$ (or $(^{13}C/^{12}C)_{V\text{-}PDB}$) is 0.0112372, and established as $\delta^{13}C$ value = 0. Details of stable carbon isotope measurements are described by our previous studies~~elsewhere~~ (Cao et al., 2008, 2011, 2013).

2.4 Radiocarbon (^{14}C) measurement of OC and EC

Combustion of OC, EC and standards OC and EC were extracted separately by our aerosol combustion system (ACS) (Dusek et al., 2014). In brief, the ACS consists of a combustion tube, where aerosol filter pieces are combusted at different temperatures in pure O_2, and a purification line where the resulting CO_2 is isolated and separated from other gases, such as water vapor and NO_x. The purified CO_2 is then stored in flame-sealed ampoules until graphitization.

OC is combusted by heating filter pieces at 375 °C for 10 min. EC is combusted after complete OC removal. To remove OC completely, water-soluble OC is first removed from the filter by water extraction (Dusek et al., 2014) to minimize charring of organic material (Yu et al., 2002). Subsequently, most water-insoluble OC is removed by heating the filter pieces at 375 °C for 10 min. Then the oven temperature is increased to 450 °C for 3 min, and in this step a mixture of the most refractory OC and less refractory EC is removed from the filter. The remaining EC is then combusted by heating at 650 °C for 5 min (Zenker et al., 2017).

Two standards with known ^{14}C content are combusted~~analyzed~~ as quality control for the combustion process: an oxalic acid standard and a graphite standard. Small amounts of solid~~The~~ standard materials are directly put on the filter holder of the combustion tube and heated at 650 °C for 10 min. In the further ^{14}C analysis, the CO_2 derived from combustion of the standards is treated exactly like the samples. Therefore, t~~T~~he contamination introduced by the combustion process can be estimated from the deviation of measured values from the nominal values of the standards. The contamination is below 1.5 µgC per combustion, which is relatively small compared the samples ranging between 50 and 270 µgC in this study.

^{14}C analysis of OC and EC Graphitization and AMS measurements were conducted at the Centre for Isotope Research (CIO) at the University of Groningen. The extracted CO_2 is reduced to graphite by reaction with H_2 (g) at a molecular ratio H_2/CO_2 of 2 using a porous iron pellet as catalyst at 550 °C (de Rooij et al., 2010). The water vapor from the reduction reaction is cryogenically removed using Peltier cooling elements. The yield of graphite is higher than 90 % for samples of >50 µgC. Graphite formed on the iron pellet is then pressed into a 1.5 mm target holder, which is introduced into the AMS system for

subsequent measurement. The AMS system (van der Plicht et al., 2000) is dedicated to ^{14}C analysis, and simultaneously measures $^{14}C/^{12}C$ and $^{13}C/^{12}C$ ratios.

Varying amounts of reference materials covering the range of sample mass are graphitized and analyzed together with samples in the same wheel of AMS. Two such materials with known ^{14}C content are used: the oxalic acid OXII calibration material ($F^{14}C$ = 1.3406) and a ^{14}C-free CO_2 gas ($F^{14}C$ = 0). The differences between measured and nominal $F^{14}C$ values are used to correct the sample values (de Rooij et al., 2010; Dusek et al., 2014) for contamination during graphitization and AMS measurement (Supplemental S3). The modern carbon contamination is between 0.35 and 0.50 µg C, and the fossil carbon contamination is around 2 µg C for samples bigger than 100 µgC. ~~The contamination is typically smaller than 2 µgC (Prokopiou, 2010).~~

2.5 Source apportionment methodology using ^{14}C

$F^{14}C$ of EC ($F^{14}C_{(EC)}$) was converted to the fraction of biomass burning (f_{bb}(EC)) by dividing with $F^{14}C$ of biomass burning ($F^{14}C_{bb}$ = ~~the conversion factor of~~ 1.10 ± 0.05 ~~;for EC (~~ Lewis et al., 2004; Mohn et al., 2008; Palstra and Meijer, 2014) given that biomass burning is the only non-fossil source of EC, to eliminate the effect from nuclear bomb tests in the 1960s. EC is primarily produced from biomass burning (EC_{bb}) and fossil fuel combustion (EC_{fossil}), and absolute EC concentrations from each source can be estimated once f_{bb}(EC) is known:

$$EC_{bb} = EC \times f_{bb}(EC), \quad (3)$$

$$EC_{fossil} = EC - EC_{bb}, \quad (4)$$

Analogously, $F^{14}C$ of OC ($F^{14}C_{(OC)}$) was converted to the fraction of non-fossil (f_{nf}(OC)) by dividing the $F^{14}C$ of non-fossil sources including both biogenic and biomass burning ($F^{14}C_{nf}$=1.09 ± 0.05; ~~conversion factor of 1.09 ± 0.05 for OC (~~Lewis et al., 2004; Levin et al., 2010; Y. Zhang et al., 2014~~ab~~). The lower limit of 1.04 corresponds to current biospheric sources as the source of OC, the upper limit corresponds to burning of wood as the main source of OC, with only little input from annual crops. OC can be apportioned between OC from non-fossil sources (OC_{nf}) and from fossil-dominated combustion sources (OC_{fossil}) using f_{nf}(OC):

$$OC_{nf} = OC \times f_{nf}(OC), \quad (5)$$

$$OC_{fossil} = OC - OC_{nf}, \quad (6)$$

A Monte Carlo simulation with 10,000 individual calculations was conducted to propagate uncertainties. For each individual calculation, $F^{14}C_{(OC)}$, $F^{14}C_{(EC)}$, and OC, EC concentrations are randomly chosen from a normal distribution symmetric around the measured values with the experimental uncertainties as standard deviation. Random values for conversion factors are chosen from a triangular frequency distribution with its maximum at the central value, and is 0 at the lower limit and upper

limit. In this way 10,000 different estimation of f_{bb}(EC), f_{nf}(OC), EC_{bb}, EC_{fossil}, OC_{nf} and OC_{fossil} can be calculated. The derived average represents the best estimate, and the standard deviation represents the combined uncertainties.

2.6 Source apportionment of EC using Bayesian statistics

$F^{14}C$ and $\delta^{13}C$ signatures of EC and a mass-balance calculation were used in combination with a Bayesian Markov chain Monte Carlo (MCMC) scheme to further constrain EC sources into biomass burning (f_{bb}), liquid fossil combustion ($f_{liq.fossil}$), and coal combustion (f_{coal}):

$$F^{14}C_{(EC)} = F^{14}C_{bb} \times f_{bb} + F^{14}C_{liq.fossil} \times f_{liq.fossil} + F^{14}C_{coal} \times f_{coal}, \quad (7)$$

$$f_{bb} + f_{liq.fossil} + f_{coal} = 1, \quad (8)$$

$$\delta^{13}C_{EC} = \delta^{13}C_{bb} \times f_{bb} + \delta^{13}C_{liq.fossil} \times f_{liq.fossil} + \delta^{13}C_{coal} \times f_{coal}, \quad (9)$$

where f represents the fraction of EC mass contributed by a given source, and subscripts denote investigated sources, where "$_{bb}$" denotes biomass burning, "$_{liq.fossil}$" is liquid fossil, and "$_{coal}$" is fossil coal. $F^{14}C_{(EC)}$ is included in this model which allows separating the input from biomass (f_{bb}) from fossil sources ($f_{liq.fossil}$ and f_{coal}). $F^{14}C_{bb}$ is the $F^{14}C$ of biomass burning (1.10 ± 0.05 as mentioned~~, the conversion factor for EC~~ in Sect. 2.5). $F^{14}C_{liq.fossil}$ and $F^{14}C_{coal}$ is zero due to the long-time decay. $\delta^{13}C_{bb}$, $\delta^{13}C_{liq.fossil}$ and $\delta^{13}C_{coal}$ are the $\delta^{13}C$ signature emitted from biomass burning, liquid fossil fuel combustion and coal combustion, respectively. The means and the standard deviations for $\delta^{13}C_{bb}$ (-26.7 ± 1.8 ‰ for C3 plants, and -16.4 ± 1.4 ‰ for corn stalk), $\delta^{13}C_{liq.fossil}$ (-25.5 ± 1.3 ‰) and $\delta^{13}C_{coal}$ (-23.4 ± 1.3 ‰) are presented in Table S1 (Andersson et al., 2015 and reference therein; Sect. 4.3.1), and serves as input of MCMC. The source endmembers for $\delta^{13}C$ are less well-constrained than for $F^{14}C$, as $\delta^{13}C$ varies with fuel types and combustion conditions. For example, the range of possible $\delta^{13}C$ values for liquid fossil fuel combustion overlaps to a small extent with the range for coal combustion, although liquid fossil fuels are usually more depleted than coal. The MCMC technique takes into account the variability in the source-signatures of $F^{14}C$ and $\delta^{13}C$ (Table S1), where $\delta^{13}C$ introduces a larger uncertainty than $F^{14}C$. Uncertainties of both source endmembers for each source and the measured ambient $\delta^{13}C_{EC}$ and $F^{14}C_{(EC)}$ are propagated.

MCMC-driven Bayesian approaches have been recently implemented to account for multiple sources of uncertainties and variabilities for isotope-based source apportionment applications (Parnell et al., 2010; Andersson, 2011). MCMC works by repeatedly guessing the values of the source contributions and find those values, which fit the data best. The initial guesses are usually poor and are discarded as part of an initial phase known as the burn-in. Subsequent iterations are then stored and used for the posterior distribution. MCMC was implemented in the freely available R software (https://cran.r-project.org/), using the *simmr* package (https://CRAN.R-project.org/package=simmr). Convergence diagnostics were created to make sure the model has converged properly. The simulation for each sample was run with 10,000 iterations, using a burn-in of 1000 steps, and a data thinning of 100.

3 Results

3.1 Temporal variation of OC and EC mass concentrations

During the sampling period, extremely high OC and EC mass concentrations were sometimes observed (Fig. S1). OC mass concentrations ranged from 3.3 μg m^{-3} to 67.0 μg m^{-3}, with an average of 21.5 μg m^{-3}. EC mass concentrations ranged from 2 μg m^{-3} to 16 μg m^{-3}, with an average of 7.6 μg m^{-3} (Table S2). OC and EC mass concentrations were comparable to those reported values in previous studies for Xi'an, which had an average of 19.7 ± 10.7 μg m^{-3} (average ± standard deviation) OC and 8.0 ± 4.7 μg m^{-3} EC from March, 2012 to March, 2013 (Han et al., 2016).

OC and EC concentrations showed a clear seasonal variation with higher concentrations in cold period than those in warm period. The differences between winter and summer concentrations were significant (p<0.05). The mean winter to summer concentration ratios were 3 for OC and 1.5 for EC. Similar seasonal trends of OC and EC were also observed in Xi'an, China in earlier studies (e.g., Han et al. (2016) and Niu et al. (2016)).

3.2 Temporal variation of fossil and non-fossil fractions of OC and EC

To investigate the sources of OC and EC, twenty-four samples representing different loadings of carbonaceous aerosols from different seasons were selected for radiocarbon measurement (Supplemental S1, Fig. S2, Table S3). The highest biomass burning contribution to EC (f_{bb}(EC)) of 46 % was detected on 25 January 2009 (Fig. 1(a)). This can be related to enhanced biomass burning emissions indicated by the comparably high biomass-indicative levoglucosan/EC ratio, and relatively low fossil-fuel associated Σhopanes/EC ratio, picene/EC ratio (Supplemental S2 and Fig. S3), along with unfavorable meteorological condition (e.g., substantially low wind speed (~1 m/s) and low temperature (-0.5 °C)). The highest non-fossil contribution to OC (f_{nf}(OC)) of 70 % was observed on the same day. Note that 25 January 2009 was the Chinese New Year eve with many fireworks. Since the influence of fireworks on $F^{14}C$ signature is not known yet, the following source apportionment will not include the Chinese New Year eve.

EC is predominantly influenced by fossil sources, with relative contribution of fossil fuel to EC (f_{fossil}(EC)) ranging from 71 % to 89 %, with an annual average of 83 ± 5 %. Lower f_{fossil}(EC) were observed in winter (77 ± 5 %) compared with other seasons. This is due to the substantial contribution from biomass burning to EC in winter, with a larger f_{bb}(EC) in winter (23 ± 5 %) than other seasons (14 ± 2 %, 16 ± 1 % and 18 ± 5 % in summer, spring and autumn, respectively; Fig. 1(a)). This is consistent with the evaluated levoglucosan/EC ratios observed in winter (96 ng/μg), 1.6 times higher than that of yearly average (Fig. S3). Lowest f_{bb}(EC) in summer (14 ± 2 %) suggests the importance of fossil fuel sources for EC concentrations. Since the residential usage of coal in summer is much reduced compared with other seasons, we can expect higher contribution from vehicle emissions than coal burning to fossil EC in summer. EC concentrations from fossil fuel (EC_{fossil}) varied by a factor of 4, ranging from 3.1 μg m^{-3} to 11.6 μg m^{-3} with a mean of 6.7 ± 2.0 μg m^{-3}, which was 4 times higher than averaged biomass-burning EC concentrations (EC_{bb} = 1.5 ± 0.9 μg m^{-3}). A stronger variation was observed in the

EC_{bb}, varying 9-fold from 0.5 μg m^{-3} to 4.7 μg m^{-3} (Table S4, Table S5).

The relative contribution of non-fossil sources to OC (f_{nf}(OC)) ranged from 31 % to 66 %, with an annual average of 54 ± 8 %, which is larger than that to EC (yearly average of 17 ± 5 %). Higher f_{nf}(OC) was observed in winter (62 ± 5 %) and autumn (57 ± 4 %), compared to summer and spring, when about half of OC was contributed by non-fossil sources (48 ± 3 % and 48 ± 8 %, respectively. Table S5). The lowest f_{nf}(OC) of 31 % was detected on 28 April 2009 (Fig. 1(b)), caused by the enhanced fossil emissions indicated by the highest Σhopanes/EC ratios (5 ng/μg. Fig. S3). Averaged OC concentrations from non-fossil sources (OC_{nf}) were 12 ± 10 μg m^{-3}, ranging from 2.3 μg m^{-3} to 38.6 μg m^{-3}. OC concentrations from fossil sources (OC_{fossil}) varied from 3.2 μg m^{-3} to 20.4 μg m^{-3}, with an average of 9.0 ± 4.8 μg m^{-3}. Clear seasonal variations were seen in OC concentrations both from fossil fuel and non-fossil sources, with maxima in winter (OC_{fossil} = 13.2 ± 6.0 μg m^{-3}, OC_{nf} = 23.3 ± 13.3 μg m^{-3}) and minima in summer (OC_{fossil} = 5.5 ± 1.0 μg m^{-3}, OC_{nf} = 5.1 ± 1.4 μg m^{-3}), because of enhanced fossil and non-fossil activities in winter, mainly biomass burning and domestic coal burning (Cao et al., 2009, 2011; Han et al., 2010, 2016).

3.3 ^{13}C signature of OC and EC

The $\delta^{13}C_{EC}$ preserves the signature of emission sources, as EC is inert to chemical or physical transformations (Huang et al., 2006; Andersson et al., 2015; Winiger et al., 2015, 2016). Major EC sources in Xi'an include biomass burning, coal combustion, and liquid fossil fuel (e.g., diesel and gasoline) combustion (i.e., vehicular emissions)~~(e.g., diesel and gasoline)~~ (Cao et al., 2005, 2009, 2011; Han et al., 2010; Wang et al., 2016). C3 plants and C4 plants, biomass subtypes, have a different $\delta^{13}C$ signature. Aerosols from burning C4 plants are more enriched in $\delta^{13}C$ (-16.4~~5~~ ± 1.4 ‰) than that of C3 plants (-26.7 ± 1.8 ‰, Table S1). C3 plants are the dominant biomass type (e.g., wood, wheat straw etc.) in North China (Cheng et al., 2013; Cao et al., 2016). This is also evident from our observation that $\delta^{13}C$ values of the ambient aerosol fall within the range of C3 plants, coal and liquid fossil fuel combustion (i.e., vehicular emissions) (Fig. 2).

The annually averaged $\delta^{13}C_{EC}$ is -24.9~~2~~ ± 1.1~~4~~ ‰, varying between -26.5~~0~~ ‰ and -22.8~~1~~‰. Considerable seasonal variation is observed, suggesting a shift among combustion sources. The $\delta^{13}C_{EC}$ signature for winter (-23.2~~0~~ ± 0.~~35~~ 4 ‰) clearly locates in the $\delta^{13}C$ range for coal combustion (-23.~~38~~ 4 ± 1.3 ‰, Table S1), and is more enriched compared to other seasons. This indicates a strong influence of coal combustion in winter, but the ^{14}C values indicate that coal combustion cannot be the only source of EC. Moreover, the $\delta^{13}C_{EC}$ values in winter ranging from -23.7~~2~~ ‰ to -22.8~~1~~ ‰ are at the higher (i.e., enriched) end of coal combustion, indicating some additional contributions from C4 plants, such as corn stalk burning. In northern China, large quantities of coal are used for heating during a formal residential "heating season" in winter (Cao et al., 2007), and in rural Xi'an, burning corn stalk (C4 plant) in "Heated Kang" (Zhuang et al., 2009) is a traditional way for heating in winter (Sun et al., 2017). The most depleted $\delta^{13}C_{EC}$ values in summer (-25.9~~4~~ ± 0.~~46~~ 5 ‰) and spring (-25.4~~0~~ ± 0.3~~3~~ ‰) falls into the overlap of liquid fossil fuel emission (-25.5 ± 1.3 ‰) and C3 plant combustion (-26.7 ± 1.8 ‰, Fig. 2), when little or

no coal is used for residential heating but has some coal emissions from industries. As the biomass burning contribution to EC in summer and spring is relatively low (14 ± 2% and 16 ± 1%, respectively), we can expect liquid fossil fuel combustion dominates EC emissions. $\delta^{13}C_{EC}$ signatures in autumn (-25.14 ± 0.66 7 ‰) fall in the overlapped area of C3 plant, liquid fuel and coal, implying EC is influenced by the mixed sources.

$\delta^{13}C_{OC}$ was in general similar to $\delta^{13}C_{EC}$. This suggests that biogenic OC is probably not very important, as could be expected from the high TC concentrations. ^{14}C analysis indicates a considerably higher fraction of non-fossil OC than non-fossil EC, and it would seem that this is mainly related to the biomass burning, which has higher OC/EC ratios than fossil fuel burning. If the contribution of biogenic OC plays an important role, then the biogenic $\delta^{13}C$ signatures should be relatively similar to the source mixture of EC, which is rather unlikely, especially as this source mixture is not constant. $\delta^{13}C_{OC}$ it varies from -27.42 ‰ to -23.23 ‰, with an annual average of -25.32 ± 1.19 2 ‰ (Fig. 2). This range overlaps with C3 plants, liquid fossil and coal combustion. Influence from marine sources (-21 ± 2 ‰; Chesselet et al., 1981; Miyazaki et al., 2011) should be minimal, as Xi'an is a far inland city in China. $\delta^{13}C_{OC}$ shows a similar seasonal variation pattern as $\delta^{13}C_{EC}$. $\delta^{13}C_{OC}$ is most enriched in winter (-24.13 ± 0.83 ‰), followed by autumn (-24.85 9 ± 0.79 8 ‰), summer (-25.73 ± 0.90 ‰), and spring (-26.58 6 ± 0.57 6 ‰). In addition to source mixtures, atmospheric processing also influences $\delta^{13}C_{OC}$ (Irei et al., 2006, 2011; Fisseha et al., 2009). In spring, $\delta^{13}C_{OC}$ is much more depleted than $\delta^{13}C_{EC}$ (1.1−2.4 ‰), indicating the importance of secondary formation of OC (e.g., from volatile organic compound precursors) in addition to primary sources (Anderson et al., 2004; Iannone et al., 2010). In summer and autumn 2008, $\delta^{13}C_{OC}$ was very similar to $\delta^{13}C_{EC}$ (Table S3), and showed strong correlations (r^2 = 0.90), indicating that OC originates from a similar source mixture as EC. There are no depleted $\delta^{13}C_{OC}$ values in summer and autumn as would be expected from significantdue to the secondary OC formation. In summer this could be t is partially due to the high temperature: (i) high temperature favors equilibrium shifts to the gas phase, and the formed SOA less efficiently partitions to the particle phase; (ii) aging processes also intensifyerease which causes enriched $\delta^{13}C_{OC}$ in the particle phase. This is further discussed in Sect. 4.45.

4 Discussion

4.1 Aerosol characteristics in Xi'an compared to other Chinese cities

There are few annual ^{14}C measurements in China (Table 1). The annual average f_{fossil}(EC) derived from ^{14}C data in Xi'an is 83 %. This falls in the range of annual f_{fossil}(EC) measured in China, depending on the location. Comparable annual f_{fossil}(EC) was reported at an urban site of Beijing (79 ± 6% (Zhang et al., 2015b); 82% ± 7% (Zhang et al., 2017)) and a background receptor site of Ningbo (77 ± 15% (Liu et al., 2013)). Much lower f_{fossil}(EC) was found at a regional background site in Hainan (38 ± 11 % (Y. Zhang et al., 2014b2014a)). The big differences between the two background sites are due to different air-mass transport to the receptor site. The background site in Ningbo was more often influenced by air-masses transported from highly urbanized regions of East China associated with lots of fossil-fuel combustion, whereas the

decreased fossil contribution observed in Hainan could be attributed to enhanced open burning of biomass in Southeast Asia or Southeast China.

In this study, f_{fossil}(EC) was lowest in winter (77 %). This is comparable with previously reported f_{fossil}(EC) at the same sampling site during winter 2013 (78 ± 3 % (Zhang et al., 2015a)), Shanghai (79 ± 4 %, Zhang et al., 2015a), Wuhan (74 ± 8 % (Liu et al., 2016b)), North China Plain (73–75 %, Andersson et al., 2015) and Guangzhou (71 ± 10 %, J. Liu et al., 2014b). Higher f_{fossil}(EC) in winter are reported in Beijing (80–87%, Sun et al., 2012; 83 ± 4 %, Chen et al., 2013), Xiamen (87 ± 3 %, Chen et al., 2013). Lower winter f_{fossil}(EC) was observed in Guangzhou (69 %, Zhang et al., 2015a), Yangtze River Delta (66–69 %, Andersson et al., 2015), and Pearl River Delta (67–70 %, Andersson et al., 2015), indicating different influence of biomass burning emissions over China during winter. ^{14}C measurements in other seasons are still very scarce in China.

The annual average f_{fossil}(OC) in Xi'an is 46%, with the lowest values in winter (38 %) and the highest in summer (52 %). The annual average f_{fossil}(OC) in this study is comparable to the results found in an urban site of Beijing (48 ± 12 %) (Zhang et al., 2017), but higher than 19 ± 10 % at a background site of Hainan (Y. Zhang et al., 2014b2014a). Similar contributions from fossil sources to OC were reported for the same sampling site at Xi'an in winter 2013 (38 ± 3%, Zhang et al., 2015a), Wuhan in January 2013 (38 ± 5 %, Liu et al., 2016b), and Guangzhou in winter 2012/2013 (37 ± 4 %, J. Liu et al., 2014b). A higher fossil contribution to OC was found in Beijing with f_{fossil}(OC) of 58 ± 5 % in winter 2013 and 59 ± 6 % in winter 2013/2014 (Zhang et al., 2015a, 2017), and in Shanghai with f_{fossil}(OC) of 49 ± 2 % in winter 2013 (Zhang et al., 2015a)). Previous studies in Beijing observed different seasonal trends, with higher contribution by fossil sources in winter (higher f_{fossil}(OC)) than in other seasons (Yan et al., 2017; Zhang et al., 2017). This is consistent with findings by online aerosol mass spectrometer analysis in winter 2013/2014 (Elser et al., 2016), where organic matter in Xi'an was found to be dominated by biomass burning, in contrast to Beijing where it is dominated by coal burning. This implies different pollution patterns over Chinese cities.

The $\delta^{13}C_{EC}$ is most enriched in winter (-23.20 ± 0.35 4 ‰), and most depleted in summer (-25.94 ± 0.46 5 ‰). This is consistent with previous studies in northern China, with the winter-to-summer difference ranging from 0.76 to 2.79 ‰ for all the 7 northern Chinese cities (e.g., Cao et al., 2011; Table S8S6), supporting the important influence on EC from coal combustion in winter. By contrast, no notable difference between winter and summer $\delta^{13}C_{EC}$ is reported in southern China, where there is no official heating season. (e.g., Ho et al., 2006; Cao et al., 2011; Table S8S6). $\delta^{13}C_{OC}$ showed a seasonal variation pattern similar to $\delta^{13}C_{EC}$. $\delta^{13}C_{OC}$ is most enriched in winter (-24.13 ± 0.83 ‰), comparable with previously reported winter data in North China, for example Beijing (-24.26 ± 0.29 ‰) by Yan et al. (2017), and seven northern cities in China (-25.54 ‰ to -23.08 ‰) by Cao et al. (2011), but our winter $\delta^{13}C_{OC}$ is more enriched than those found in South China, for example Hong Kong (-26.9 ± 0.6 ‰) by Ho et al. (2006), and seven southern cities in China (-26.62 ‰ to -25.79 ‰) by Cao et al. (2011) (Table S8S6). The differences in North and South China reveal the influence from coal burning to OC.

4.2 Correlations between $F^{14}C_{(EC)}$ and biomass burning markers

In ^{14}C-based source apportionment, biomass burning is considered the only source of non-fossil EC. Here we evaluate $F^{14}C_{(EC)}$ with other biomass burning markers, including levoglocosan and water-soluble potassium (K^+). In summer, a very strong positive correlation (r^2 = 0.98) was found between $F^{14}C_{(EC)}$ and K^+/EC ratios, in contrast to the significant negative correlation (r^2 = 0.96) between $F^{14}C_{(EC)}$ and levoglucosan/EC ratios (Fig. ~~6~~3). Previous studies have found that burning of crop residues emitted more K^+ than levoglucosan, with significantly lower levoglucosan/K^+ ratios than burning of wood (Cheng et al., 2013; Zhu et al., 2017). The levoglucosan/K^+ ratio for wood is ~~23.96~~24.0 ± 1.8~~2~~, much higher than those for crop residues (0.10 ± 0.00 for wheat straw, 0.21 ± 0.08 for corn straw, 0.62 ± 0.32 for rice straw) (Cheng et al., 2013). Emissions from crop residue burning therefore increase both the fraction of EC from non-fossil sources and K^+. This results in a positive correlation between K^+/EC ratios and $F^{14}C_{(EC)}$. At the same time emissions from crop residue burning contain relatively little levoglucosan and atmospheric levoglucosan concentrations are expected to be dominated by wood burning emissions. If wood burning emissions stay relatively constant, an increase in crop burning emissions will increase EC concentrations, but have little effect on levoglucosan concentrations, leading to lower levoglucosan/EC ratios. The significant positive correlation of $F^{14}C_{(EC)}$ with K^+ /EC ratios coinciding with a negative correlation of $F^{14}C_{(EC)}$ with levoglucosan/EC ratios in summer therefore suggests strong impacts from crop residues burning and little influence from wood burning on the variability of EC. Variable crop burning activities superimposed on a relatively constant background contribution from wood burning can explain the observed correlations. In summer, extensive open burning in croplands is also detected in the MODIS fire counts map (NASA, 2017) (Fig. ~~S10~~S4), when farmers in the surrounding area of Xi'an (i.e., Guanzhong Plain) burned crop residues in fields. No significant correlations of $F^{14}C_{(EC)}$ with K^+/EC or levoglucosan/EC were found in other seasons (Fig. ~~S11~~S5), suggesting a changing mixture of ~~both~~ biomass subtypes with different levoglucosan/K^+ ratios. In this case, the same amount of modern carbon contribution in EC (i.e., same $F^{14}C_{(EC)}$) can be associated with very different K^+/EC and levoglucosan/EC ratios, depending on which type of biomass is dominating at a given time.

~~3.4~~ 4.3 $\delta^{13}C/F^{14}C$-based statistical source apportionment of EC

Figure ~~3~~ 4 shows ^{14}C-based f_{fossil}(EC) against $\delta^{13}C_{EC}$ together with the isotopic signature of their source endmembers. The source endmembers for $\delta^{13}C$ are less well constrained than for ^{14}C. For example, $\delta^{13}C$ values for liquid fossil fuel combustion overlaps with $\delta^{13}C$ values for both coal and C3 plant combustion. In contrast to $\delta^{13}C$, f_{bb} and f_{fossil} are clearly different and the uncertainties in the endmembers are related to the combined uncertainties of ^{14}C measurements and the factor used to eliminate the bomb test effect ($F^{14}C_{bb}$, see Sect. 2.5). All data points fall reasonably well within the "source triangle" of C3 plant, liquid fossil fuel (e.g., traffic or vehicular emission) and coal combustion, except that $\delta^{13}C_{EC}$ in winter are on the higher (i.e., enriched) end of coal combustion, indicating possible influence of C4 plants combustion as discussed above in Sect. 3.3.

~~3.4.1~~4.3.1 Selection of $\delta^{13}C$ endmembers for ~~C4 plants~~aerosols from corn stalk burning in the study area

To incorporate possible contribution from C4 plants into the source apportionment, we need to estimate the $\delta^{13}C$ signature of aerosols emitted by C4 biomass burning. Corn stalk is the dominant C4 plant in Xi'an and its surrounding areas (Guanzhong Plain), with little sugarcane and other C4 plants (Sun et al., 2017; Zhu et al., 2017). Estimates of $\delta^{13}C$ of corn stalk burning emissions range from -19.3 ‰ to -13.6 ‰ (Chen et al., 2012; Kawashima and Haneishi, 2012; G. Liu et al., 2014~~a~~; Guo et al., 2016). $\delta^{13}C$ values of aerosols from corn stalk burning were compiled from literature (Fig. ~~S4~~S6). The mean was computed as the average of the different data sets, and standard deviation analogously calculated. $\delta^{13}C$ source signatures for corn stalk burning are -16.4 ± 1.4 ‰ (Fig. ~~S4~~S6).

~~3.4.2~~4.3.2 Influence of C4 biomass on EC source apportionment

Bayesian Markov chain Monte Carlo techniques (MCMC) were used to account for the variability of the isotope signatures from the different sources (Andersson et al., 2015; Winiger et al., 2015; Fang et al., 2017). Results from a four-source (C3 biomass, C4 biomass, coal and liquid fossil fuel) MCMC4 model and a three-source (C3 biomass, coal and liquid fossil fuel) MCMC3 model were compared to underscore the influence of C4 biomass on source apportionment. The results of the Bayesian calculations are the posterior probability density functions (PDF) for the relative contributions from the sources (Fig. ~~S5~~S7, Fig. ~~S6~~S8). For MCMC4, we did a posteriori combination of PDF for C3 biomass and C4 biomass, and named the combined PDF as biomass burning, to better compare results with MCMC3.

To estimate seasonal source contributions to EC, we combined all the data points from each season in the MCMC calculations. Yearly source apportionment was conducted by combining all the data points, to improve the precision of the estimated source contributions. The median was used to represent the best estimate of the contribution of any particular source to EC. Uncertainties of this best estimate are expressed as interquartile range and 95 % range of corresponding PDF. For both MCMC4 and MCMC3, the MCMC-derived fraction of biomass burning EC (f_{bb}, median with interquartile range calculated by Eq. (7)) is similar to that obtained from radiocarbon data (f_{bb}(EC), median with one standard deviation by Eq. (3)) as both of them are well-constrained by $F^{14}C$ (Table 2, Table S5, Table ~~S6~~S7, Fig. ~~S7~~S9). Compared to MCMC4, MCMC3 overestimated the contributions from coal combustion, and underestimated the contributions from liquid fossil fuel combustion (Fig. 45). In MCMC3, the $\delta^{13}C$ signature for biomass burning ($\delta^{13}C_{bb}$) is taken from C3 plants only (-26.7 ± 1.8 ‰), and is therefore more depleted compared the $\delta^{13}C_{bb}$ of combined C3 (-26.7 ± 1.8 ‰) and C4 (-16.4 ± 1.4 ‰) signatures in MCMC4. With the same f_{bb} in both MCMC3 and MCMC4, MCMC3 calculations apportion a bigger fraction of EC to $\delta^{13}C$-enriched coal combustion in order to explain the enriched winter $\delta^{13}C_{EC}$. As a result, MCMC3-derived contributions of liquid fossil fuel combustion to EC was only 14 % in winter, 5 times ~~less~~ lower than in summer. This implies the absolute EC concentrations from liquid fossil fuel combustion were much smaller in winter than in summer, considering that the total EC concentrations in winter were only 1.5 times higher than that in summer. This is inconsistent with our expectation that absolute EC concentrations from liquid fossil fuel combustion should be roughly constant all over the year, or even higher in

winter due to unfavourable meteorological conditions. If we do not include C4 biomass in calculation, coal combustion contributions will be overestimated, and combustion of liquid fossil fuel be underestimated, especially in winter when $\delta^{13}C_{EC}$ are most enriched combined with highest contribution from biomass burning.

MCMC4 calculations reveal that on a yearly average the highest contribution to EC is from liquid fossil sources (median, 72 %; interquartile range, (65−77 %); Table 2), followed by biomass burning (17 %, 16−18 %), and coal combustion (11 %, 6–18 %). However, source patterns changed substantially between different seasons. Coal combustion was the dominant contributor to EC concentrations in winter, with a median of 45 % (29–58 %). Contrary to winter, EC in other seasons was mainly derived from liquid fossil usage, accounting for 67 % (56–74 %), 71 % (63–77 %) and 77 % (71–82 %) of EC in autumn, spring, and summer, respectively. The larger contribution from coal combustion in winter was associated with the extensive coal use for residential heating and cooking in Xi'an, in addition to contributions from coal-fired industries and power plants. This is in line with the findings from $\delta^{13}C$ results. We consider that EC from coal-fired industries and power plants are much lower than that from residential coal combustion, because they have high combustion efficiency and widely-used dust removal facilities. For example, a previous study reported that EC emission factors (emitted EC amount per kg fuel) from residential coal combustion are up to 3 orders of magnitudes higher than those from industries and power plants (Zhang et al., 2008). However, relative contributions from fossil combustion ($f_{coal} + f_{liq.fossil}$) were on average lower in winter than in other seasons (warm period), implying that contributions from biomass burning were also important for the EC increment in winter. By subtracting mean EC_{bb} and EC_{fossil} in the warm period from those in winter, the excess EC_{bb} and EC_{fossil} was 1.2 μg m^{-3} and 0.8 μg m^{-3}, respectively. Biomass burning contributed on average 60 % of EC increment in winter.

~~3.5~~ 4.4 Estimating mass concentrations and sources of primary OC

Comparing concentrations and sources of primary OC to total OC can give insights into the importance of secondary formation and other chemical processes, such as photochemical loss mechanisms. Based on the EC concentrations from biomass, coal, and liquid fossil fuel combustion derived from MCMC4 model, the total primary OC mass concentrations due to these three major combustion sources can be estimated ($OC_{pri,e}$; OC primary, estimated). The respective EC concentrations apportioned to each source are multiplied by the characteristic primary OC/EC ratios for each source (Eq. (10)). The non-fossil fraction (i.e., biomass burning) in $OC_{pri,e}$ ($f_{bb}(OC_{pri,e})$) is approximated by Eq. (11):

$$OC_{pri,e} = POC_{bb,e} + POC_{coal,e} + POC_{liq.fossil,e} = \left(r_{bb} \times f_{bb} + r_{coal} \times f_{coal} + r_{liq.fossil} \times f_{liq.fossil}\right) \times EC, \quad (10)$$

$$f_{bb}\left(OC_{pri,e}\right) = \frac{POC_{bb,e}}{OC_{pri,e}} = \frac{r_{bb} \times f_{bb}}{r_{bb} \times f_{bb} + r_{coal} \times f_{coal} + r_{liq.fossil} \times f_{liq.fossil}}, \quad (11)$$

where $POC_{bb,e}$, $POC_{coal,e}$, and $POC_{liq.fossil,e}$ are estimated primary OC mass concentrations from biomass burning, coal combustion and liquid fossil fuel combustion, respectively. r_{bb}, r_{coal}, and $r_{liq.fossil}$ are OC/EC ratios for primary emissions from biomass burning, coal combustion, and liquid fossil fuel combustion, respectively. The selection of r_{bb} (5 ± 2), r_{coal} (2.38 ± 0.44), and $r_{liq.fossil}$ (0.85 ± 0.16) is done by literature searches and described in Supplemental ~~S3~~S4. f_{bb}, f_{coal}, and $f_{liq.fossil}$ are the

relative contribution to EC from combustion of biomass, coal, and liquid fossil fuel derived from MCMC4 model. EC denotes EC mass concentrations (μg m^{-3}).

A Monte Carlo simulation with 10,000 individual calculations of $OC_{pri,e}$ and $f_{bb}(OC_{pri,e})$ was conducted to propagate uncertainties. For each individual calculation input, EC concentrations are randomly chosen from a normal distribution symmetric around the measured values with uncertainties as standard deviation; the random values for r_{bb}, r_{coal} and $r_{liq.fossil}$ are taken from a triangular distribution, which has its maximum at the central value and 0 at the upper and lower limits. For f_{bb}, f_{coal} and $f_{liq.fossil}$, the PDF derived from MCMC4 model was used (Fig. S119). Then 10,000 different estimations of $OC_{pri,e}$ and $f_{bb}(OC_{pri,e})$ were calculated. The derived median represents the best estimate, and interquartile ranges (25^{th}-75^{th} percentile) were calculated to represent the combined uncertainties.

The observed OC concentrations and non-fossil fractions $f_{nf}(OC)$ as well as estimated $OC_{pri,e}$, $f_{bb}(OC_{pri,e})$ are shown in Fig. 56. $OC_{pri,e}$ tracks the observed concentrations and seasonality of OC very well, with correlation of $r^2 = 0.71$ ($p<0.05$). $OC_{pri,e}$ are only substantially lower than OC, when observed OC concentrations > 25 μg m^{-3} (Fig. 56(a)). Observed OC mass concentrations that exceed $OC_{pri,e}$ can be explained by contribution from secondary OC from coal combustion (SOC_{coal}), and liquid fossil fuel usage ($SOC_{liq.fossil}$) and by other non-fossil OC ($OC_{o,nf}$). $OC_{o,nf}$ ~~that~~ includes secondary OC from biomass burning and biogenic sources (SOC_{nf}; SOC non-fossil), and primary OC from vegetative detritus, bioaerosols, resuspended soil organic matter, or cooking. So:

$$\text{Observed OC conentrations} - OC_{pri,e} = OC_{o,nf} + SOC_{coal} + SOC_{liq.fossil}, \quad (12)$$

In most cases, the contributions to $PM_{2.5}$ from vegetative detritus, bioaerosols and soil dust in the air are likely small, because their sizes are usually much larger than 2.5 μm. For example, Guo et al. (2012) estimated that vegetative detritus only accounts for ~1% of OC in $PM_{2.5}$ in Beijing, China, using chemical mass balance (CMB) modeling and tracer-yield method. Thus, this fraction of OC can be ignored (i.e., $OC_{o,nf} \approx SOC_{nf}$). A previous ^{14}C study in Xi'an during severe winter pollution days in 2013 also reveals that increased total carbon (TC = OC + EC) was mainly driven by enhanced SOC from fossil and non-fossil sources (Zhang et al., 2015a), that is SOC_{coal}, $SOC_{liq.fossil}$, and SOC_{nf}, all of which are not modelled in $OC_{pri,e}$.

$OC_{pri,e}$ was higher than the total observed OC in summer 2008, which may indicate an overestimate of primary OC/EC ratios, or loss of OC due to photochemical processing. Xi'an is one of the four "stove cities" in China. In summer, daily average temperature was 25–31°C, and occasionally exceeded 38°C. At these temperatures, semi-volatile OC from emission sources becomes volatilized more quickly owning to higher temperatures, leading to lower primary OC/EC ratios than other seasons. These low OC/EC ratios in summer are commonly observed in urban China (e.g. median, 2.7; interquartile range, (1.9−4) from an overview of $PM_{2.5}$ composition in China by Tao et al. (2017)). This evaporation can be compounded by loss through photochemical reactions that lead to fragmentation of organic compounds.

On the other hand, the estimated $f_{bb}(OC_{pri,e})$ are consistently lower than observed ^{14}C-based $f_{nf}(OC)$, and weak correlations were observed (r^2=0.31). Differences between the non-fossil carbon fraction in primary aerosol ($f_{bb}(OC_{pri,e})$) and in the total organic aerosol $f_{nf}(OC)$ can in principle be expected due to secondary organic aerosol formation. A higher fraction of non-fossil carbon in total OC than in estimated primary OC implies that non-fossil sources contribute more strongly to SOC formation than fossil sources. Some previous observations support this hypothesis. Zhang et al. (2015a) also reported that the relative contribution of $OC_{o,nf}$ is ~2 times higher than that of SOC_{coal} and $SOC_{liq.fossil}$ in January 2013 at the same sampling site. In winter, $OC_{o,nf}$ is likely dominated by SOC from biomass-burning emissions, while contributions from biogenic SOC is small. In spring and summer, additional contributions from biogenic SOC can further elevate $f_{nf}(OC)$ compared to $f_{bb}(OC_{pri,e})$.

However, considering both $f_{nf}(OC)$ and OC concentrations, this simple model of total OC as the sum of primary and secondary OC leads to an apparent contradiction for spring and summer observations. $OC_{pri,e}$ already equals to or exceeds the total measured OC concentrations, whereas additional SOC is necessary to explain the observed higher $f_{nf}(OC)$. Spring and summer temperatures in Xi'an are generally high, which favours active photochemistry. The resulting loss of OC due to photochemistry probably also needs to be considered to explain the observations.

4.4 5 Differences between observed and estimated primary OC concentrations and sources

The estimated $OC_{pri,e}$ concentrations are comparable to the observed OC concentrations except for samples with observed OC concentrations >25 μg m^{-3}. However, $f_{bb}(OC_{pri,e})$ is considerably lower than the observed $f_{nf}(OC)$. It is worth investigating, whether this might be due to the model assumptions, for example the OC/EC emission ratios used for the primary sources. OC/EC ratios are known to be dependent on the measurement protocol applied to the samples (Chow et al., 2001, 2004). For examples, Han et al. (2016) found that for fresh biomass burning emissions, OC/EC ratios by EUSAAR_2 (Cavalli et al., 2010) is 2 times higher than those by IMPROVE_A (Chow et al., 2007). According to Eq. (11), underestimated r_{bb} or overestimated r_{coal} and $r_{liq.fossil}$ would result in a $f_{bb}(OC_{pri,e})$ that is biased towards low values. Impacts of r_{bb} on $f_{bb}(OC_{pri,e})$ are presented in Fig. 56(b). With higher r_{bb}= 5 (3–7, minimum–maximum; our best estimate from the literature review presented in Supplemental S3S4) compared to r_{bb}= 4 (3–5), $f_{bb}(OC_{pri,e})$ increases only by 4 % to 7 %. Any further increase of r_{bb} would result in a modelled $OC_{pri,e}$ that is substantially higher than that total measured OC.

On the other hand, $r_{liq.fossil}$ of 0.85 ± 0.16 was applied without considering its seasonal variations. However, it is found that $r_{liq.fossil}$ is lower in summer compared with other seasons, which is related to increased volatilization of semi-VOCs and faster catalyst and engine warm-up times in summer (Xie et al., 2017). X. Huang et al. (2014b) found OC/EC ratios from fresh vehicular emissions in summer to be ~80 % of the yearly average, based on the lowest 5 % OC/EC ratios measured in a roadside environment in Hongkong, China. The $f_{bb}(OC_{pri,e})$ would increase 3 % to 5 % in summer, if we apply 80 % of the

yearly average $r_{liq.fossil}$ for the summer (Fig. 56(b)), which is also not a substantial increase. In summary, it is not feasible to model the observed f_{nf}(OC) by primary emissions, even though the total OC concentrations are in the range of modelled primary OC for spring and summer. Moreover, in spring $\delta^{13}C_{OC}$ is lower than $\delta^{13}C_{EC}$ (Fig. 2). This points to a depleted OC source, which can be an indication of secondary formation of OC. In summary, the isotopic composition of OC makes a predominantly primary origin very unlikely.

A more realistic model for OC concentrations and f_{nf}(OC) needs to account for $OC_{o,nf}$, SOC_{coal} and $SOC_{liq.fossil}$:

$$f_{nf}(OC) = \frac{POC_{bb,e}+OC_{o,nf}}{OC_{pri,e}+OC_{o,nf}+SOC_{coal}+SOC_{liq.fossil}} \quad (13)$$

Then the estimated total OC (OC_e) will be:

$$OC_e = OC_{pri,e} + OC_{o,nf} + SOC_{coal} + SOC_{liq.fossil}, \quad (14)$$

As a sensitivity study with minimum addition to $OC_{pri,e}$ (thus minimum OC_e, $OC_{e,min}$), we make the unrealistic assumption that there is no SOC from coal and liquid fossil fuel combustion (SOC_{coal} = 0, $SOC_{liq.fossil}$ = 0). Only the required $OC_{o,nf}$ is added until the modelled f_{nf}(OC) is equal to the measured one. Figure 8 7 presents the modelled $OC_{e,min}$ and observed OC concentrations. Nearly half of $OC_{e,min}$ are higher than observed OC and especially in summer, the OC concentrations are consistently overestimated. For many of the data points in fall and spring there is a reasonable agreement between model and measurements. There are only a few haze episodes in winter, where additional SOC formation would be required to explain observed OC concentrations. However, a previous study in winter 2013 at the same sampling site found the secondary fossil OC was 0.75–1.6 times that of primary fossil OC (Zhang et al., 2015a), which indicates that that fossil SOC is likely also of importance. If we also include SOC_{coal} and $SOC_{liq.fossil}$, this leads to a further overestimate of absolute OC concentrations, if we simply estimate total OC as the sum of primary and secondary OC. Therefore, the more reasonable explanation is OC loss. The primary OC/EC ratios do not preserve the characteristics of sources any more in a warm period due to active photochemistry under high temperature and humidity. The conclusion will not change if we apply EC apportion results from MCMC3 (Fig. S12, Fig. S13).

4.3 6 Changes in emission sources in Xi'an, China (2008/2009 vs. 2012/2013)

EC is a primary emission product, and thus changes in EC sources can reflect the changes in emission sources. The contributions from biomass burning to EC was 24 % (median; interquartile range 22–26 %) in winter 2008/2009 (Fig. 78, Table 2) with no considerable change in f_{bb}(EC) between polluted days and clean days (Fig. 1(a), except the Chinese New Year eve). Taken into account of the uncertainties, ~~Comparable~~ comparable contributions were also reported at the same sampling site for winter 2012/2013 based on ^{14}C measurements (22 ± 3 %, Zhang et al., 2015a), and positive matrix factorization (PMF) receptor model simulation (20.1 ± 7.9 %, Wang et al., 2016) (Fig. 78). This suggests that from 2008 to 2013, biomass burning contributions to EC remained rather stable, although with a slight decrease from 24 % (22–26 %) to

20 % (SD = 7.9 %). Biomass burning in Xi'an mainly includes open burning of crop residues, and household usage of crop residues and wood. The slight decrease can be explained by more strict rules to minimize crop open burning, but implementation of regulations was still weak and slow. Moreover, there are no regulations yet that target household biomass usage (Zhang and Cao, 2015b).

The contributions of coal combustion to EC decreased from 45 % (29–58 %) in winter 2008/2009 to 33.9 % (SD = 23.8 %) in winter 2012/2013, with increased contributions from vehicle emission from 31 % (18–46 %) to 46 % (SD = 25.1 %) (Fig. ~~7~~8). For EC source apportionment, it is noted that the quartile ranges for 2008/2009 values overlaps ranges for 2012/2013 values (average ± SD). Compared to the uncertainties of ^{14}C measurements, the uncertainties of PMF results are always larger, making the overlapped ranges very likely. However, comparing the probability distribution functions for both cases give a more complete picture. Figure S14 and S15 shows the PDF of the relative source contributions to EC from coal combustion and vehicle emissions, respectively. For the PDF by Wang et al. (2016), we assume normal distribution as their source apportionment results are not known and given in the form of average ± SD. As shown in Fig. S14 and Fig. S15, though with some overlaps, the PDF of the relative source contribution of coal combustion (vehicle emissions) does clearly shift to the lower side (higher side) from the year 2008/2009 to 2012/2013.

Vehicle emissions become increasingly important and coal combustion less from 2008 to 2013. This change could not be detected from ^{14}C measurements alone, since the total fossil contribution to EC stayed relatively constant. Further apportionment of fossil sources into coal combustion and vehicle emissions could be achieved by combining ^{14}C measurements with $\delta^{13}C$ (Andersson et al., 2015; Winiger et al., 2016) or organic source markers (Zhang et al., 2015b).

The decreased contribution from coal combustion to EC from 2008 to 2013 resulted from stepwise replacement of coal combustion by natural gas for residential heating and cooking since the second half of the 2000s. Natural gas usage in Xi'an increased by 94 % from 2009 to 2013 (Xi'an Statistical Yearbook, 2010, 2014). Although coal combustion in Xi'an had been increasing from 6.6 million ton 2008 to 10.3 million ton in 2013, the proportion of coal used as energy reduced from 71 % to 66 % (Xi'an Statistical Yearbook, 2009, 2014). The reinforcement of environmental laws and regulations, encouragement of using high-efficiency improved coal burners and high-quality coals are important factors as well. The decreased coal combustion emissions are also evidenced from the declined enrichment factor (EF) of As and Pb. As and Pb can indicate coal combustion, as Pb-containing gasoline has been forbidden since 2000 in Xi'an (Xu et al., 2012). Annual EFs of As and Pb dropped from 802 and 804 in 2008 to 465 and 490 in 2010, respectively (Xu et al., 2016).

Vehicular emissions to EC increased from 31 % to 46 % (an absolute relative increase by roughly 50 %) from 2008 to 2013 (Fig. ~~7~~8). This is supported by increasing levels of NO_2 in urban Xi'an, which is another indicator for the contribution of vehicular emissions to air pollution. The NO_2 concentrations in Xi'an increased by 15.5 % from 2006 to 2010 (Xu et al., 2016). The increased vehicular contribution likely resulted from a strong increase in civil vehicles. The processing

(registration) of civil vehicles increased > twofold from 0.9 million unit in 2008 to 1.9 million unit in 2013 (Xi'an Statistical Yearbook, 2009, 2014). However, vehicular contributions to EC and NO_2 concentrations have not increased to the same extent as the increase in vehicle numbers. This can be attributed to the upgrade of vehicle emission standard from National II to National III for light-duty gasoline and heavy-duty diesel vehicles in 2007 and for heady-duty gasoline vehicles in 2010 in Xi'an (GB18352.3-2005, 2005; GB17691-2005, 2005), which somewhat offset the increase of vehicle numbers.

5 Conclusions

Sources of OC and EC in Xi'an, China are constrained based on a full year of radiocarbon and stable carbon isotopic measurements for the year 2008–2009. Radiocarbon measurement reveals that EC is dominated by fossil sources with contributions ranging from 71 % to 89 %, with an average of 83 ± 5 %. Compared with EC, OC has much higher contribution from non-fossil sources (54 ± 8 %), with higher contribution in winter (62 ± 5 %). Fossil contributions to OC and EC in this study fall within the range of published values from other ^{14}C-based source apportionments in Chinses cities. ~~The annual fossil contribution to OC and EC in Xi'an was comparable to Beijing (Zhang et al., 2015b, 2017), but higher than that from a regional background site in Hainan (Zhang et al., 2014b).~~ In this study, the non-fossil contribution to OC in winter (f_{nf}(OC) = 62 ± 5 %) was observed to be higher than in summer (48 ± 3 %) in Xi'an. A different seasonal variation pattern for f_{nf}(OC) was reported in Beijing, where the fossil contribution to OC was higher in winter than in summer (Yan et al., 2017; Zhang et al., 2017). This implies that different pollution patterns exist in individual Chinese cities.

In summer, a strong positive correlation was found between $F^{14}C_{(EC)}$ and K^+/EC ratios, and a significant negative correlation between $F^{14}C_{(EC)}$ and levoglucosan/EC ratios. This suggests that burning of crop residues, with significant lower levoglucosan/K^+ ratios than wood, accounted for most of the variability in non-fossil EC in the summer. No significant correlations of $F^{14}C_{(EC)}$ with K^+/EC or levoglucosan/EC were found in other seasons (Fig. ~~S11~~S5), suggesting a variable mixture of biomass subtypes.

~~The annual averaged $\delta^{13}C_{EC}$ is -24.92 ± 1.14 ‰, varying between −26.50 ‰ and -22.81 ‰. The $\delta^{13}C_{EC}$ is most enriched in winter, ranging from -23.72 ‰ to -22.81 ‰. Winter $\delta^{13}C_{EC}$ values are at the higher (i.e., less negative) end of pure coal combustion emissions even though considerable contributions from more depleted liquid fuel combustion and wood burning to EC are expected. This indicates some contribution from C4 plants, such as corn stalk burning, in addition to coal combustion.~~ To further refine EC sources, radiocarbon and stable carbon signatures are combined and used in a Bayesian Markov Chain Monte Carlo (MCMC) approach, in which burning of C4 plants is included as a subtype of biomass burning. The MCMC results indicate that coal combustion dominated EC in winter, and liquid fossil fuel combustion dominated EC in other seasons. However, increased contributions from biomass burning were important for the EC increment in winter as well. Comparisons with the results of other studies at the same sampling site in winter suggest that the sources ~~contributions~~ of fossil ~~primary carbonaceous aerosol~~EC have changed from 2008/2009 to 2013/2014, with decreasing contributions from

coal burning and increasing contributions from motor vehicles. ~~The changes in source contributions to EC in Xi'an~~This is consistent with recent changes in Xi'an ~~the region~~: changes in energy consumption, and the expansion of the civil vehicular fleet resulting from urbanization and economic improvement.

$\delta^{13}C_{OC}$ exhibited similar values to $\delta^{13}C_{EC}$, and showed strong correlations (r^2 = 0.90) in summer and autumn, indicating similar source mixtures as EC and influence of high temperature on atmospheric processing of OC. In spring, $\delta^{13}C_{OC}$ is more depleted than $\delta^{13}C_{EC}$, indicating the possible importance of secondary formation of OC (e.g., from volatile organic compound precursors) in addition to primary sources. Comparing the observations (OC mass, ^{14}C-based f_{nf}(OC)) with estimated total primary OC concentrations related to combustion sources (i.e., estimated by apportioned EC and corresponding OC to EC ratios) and the non-fossil fraction in the estimated primary OC makes it possible to provide some insights into the importance of secondary formation and other chemical processes, such as photochemical loss mechanisms. It is found that estimated primary OC mass follows the observed total OC concentrations and seasonality (r^2 = 0.71), but source contributions to total OC differ from the estimated source contributions to primary OC (r^2 = 0.31). The estimated primary OC is similar to the observed OC concentrations except for samples with observed OC concentrations >25 μg m^{-3}. However, the non-fossil fraction in estimated primary OC is significantly lower than the observed f_{nf}(OC). Those differences can be explained by the contribution of other non-fossil primary OC (excluding biomass burning), or secondary non-fossil OC, which are not included in the estimation. But we cannot reconcile the differences between observed and estimated non-fossil OC fraction without overestimating the absolute OC concentrations, especially in summer. Therefore, we hypothesize that OC loss due to active photochemistry cannot be neglected, especially not in summer.

Acknowledgments

This work was supported by the KNAW project (Nr. 530-5CDP30). The authors acknowledge the financial support from the Gratama foundation. Special thanks to Henk Been and Marc Bleeker for their help with the AMS measurements at CIO, and to Anita Aerts-Bijma and Dicky van Zonneveld for their help with ^{14}C data correction at CIO.

References

Anderson, R. S., Huang, L., Iannone, R., Thompson, A. E., and Rudolph, J.: Carbon kinetic isotope effects in the gas phase reactions of light alkanes and ethene with the OH radical at 296 ± 4 K, J. Phys. Chem. A., 108, 11537–11544, 2004.

Andersson, A.: A systematic examination of a random sampling strategy for source apportionment calculations, Sci. Total Environ., 412, 232–238, 2011.

Andersson, A., Deng, J., Du, K., Zheng, M., Yan, C., Sköld, M., and Gustafsson, Ö.: Regionally-varying combustion sources of the January 2013 severe haze events over eastern China, Environ. Sci. Technol., 49, 2038–2043, 2015.

Bandowe, B. A. M., Meusel, H., Huang, R. J., Ho, K., Cao, J., Hoffmann, T., and Wilcke, W.: $PM_{2.5}$-bound oxygenated PAHs, nitro-PAHs and parent-PAHs from the atmosphere of a Chinese megacity: seasonal variation, sources and cancer risk assessment, Sci. Total Environ., 473–474, 77–87, http://dx.doi.org/10.1016/j.scitotenv.2013.11.108, 2014.

Bikkina, S., Andersson, A., Sarin, M., Sheesley, R., Kirillova, E., Rengarajan, R., Sudheer, A., Ram, K., and Gustafsson, Ö.: Dual carbon isotope characterization of total organic carbon in wintertime carbonaceous aerosols from northern India, J.Geophys. Res. -Atmos., 121, 4797–4809, 2016.

Bikkina, S., Andersson, A., Ram, K., Sarin, M., Sheesley, R. J., Kirillova, E. N., Rengarajan, R., Sudheer, A., and Gustafsson, Ö.: Carbon isotope-constrained seasonality of carbonaceous aerosol sources from an urban location (Kanpur) in the Indo-Gangetic Plain, J.Geophys. Res.-Atmos., 122, 4903–4923, 2017.

Bond, T. C., Doherty, S. J., Fahey, D. W., Forster, P. M., Berntsen, T., DeAngelo, B. J., Flanner, M. G., Ghan, S., Kärcher, B., Koch, D., Kinne, S., Kondo, Y., Quinn, P. K., Sarofim, M. C., Schultz, M. G., Schulz, M., Venkataraman, C., Zhang, H., Zhang, S., Bellouin, N., Guttikunda, S. K., Hopke, P. K., Jacobson, M. Z., Kaiser, J. W., Klimont, Z., Lohmann, U., Schwarz, J. P., Shindell, D., Storelvmo, T., Warren, S. G., and Zender, C. S.: Bounding the role of black carbon in the climate system: a scientific assessment, J.Geophys. Res.-Atmos., 118, 5380–5552, doi:10.1002/jgrd.50171, 2013.

Bosch, C., Andersson, A., Kirillova, E. N., Budhavant, K., Tiwari, S., Praveen, P., Russell, L. M., Beres, N. D., Ramanathan, V., and Gustafsson, Ö.: Source-diagnostic dual-isotope composition and optical properties of water-soluble organic carbon and elemental carbon in the South Asian outflow intercepted over the Indian Ocean, J.Geophys. Res. -Atmos., 119, 2014.

Cao, F., Zhang, S.-C., Kawamura, K., and Zhang, Y.-L.: Inorganic markers, carbonaceous components and stable carbon isotope from biomass burning aerosols in Northeast China, Sci. Total Environ., 572, 1244–1251, http://dx.doi.org/10.1016/j.scitotenv.2015.09.099, 2016.

Cao, J. J., Lee, S. C., Ho, K. F., Zhang, X. Y., Zou, S. C., Fung, K., Chow, J. C., and Watson, J. G.: Characteristics of carbonaceous aerosol in Pearl River Delta Region, China during 2001 winter period, Atmos. Environ., 37, 1451–1460, 2003.

Cao, J. J., Wu, F., Chow, J. C., Lee, S. C., Li, Y., Chen, S. W., An, Z. S., Fung, K. K., Watson, J. G., Zhu, C. S., and Liu, S. X.: Characterization and source apportionment of atmospheric organic and elemental carbon during fall and winter of 2003 in Xi'an, China, Atmos. Chem. Phys., 5, 3127–3137, 2005.

Cao, J. J., Lee, S. C., Chow, J. C., Watson, J. G., Ho, K. F., Zhang, R. J., Jin, Z. D., Shen, Z. X., Chen, G. C., Kang, Y. M., Zou, S. C., Zhang, L. Z., Qi, S. H., Dai, M. H., Cheng, Y., and Hu, K.: Spatial and seasonal distributions of carbonaceous aerosols over China, J.Geophys. Res.-Atmos., 112, 2007.

Cao, J. J., Zhu, C. S., Chow, J. C., Liu, W. G., Han, Y. M., and Watson, J. G.: Stable carbon and oxygen isotopic composition of carbonate in fugitive dust in the Chinese Loess Plateau, Atmos. Environ., 42, 9118–9122, 2008.

Cao, J. J., Zhu, C. S., Chow, J. C., Watson, J. G., Han, Y. M., Wang, G.H., Shen, Z. X., and An, Z. S.: Black carbon relationships with emissions and meteorology in Xi'an, China, Atmos. Res., 94, 194–202, 2009.

Cao, J. J., Chow, J. C., Tao, J., Lee, S.C., Watson, J. G., Ho, K.F., Wang, G.H., Zhu, C.S., and Han, Y.M.: Stable carbon isotopes in aerosols from Chinese cities: influence of fossil fuels, Atmos. Environ., 45, 1359–1363, 2011.

Cao, J. J, Xu, H. M, Xu, Q., Chen, B. H., and Kan, H. D.: Fine particulate matter constituents and cardiopulmonary mortality in a heavily polluted Chinese city, Environ. Health Persp., 120, 373, 2012.

Cao, J. J., Zhu, C. S., Tie, X. X., Geng, F. H., Xu, H. M., Ho, S. S. H., Wang, G. H., Han, Y. M., and Ho, K. F.: Characteristics and sources of carbonaceous aerosols from Shanghai, China, Atmos. Chem. Phys., 13, 803–817, https://doi.org/10.5194/acp-13-803-2013 , 2013.

Cavalli, F., Viana, M., Yttri, K., Genberg, J., and Putaud, J.-P.: Toward a standardised thermal-optical protocol for measuring atmospheric organic and elemental carbon: the EUSAAR protocol, Atmos. Meas. Tech., 3, 79–89, https://doi.org/10.5194/amt-3-79-2010, 2010.

Chen, B., Andersson, A., Lee, M., Kirillova, E. N., Xiao, Q., Kruså, M., Shi, M., Hu, K., Lu, Z., Streets, D. G., Du, K., and Gustafsson, Ö.: Source forensics of black carbon aerosols from China, Environ. Sci. Technol., 47, 9102–9108, 2013.

Chen, Y., Cai, W., Huang, G., Li, J., and Zhang, G.:Stable carbon isotope of black carbon from typical emission sources in China. Environ. Sci. 33, 673–678, 2012 (in Chinese).

Cheng, Y., Engling, G., He, K. B., Duan, F. K., Ma, Y. L., Du, Z. Y., Liu, J. M., Zheng, M., and Weber, R. J.: Biomass burning contribution to Beijing aerosol, Atmos. Chem. Phys., 13, 7765–7781, https://doi.org/10.5194/acp-13-7765-2013, 2013.

Chesselet, R., Fontugne, M., Buat-Ménard, P., Ezat, U., and Lambert, C. E.: The origin of particulate organic carbon in the marine atmosphere as indicated by its stable carbon isotopic composition, Geophys. Res. Lett. , 8, 345–348, 1981.

Chow, J. C., Watson, J. G., Pritchett, L. C., Pierson, W. R., Frazier, C. A., and Purcell, R. G.: The DRI thermal/optical reflectance carbon analysis system: description, evaluation and applications in U.S. air quality studies, Atmos. Environ. Part A. General Topics, 27, 1185–1201, 1993.

Chow, J. C., Watson, J. G., Crow, D., Lowenthal, D. H., and Merrifield, T.: Comparison of IMPROVE and NIOSH carbon measurements, Aerosol Sci. Technol., 34, 23–34, 2001.

Chow, J. C., Watson, J. G., Chen, L.-W. A., Arnott, W. P., Moosmüller, H., and Fung, K. K.: Equivalence of elemental carbon by Thermal/Optical Reflectance and Transmittance with different temperature protocols, Environ. Sci. Technol., 38, 4414–4422, 2004.

Chow, J. C., Watson, J. G., Chen, L.-W. A., Chang, M. O., Robinson, N. F., Trimble, D., and Kohl, S.: The IMPROVE_A temperature protocol for thermal/optical carbon analysis: maintaining consistency with a long-term database, J. Air Waste Manage., 57, 1014–1023, 2007.

Chow, J. C., Watson, J. G., Chen, L.-W. A., Rice, J., and Frank, N. H.: Quantification of $PM_{2.5}$ organic carbon sampling artifacts in US networks, Atmos. Chem. Phys., 10, 5223–5239, https://doi.org/10.5194/acp-10-5223-2010, 2010.

Chow, J. C., Watson, J. G., Robles, J., Wang, X. L., Chen, L.-W. A., Trimble, D. L., Kohl, S. D., Tropp, R. J., and Fung, K. K.: Quality assurance and quality control for thermal/optical analysis of aerosol samples for organic and elemental carbon, Anal. Bioanal. Chem., 401, 3141–3152, 2011.

Chung, S. H. and Seinfeld, J. H.: Global distribution and climate forcing of carbonaceous aerosols, J.Geophys. Res. -Atmos., 107 (D19), 4407, 2002.

de Rooij, M., van der Plicht, J., and Meijer, H.: Porous iron pellets for AMS ^{14}C analysis of small samples down to ultra-microscale size (10–25 μgC), Nucl. Instrum. Meth. B, 268, 947–951, 2010.

Dusek, U., Ten Brink, H., Meijer, H., Kos, G., Mrozek, D., Röckmann, T., Holzinger, R., and Weijers, E.: The contribution of fossil sources to the organic aerosol in the Netherlands, Atmos. Environ., 74, 169-176, 2013.

Dusek, U., Monaco, M., Prokopiou, M., Gongriep, F., Hitzenberger, R., Meijer, H.A.J. and Röckmann, T.: Evaluation of a two-step thermal method for separating organic and elemental carbon for radiocarbon analysis, Atmos. Meas. Tech., 7(7), 1943–1955, https://doi.org/10.5194/amt-7-1943-2014, 2014.

Dusek, U., Hitzenberger, R., Kasper-Giebl, A., Kistler, M., Meijer, H. A. J., Szidat, S., Wacker, L., Holzinger, R., and Röckmann, T.: Sources and formation mechanisms of carbonaceous aerosol at a regional background site in the Netherlands: insights from a year-long radiocarbon study, Atmos. Chem. Phys., 17, 3233–3251, https://doi.org/10.5194/acp-17-3233-2017, 2017.

Elser, M., Huang, R. J., Wolf, R., Slowik, J. G., Wang, Q., Canonaco, F., Li, G., Bozzetti, C., Daellenbach, K. R., Huang, Y., Zhang, R., Li, Z., Cao, J., Baltensperger, U., El-Haddad, I., and Prévôt, A. S. H.: New insights into $PM_{2.5}$ chemical composition and sources in two major cities in China during extreme haze events using aerosol mass spectrometry, Atmos. Chem. Phys., 16, 3207–3225, https://doi.org/10.5194/acp-16-3207-2016, 2016.

Fang, W., Andersson, A., Zheng, M., Lee, M., Holmstrand, H., Kim, S.-W., Du, K., and Gustafsson, Ö.: Divergent evolution of carbonaceous aerosols during dispersal of East Asian haze, Sci. Rep., 7, 10422, 2017.

Fisseha, R., Saurer, M., Jäggi, M., Siegwolf, R. T. W., Dommen, J., Szidat, S., Samburova, V., and Baltensperger, U.: Determination of primary and secondary sources of organic acids and carbonaceous aerosols using stable carbon isotopes, Atmos. Environ., 43, 431–437, http://dx.doi.org/10.1016/j.atmosenv.2008.08.041, 2009.

GB17691-2005:Limits and measurement methods for emissions from heavy-duty vehicles (III, IV). Ministry of Environmental Protection and General Administration of Quality Supervision, Inspection and Quarantine of the People's Republic of China, 2005.

GB18352.3-2005: Limits and measurement methods for emissions from light-duty vehicles (III, IV). Ministry of Environmental Protection and General Administration of Quality Supervision, Inspection and Quarantine of the People's Republic of China, 2005.

Genberg, J., Hyder, M., Stenström, K., Bergström, R., Simpson, D., Fors, E., Jönsson, J. Å., and Swietlicki, E.: Source apportionment of carbonaceous aerosol in southern Sweden, Atmospheric Chemistry and Physics, 11, 11387-11400, 2011.

Gilardoni, S., Vignati, E., Cavalli, F., Putaud, J. P., Larsen, B. R., Karl, M., Stenström, K., Genberg, J., Henne, S., and Dentener, F.: Better constraints on sources of carbonaceous aerosols using a combined ^{14}C – macro tracer analysis in a European rural background site, Atmos. Chem. Phys., 11, 5685-5700, https://doi.org/10.5194/acp-11-5685-2011, 2011.

Guo, S., Hu, M., Guo, Q., Zhang, X., Zheng, M., Zheng, J., Chang, C.C., Schauer, J.J. and Zhang, R.: Primary sources and secondary formation of organic aerosols in Beijing, China, Environ. Sci. Technol., 46(18), 9846-9853, 2012.

Guo, Z., Jiang, W., Chen, S., Sun, D., Shi, L., Zeng, G., and Rui, M.: Stable isotopic compositions of elemental carbon in $PM_{1.1}$ in north suburb of Nanjing region, China, Atmos. Res., 168, 105–111, 2016.

Hallquist, M., Wenger, J. C., Baltensperger, U., Rudich, Y., Simpson, D., Claeys, M., Dommen, J., Donahue, N. M., George, C., Goldstein, A. H., Hamilton, J. F., Herrmann, H., Hoffmann, T., Iinuma, Y., Jang, M., Jenkin, M. E., Jimenez, J. L., Kiendler-Scharr, A., Maenhaut, W., McFiggans, G., Mentel, Th. F., Monod, A., Prévôt, A. S. H., Seinfeld, J. H., Surratt, J. D., Szmigielski, R., and Wildt, J.: The formation, properties and impact of secondary organic aerosol: current and emerging issues, Atmos. Chem. Phys., 9, 5155–5236, https://doi.org/10.5194/acp-9-5155-2009, 2009.

Han, Y. M., Cao, J. J., Lee, S. C., Ho, K. F., and An, Z. S.: Different characteristics of char and soot in the atmosphere and their ratio as an indicator for source identification in Xi'an, China, Atmos. Chem. Phys., 10, 595–607, https://doi.org/10.5194/acp-10-595-2010, 2010.

Han, Y. M., Chen, L.W., Huang, R.J., Chow, J. C., Watson, J. G., Ni, H. Y., Liu, S. X., Fung, K. K., Shen, Z. X, Wei, C., Wang, Q. Y., Tian, J., Zhao, Z. Z., Prévôt, A. S. H., and Cao, J. J.: Carbonaceous aerosols in megacity Xi'an, China: implications of thermal/optical protocols comparison, Atmos. Environ., 132, 58–68, 2016.

Ho, K. F., Lee, S. C., Cao, J. J., Li, Y. S., Chow, J. C., Watson, J. G., and Fung, K.: Variability of organic and elemental carbon, water soluble organic carbon, and isotopes in Hong Kong, Atmos. Chem. Phys., 6, 4569–4576, https://doi.org/10.5194/acp-6-4569-2006, 2006.

Huang, L., Brook, J., Zhang, W., Li, S., Graham, L., Ernst, D., Chivulescu, A., and Lu, G.: Stable isotope measurements of carbon fractions (OC/EC) in airborne particulate: a new dimension for source characterization and apportionment, Atmos. Environ., 40, 2690–2705, 2006.

Huang, R. J., Zhang, Y., Bozzeti, C., Ho, K. F., Cao, J. J., Han, Y., Daellenbach, K. R., Slowik, J.G., Platt, S. M., Canonaco, F., Zotter, P., Wolf, R., Pieber, S. M., Bruns, E. A., Crippa, M., Ciarelli, G., Piazzalunga, A., Schwikowski, M., Abbaszade, G., SchnelleKreis, J., Zimmermann, R., An, Z., Szidat, S., Baltensperger, U., El Haddad, I., and Prévôt, A. S. H.: High secondary aerosol contribution to particulate pollution during haze events in China, Nature, 514, 218–222, doi:10.1038/nature13774, 2014~~a~~.

Huang, X. H. H., Bian, Q. J., Louie, P. K. K., and Yu, J. Z.: Contributions of vehicular carbonaceous aerosols to $PM_{2.5}$ in a roadside environment in Hong Kong, Atmos. Chem. Phys., 14, 9279–9293, https://doi.org/10.5194/acp-14-9279-2014, 2014~~b~~.

Iannone, R., Koppmann, R., and Rudolph, J.: Stable carbon kinetic isotope effects for the production of methacrolein and methyl vinyl ketone from the gas-phase reactions of isoprene with ozone and hydroxyl radicals, Atmos. Environ., 44, 4135–4141, 2010.

IPCC: Climate Change 2013: The Physical Science Basis, Cambridge University Press, Cambridge, United Kingdom and New York, NY, USA, 2013.

Irei, S., Huang, L., Collin, F., Zhang, W., Hastie, D., and Rudolph, J.: Flow reactor studies of the stable carbon isotope composition of secondary particulate organic matter generated by OH-radical-induced reactions of toluene, Atmos. Environ., 40, 5858–5867, 2006.

Irei, S., Rudolph, J., Huang, L., Auld, J., and Hastie, D.: Stable carbon isotope ratio of secondary particulate organic matter formed by photooxidation of toluene in indoor smog chamber, Atmos. Environ., 45, 856–862, 2011.

Jacobson, M. C., Hansson, H. C., Noone, K. J., and Charlson, R. J.: Organic atmospheric aerosols: review and state of the science, Rev. Geophys., 38, 267–294, 2000.

Kawashima, H. and Haneishi, Y.: Effects of combustion emissions from the Eurasian continent in winter on seasonal $\delta^{13}C$ of elemental carbon in aerosols in Japan, Atmos. Environ., 46, 568–579, 2012.

Kirillova, E. N., Andersson, A., Sheesley, R. J., Kruså, M., Praveen, P., Budhavant, K., Safai, P., Rao, P., and Gustafsson, Ö.: ^{13}C- and ^{14}C-based study of sources and atmospheric processing of water-soluble organic carbon (WSOC) in South Asian aerosols, J.Geophys. Res. -Atmos., 118, 614–626, 2013.

Kirillova, E. N., Andersson, A., Han, J., Lee, M., and Gustafsson, Ö.: Sources and light absorption of water-soluble organic carbon aerosols in the outflow from northern China, Atmos. Chem. Phys., 14, 1413-1422, https://doi.org/10.5194/acp-14-1413–2014, 2014a.

Kirillova, E. N., Andersson, A., Tiwari, S., Srivastava, A. K., Bisht, D. S., and Gustafsson, Ö.: Water-soluble organic carbon aerosols during a full New Delhi winter: isotope-based source apportionment and optical properties, J.Geophys. Res. -Atmos., 119, 3476–3485, 2014b.

Laskin, A., Laskin, J., and Nizkorodov, S. A.: Chemistry of Atmospheric Brown Carbon, Chemical Reviews, 115, 4335-4382, 10.1021/cr5006167, 2015.

Lelieveld, J., Evans, J., Fnais, M., Giannadaki, D., and Pozzer, A.: The contribution of outdoor air pollution sources to premature mortality on a global scale, Nature, 525, 367-371, 2015.

Levin, I., Naegler, T., Kromer, B., Diehl, M., Francey, R. J., GOMEZ-PELAEZ, A. J., Steele, L., Wagenbach, D., Weller, R., and Worthy, D. E.: Observations and modelling of the global distribution and long-term trend of atmospheric $^{14}CO_2$, Tellus B, 62, 26–46, 2010.

Lewis, C. W., Klouda, G. A., and Ellenson, W. D.: Radiocarbon measurement of the biogenic contribution to summertime PM-2.5 ambient aerosol in Nashville, TN, Atmos. Environ., 38, 6053–6061, 2004.

Liu, D., Li, J., Zhang, Y., Xu, Y., Liu, X., Ding, P., Shen, C., Chen, Y., Tian, C., and Zhang, G.: The use of levoglucosan and radiocarbon for source apportionment of $PM_{2.5}$ carbonaceous aerosols at a background site in East China, Environ. Sci. Technol., 47, 10454–10461, 2013.

Liu, G., Li, J., Xu, H., Wu, D., Liu, Y., and Yang, H.: Isotopic compositions of elemental carbon in smoke and ash derived from crop straw combustion, Atmos. Environ., 92, 303–308, http://dx.doi.org/10.1016/j.atmosenv.2014.04.042, 2014a.

Liu, J., Li, J., Zhang, Y., Liu, D., Ding, P., Shen, C., Shen, K., He, Q., Ding, X., Wang, X., Chen, D., and Zhang, G.: Source apportionment using radiocarbon and organic tracers for $PM_{2.5}$ carbonaceous aerosols in Guangzhou, South China: contrasting local-and regional-scale aaze events, Environ. Sci. Technol., 48, 12002–12011, 2014b.

Liu, J., Li, J., Liu, D., Ding, P., Shen, C., Mo, Y., Wang, X., Luo, C., Cheng, Z., Szidat, S., Zhang, Y., Chen, Y., and Zhang, G.: Source apportionment and dynamic changes of carbonaceous aerosols during the haze bloom-decay process in China based on radiocarbon and organic molecular tracers, Atmos. Chem. Phys., 16, 2985-2996, https://doi.org/10.5194/acp-16-2985–2016, 2016a.

Liu, J., Li, J., Vonwiller, M., Liu, D., Cheng, H., Shen, K., Salazar, G., Agrios, K., Zhang, Y., He, Q., Ding, X., Zhong, G.,

Wang, X., Szidat, S., and Zhang, G.: The importance of non-fossil sources in carbonaceous aerosols in a megacity of central China during the 2013 winter haze episode: a source apportionment constrained by radiocarbon and organic tracers, Atmos. Environ., 144, 60–68, 2016b.

Masalaite, A., Holzinger, R., Remeikis, V., Roeckmann, T., and Dusek, U.: Characteristics, sources and evolution of fine aerosol (PM_1) at urban, coastal and forest background sites in Lithuania, Atmos. Environ., 148, 62-76, 2017.

Minguillón, M. C., Perron, N., Querol, X., Szidat, S., Fahrni, S. M., Alastuey, A., Jimenez, J. L., Mohr, C., Ortega, A. M., Day, D. A., Lanz, V. A., Wacker, L., Reche, C., Cusack, M., Amato, F., Kiss, G., Hoffer, A., Decesari, S., Moretti, F., Hillamo, R., Teinilä, K., Seco, R., Peñuelas, J., Metzger, A., Schallhart, S., Müller, M., Hansel, A., Burkhart, J. F., Baltensperger, U., and Prévôt, A. S. H.: Fossil versus contemporary sources of fine elemental and organic carbonaceous particulate matter during the DAURE campaign in Northeast Spain, Atmos. Chem. Phys., 11, 12067-12084, https://doi.org/10.5194/acp-11-12067-2011, 2011.

Miyazaki, Y., Kawamura, K., Jung, J., Furutani, H., and Uematsu, M.: Latitudinal distributions of organic nitrogen and organic carbon in marine aerosols over the western North Pacific, Atmos. Chem. Phys., 11, 3037–3049, https://doi.org/10.5194/acp-11-3037-2011, 2011.

Mohn, J., Szidat, S., Fellner, J., Rechberger, H., Quartier, R., Buchmann, B., and Emmenegger, L.: Determination of biogenic and fossil CO_2 emitted by waste incineration based on $^{14}CO_2$ and mass balances, Bioresource Technol., 99, 6471–6479, 2008.

Mook, W. G. and van der Plicht, J.: Reporting ^{14}C activities and concentrations, Radiocarbon, 41, 227–239, 1999.

NASA: MODIS thermal anomalies/fire, National Aeronautics & Space Administration, Greenbelt, MD, 2017.

Nel, A.: Air pollution-related illness: effects of particles, Science, 308, 804–806, 2005.

Niu, X., Cao, J., Shen, Z., Ho, S. S. H., Tie, X., Zhao, S., Xu, H., Zhang, T., and Huang, R.: $PM_{2.5}$ from the Guanzhong Plain: chemical composition and implications for emission reductions, Atmos. Environ., 147, 458–469, 2016.

Palstra, S. W. and Meijer, H. A.: Biogenic carbon fraction of biogas and natural gas fuel mixtures determined with ^{14}C, Radiocarbon, 56, 7-28, 2014.

Parnell, A. C., Inger, R., Bearhop, S., and Jackson, A. L.: Source partitioning using stable isotopes: coping with too much variation, PloS ONE, 5, e9672, 2010.

Pavuluri, C. M. and Kawamura, K.: Enrichment of ^{13}C in diacids and related compounds during photochemical processing of aqueous aerosols: new proxy for organic aerosols aging, Sci. Rep., 6, 36467, 2016.

Pöschl, U.: Atmospheric aerosols: composition, transformation, climate and health effects, Angew. Chem. Int. Ed. Engl., 44, 7520-7540, 2005.

~~Prokopiou, M.: Characterization of a thermal method for separating organic and elemental carbon from aerosol samples using 14-C analysis, MS thesis, University of Groningen, the Netherlands, 2010.~~

Reimer, P. J., Brown, T. A., and Reimer, R. W.: Discussion: reporting and calibration of post-bomb ^{14}C data, Radiocarbon, 46, 1299–1304, 2004.

Sun, J., Shen, Z., Cao, J., Zhang, L., Wu, T., Zhang, Q., Yin, X., Lei, Y., Huang, Y., Huang, R., Liu, S., Han, Y., Xu, H., Zheng, C., and Liu, P.: Particulate matters emitted from maize straw burning for winter heating in rural areas in Guanzhong Plain, China: current emission and future reduction, Atmos. Res., 184, 66–76, 2017.

Sun, X., Hu, M., Guo, S., Liu, K., and Zhou, L.: ^{14}C-Based source assessment of carbonaceous aerosols at a rural site, Atmos. Environ., 50, 36–40, 2012.

Szidat, S.: Sources of Asian haze, Science, 323, 470–471, 2009.

Szidat, S., Jenk, T. M., Synal, H. A., Kalberer, M., Wacker, L., Hajdas, I., Kasper - Giebl, A., and Baltensperger, U.: Contributions of fossil fuel, biomass-burning, and biogenic emissions to carbonaceous aerosols in Zurich as traced by ^{14}C, J.Geophys. Res.-Atmos., 111, 2006.

Tao, J., Zhang, L., Cao, J., and Zhang, R.: A review of current knowledge concerning $PM_{2.5}$ chemical composition, aerosol optical properties and their relationships across China, Atmos. Chem. Phys., 17, 9485–9518, https://doi.org/10.5194/acp-17-9485-2017, 2017.

van der Plicht, J., Wijma, S., Aerts, A., Pertuisot, M., and Meijer, H.: Status report: the Groningen AMS facility, Nucl. Instrum. Meth. B, 172, 58–65, 2000.

Wang, Q., Huang, R. J., Zhao, Z., Cao, J., Ni, H., Tie, X., Zhao, S., Su, X., Han, Y., Shen, Z., Wang, Y., and Zhang, N.: Physicochemical characteristics of black carbon aerosol and its radiative impact in a polluted urban area of China, J.Geophys. Res. -Atmos., 121, 2016.

Watson, J. G.: Visibility: Science and regulation, J. Air Waste Manage., 52, 628–713, 2002.

Watson, J. G., Chow, J. C., Chen, L.-W. A., and Frank, N. H.: Methods to assess carbonaceous aerosol sampling artifacts for IMPROVE and other long-term networks, J. Air Waste Manage., 59, 898–911, 2009.

Winiger, P., Andersson, A., Yttri, K. E., Tunved, P., and Gustafsson, Ö.: Isotope-based source apportionment of EC aerosol particles during winter high-pollution events at the Zeppelin Observatory, Svalbard, Environ. Sci. Technol., 49, 11959–11966, 10.1021/acs.est.5b02644, 2015.

Winiger, P., Andersson, A., Eckhardt, S., Stohl, A., and Gustafsson, Ö.: The sources of atmospheric black carbon at a European gateway to the Arctic, Nat. Commun., 7, 2016.

Xi'an Municipal Bureau of Statistics and NBS Survey Office in Xi'an: Xi'an Statistical Yearbook, China Statistics Press, Beijing, China, 2009 (in Chinese).

Xi'an Municipal Bureau of Statistics and NBS Survey Office in Xi'an: Xi'an Statistical Yearbook, China Statistics Press, Beijing, China, 2010 (in Chinese).

Xi'an Municipal Bureau of Statistics and NBS Survey Office in Xi'an: Xi'an Statistical Yearbook, China Statistics Press, Beijing, China, 2014 (in Chinese).

Xie, M., Hays, M., and Holder, A.: Light-absorbing organic carbon from prescribed and laboratory biomass burning and gasoline vehicle emissions, Sci. Rep., 7, 7318, 2017.

Xu, H., Cao, J., Ho, K., Ding, H., Han, Y., Wang, G., Chow, J., Watson, J., Khol, S., Qiang, J. and Li, W.: Lead concentrations in fine particulate matter after the phasing out of leaded gasoline in Xi'an, China, Atmos. Environ., 46, 217–224, 2012.

Xu, H., Cao, J., Chow, J. C., Huang, R.-J., Shen, Z., Chen, L. A., Ho, K. F., and Watson, J. G.: Inter-annual variability of wintertime $PM_{2.5}$ chemical composition in Xi'an, China: evidences of changing source emissions, Sci. Total Environ., 545, 546–555, 2016.

Yan, C., Zheng, M., Bosch, C., Andersson, A., Desyaterik, Y., Sullivan, A. P., Collett, J. L., Zhao, B., Wang, S., He, K. and Gustafsson, Ö.: Important fossil source contribution to brown carbon in Beijing during winter, Sci. Rep., 7, 2017.

Yu, J. Z., Xu, J., and Yang, H.: Charring characteristics of atmospheric organic particulate matter in thermal analysis, Environ. Sci. Technol., 36, 754–761, 2002.

Zenker, K., Vonwiller, M., Szidat, S., Calzolai, G., Giannoni, M., Bernardoni, V., Jedynska, A. D., Henzing, B., Meijer, H. A., and Dusek, U.: Evaluation and Inter-comparison of oxygen-based OC-EC separation methods for radiocarbon analysis of ambient aerosol particle samples, Atmosphere, 8, 226, 2017.

Zhang, T., Cao, J.-J., Chow, J. C., Shen, Z.-X., Ho, K.-F., Ho, S. S. H., Liu, S.-X., Han, Y.-M., Watson, J. G., Wang, G.-H.,

and Huang, R.-J.: Characterization and seasonal variations of levoglucosan in fine particulate matter in Xi'an, China, J. Air Waste Manage., 64, 1317–1327, 10.1080/10962247.2014.944959, 2014a.

Zhang, Y. L. and Cao, F.: Fine particulate matter ($PM_{2.5}$) in China at a city level, Sci. Rep., 5, 14884, 2015a.

Zhang, Y. L. and Cao, F.: Is it time to tackle $PM_{2.5}$ air pollutions in China from biomass-burning emissions?, Environ. Pollut. , 202, 217–219, 2015b.

Zhang, Y. L., Li, J., Zhang, G., Zotter, P., Huang, R.-J., Tang, J.-H., Wacker, L., Prévôt, A. S. H., and Szidat, S.: Radiocarbon-based source apportionment of carbonaceous aerosols at a regional background site on Hainan Island, South China, Environ. Sci. Technol., 48, 2651–2659, 10.1021/es4050852, 2014ab.

Zhang, Y. L., Liu, J.W., Salazar, G. A., Li, J., Zotter, P., Zhang, G., Shen, R.R., Schäfer, K., Schnelle-Kreis, J., and Prévôt, A. S.: Micro-scale (μg) radiocarbon analysis of water-soluble organic carbon in aerosol samples, Atmos. Environ., 97, 1–5, 2014c2014b.

Zhang, Y. L., Huang, R. J., El Haddad, I., Ho, K. F., Cao, J. J., Han, Y., Zotter, P., Bozzetti, C., Daellenbach, K. R., Canonaco, F., Slowik, J. G., Salazar, G., Schwikowski, M., Schnelle-Kreis, J., Abbaszade, G., Zimmermann, R., Baltensperger, U., Prévôt, A. S. H., and Szidat, S.: Fossil vs. non-fossil sources of fine carbonaceous aerosols in four Chinese cities during the extreme winter haze episode of 2013, Atmos. Chem. Phys., 15, 1299–1312, https://doi.org/10.5194/acp-15-1299-2015, 2015a.

Zhang, Y. L., Schnelle-Kreis, J., Abbaszade, G., Zimmermann, R., Zotter, P., Shen, R. R., Schäefer, K., Shao, L., Prévôt, A , and Szidat, S.: Source apportionment of elemental carbon in Beijing, China: insights from radiocarbon and organic marker measurements, Environ. Sci. Technol., 49, 8408–8415, 2015b.

Zhang, Y. L., Ren, H., Sun, Y., Cao, F., Chang, Y., Liu, S., Lee, X., Agrios, K., Kawamura, K., Liu, D., Ren, L., Du, W., Wang, Z., Prévôt, A. S. H., Szidat, S., and Fu, P.: High contribution of nonfossil sources to submicrometer organic aerosols in Beijing, China, Environ. Sci. Technol., 51, 7842–7852, 2017.

Zhang, Y. X., Schauer, J. J., Zhang, Y. H., Zeng, L. M., Wei, Y. J., Liu, Y., and Shao, M.: Characteristics of particulate carbon emissions from real-world Chinese coal combustion, Environ. Sci. Technol., 42, 5068–5073, 2008.

Zhu, C. S., Cao, J. J., Tsai, C. J., Zhang, Z. S., and Tao, J.: Biomass burning tracers in rural and urban ultrafine particles in Xi'an, China, Atmos. Pollut. Res., 8, 614–618, http://dx.doi.org/10.1016/j.apr.2016.12.011, 2017.

Zhuang, Z., Li, Y., Chen, B., and Guo, J.: Chinese kang as a domestic heating system in rural northern China—a review, Energ. Buildings, 41, 111–119, 2009.

Table 1. Relative fossil source contribution to OC and EC (f_{fossil} (OC), f_{fossil} (EC) in percentage) in China

Location	Site type	PM fraction	Season	Year	f_{fossil} (OC)	f_{fossil} (EC)	Reference
Beijing	urban	$PM_{2.5}$	winter	2009/2010		83 ± 4	(Chen et al., 2013)
Beijing	urban	$PM_{2.5}$	spring	2013	41 ± 4	67±7	(Liu et al., 2016a)
Beijing	rural	$PM_{2.5}$	winter	2007		80–87	(Sun et al., 2012)
Beijing	rural	$PM_{2.5}$	summer	2007		80–87	(Sun et al., 2012)
Beijing	urban	$PM_{2.5}$	winter	2013	67 ± 3		(Yan et al., 2017)
Beijing	urban	$PM_{2.5}$	summer	2013	36 ± 13		(Yan et al., 2017)
Beijing	urban	PM_4	annual	2010/2011		79 ± 6	(Zhang et al., 2015b)
Beijing	urban	$PM_{2.5}$	winter	2013	58 ± 5	76 ± 4	(Zhang et al., 2015a)
Beijing	urban	PM_1	annual	2013/2014	48 ± 12	82 ± 7	(Zhang et al., 2017)
Guangzhou	urban	$PM_{2.5}$	winter	2012/2013	37 ± 4	71 ± 10	(J. Liu et al., 2014b)
Guangzhou	urban	$PM_{2.5}$	spring	2013	46 ± 6	80 ± 5	(Liu et al., 2016a)
Guangzhou	urban	PM_{10}	winter	2011	42		(Y. Zhang et al., 2014eb)
Guangzhou	urban	$PM_{2.5}$	winter	2013	35 ± 7	69	(Zhang et al., 2015a)
Shanghai	urban	$PM_{2.5}$	winter	2009/2010		83 ± 4	(Chen et al., 2013)
Shanghai	urban	$PM_{2.5}$	winter	2013	49 ± 2	79 ± 4	(Zhang et al., 2015a)
Xiamen	urban	$PM_{2.5}$	winter	2009/2010		87 ± 3	(Chen et al., 2013)
Xi'an	urban	$PM_{2.5}$	winter	2013	38 ± 3	78 ± 3	(Zhang et al., 2015a)
Xi'an	urban	$PM_{2.5}$	winter	2008/2009	46 ± 8	83 ± 5	This study[a]
Wuhan	urban	$PM_{2.5}$	winter	2013	38 ± 5	74 ± 8	(Liu et al., 2016b)
North China Plain (NCP)	urban	$PM_{2.5}$	winter	2013		73–75	(Andersson et al., 2015)
Yangtze River Delta (YRD)	urban	$PM_{2.5}$	winter	2013		66–69	(Andersson et al., 2015)
Pearl River Delta (PRD)	urban	$PM_{2.5}$	winter	2013		67–70	(Andersson et al., 2015)
Ningbo	background	$PM_{2.5}$	annual	2009/2010		77 ± 15	(Liu et al., 2013)
Hainan	background	$PM_{2.5}$	annual	2005/2006	19 ± 10	38 ± 11	(Y. Zhang et al., 2014ba)

[a] f_{fossil} (OC) and f_{fossil} (EC) in this study is calculated from the $F^{14}C$ data (see details in Sect. 2.5).

Table 2. MCMC4 results[a] from the $F^{14}C$- and $\delta^{13}C$-based Bayesian Source Apportionment Calculations of EC (Median, interquartile range (25^{th}-75^{th} percentile), and 95% Credible Intervals).

	Seasons	summer	autumn	winter[c]	spring	annual[c]
biomass burning[b]	median	0.135	0.177	0.239	0.156	0.173
(combination of	25^{th}-75^{th} percentile	(0.129–0.142)	(0.16–0.197)	(0.22–0.26)	(0.153–0.159)	(0.165–0.18)
C3 & C4 plants)	95% credible intervals	(0.114–0.159)	(0.117–0.249)	(0.172–0.332)	(0.145–0.166)	(0.15–0.195)
coal combustion	median	0.085	0.153	0.446	0.136	0.11
	25^{th}-75^{th} percentile	(0.045–0.15)	(0.083–0.261)	(0.294–0.582)	(0.075–0.219)	(0.063–0.18)
	95% credible intervals	(0.012–0.412)	(0.02–0.589)	(0.074–0.739)	(0.019–0.492)	(0.016–0.353)
liquid fossil	median	0.779	0.666	0.307	0.707	0.717
fuel combustion	25^{th}-75^{th} percentile	(0.713–0.82)	(0.555–0.74)	(0.18–0.457)	(0.627–0.768)	(0.647–0.765)
	95% credible intervals	(0.452–0.858)	(0.226–0.824)	(0.039–0.684)	(0.357–0.826)	(0.468–0.815)

[a]Results from the four-sources (C3 biomass, C4 biomass, coal and liquid fossil fuel) MCMC4 model.

[b]Contribution of biomass burning is done by a posteriori combination of PDF for C3 plants and that for C4 plants (Fig. ~~S6~~S8). Median and quartile ranges for C3 and C4 plants burning to EC is shown in Table ~~S7~~S8.

[c]Sample taken from Chinese New Year eve (25 January 2009) was excluded.

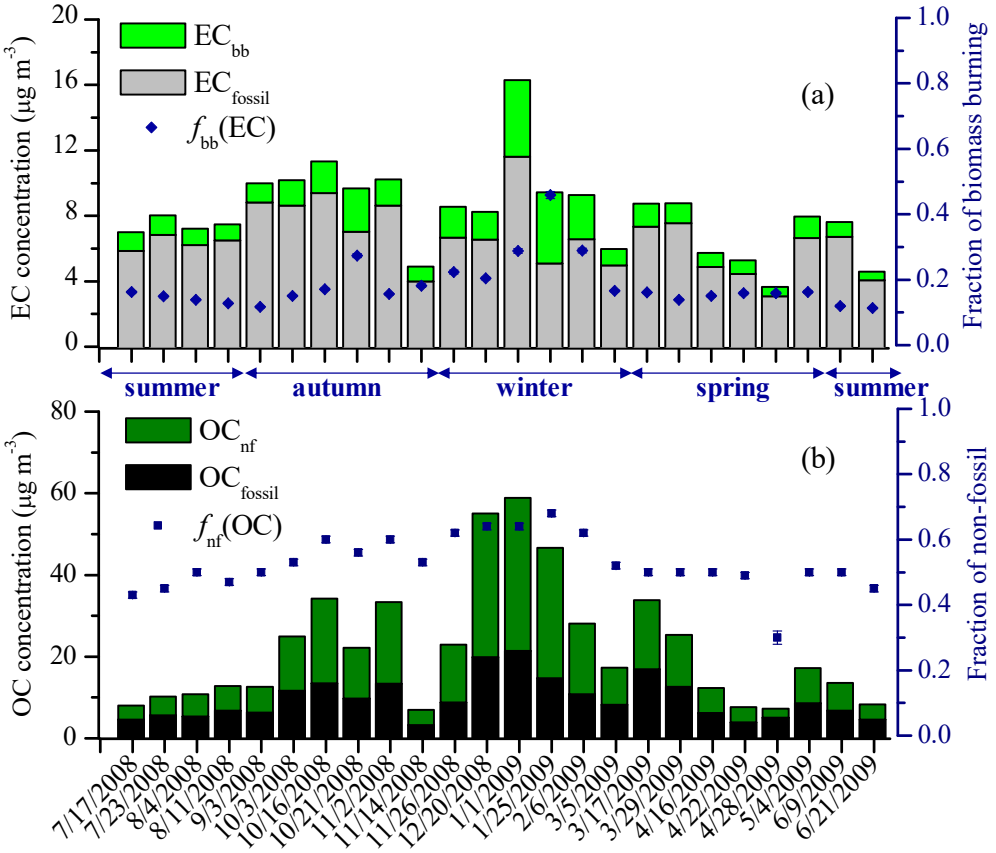

Figure 1. (a) Temporal variation of EC mass concentrations from biomass burning (EC_{bb}) and fossil-fuel sources (EC_{fossil}), and fraction of biomass burning contribution to EC (f_{bb} (EC)). (b) Temporal variation of OC mass concentrations from non-fossil sources (OC_{nf}) and fossil-fuel sources (OC_{fossil}), and fraction of non-fossil OC to total OC (f_{nf} (OC)).

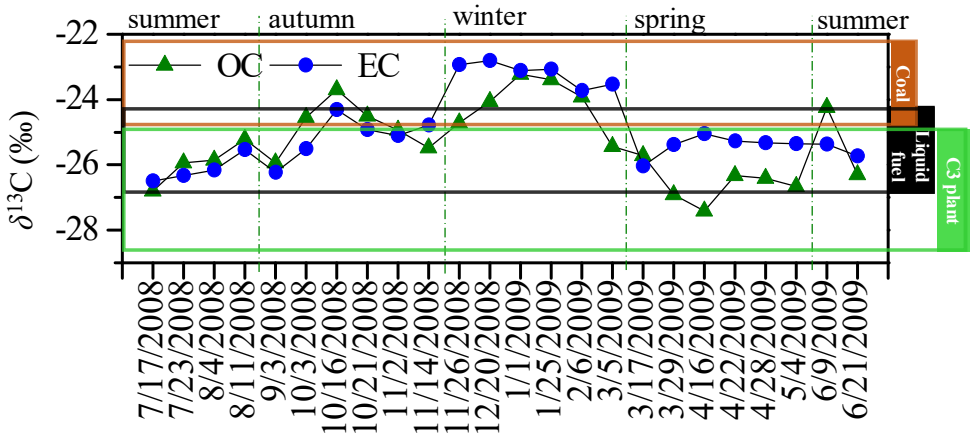

Figure 2. Stable carbon signatures ($\delta^{13}C$) in OC and EC for the samples selected for ^{14}C measurements. The $\delta^{13}C$ signatures of C3 plants (green rectangle), liquid fossil (e.g., oil, diesel, and gasoline, black rectangle), and coal (brown rectangle) are indicated as mean ± standard deviation in Table S1. The $\delta^{13}C$ endmember ranges for C4 plant burning (-16.45 ± 1.4 ‰, Table S1) are much more enriched than other sources, and are not shown in this figure.

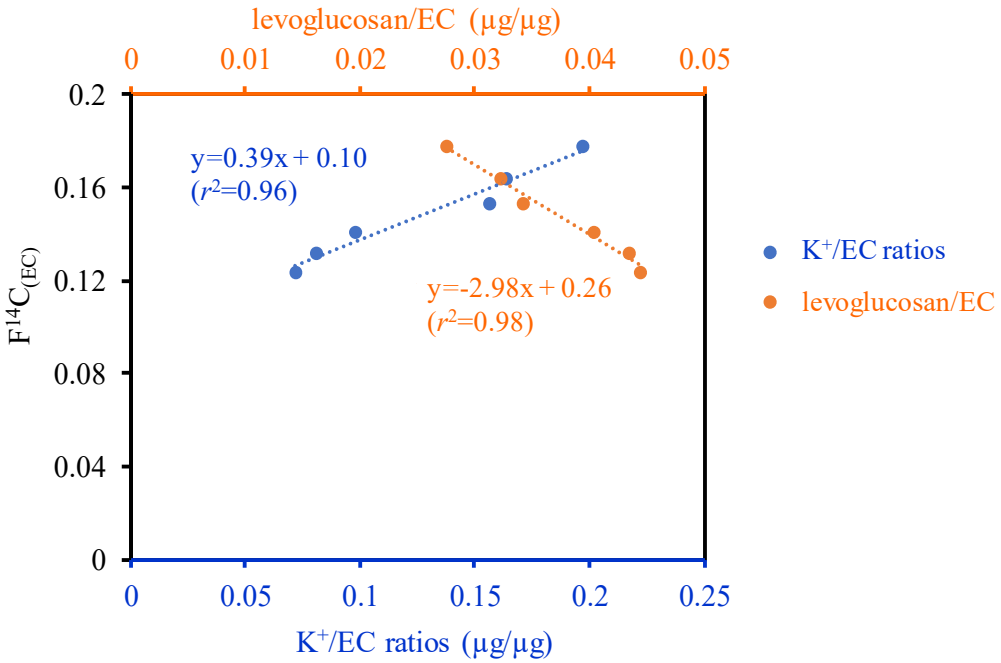

Figure 63. Correlation between $F^{14}C_{(EC)}$ and K^+/EC ratios and levoglucosan/EC ratios in summer. Data in other seasons are presented in Fig. ~~S11~~S5.

5

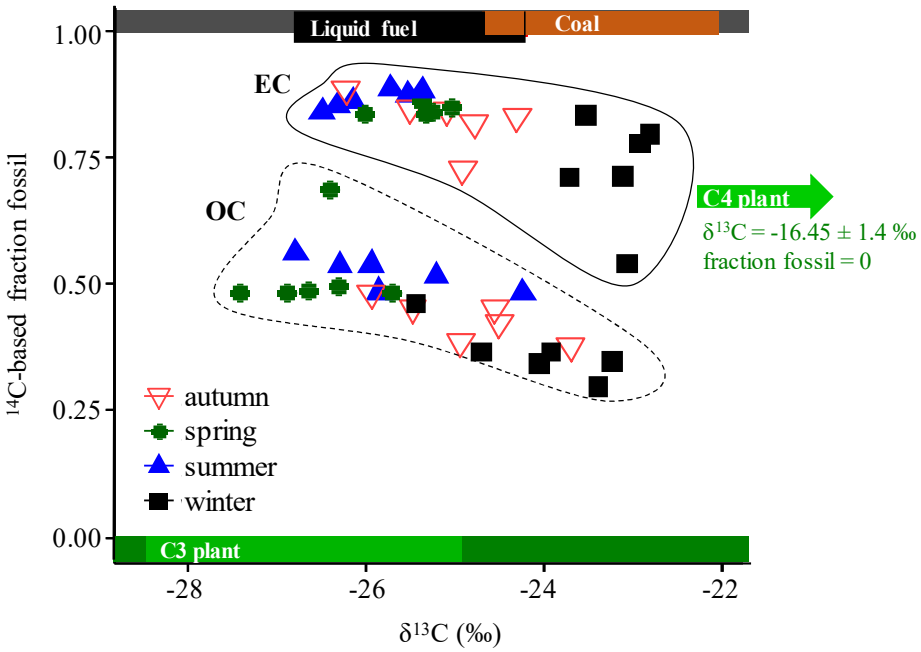

Figure 34. Two-dimensional isotope-based source characterization plot of OC and EC in different seasons. The fraction fossil (f_{fossil}(EC) and f_{fossil}(OC)) was calculated using radiocarbon data. The expected $\delta^{13}C$ and ^{14}C endmember ranges for biomass burning emissions, liquid fossil fuel combustion, and coal combustion are shown as green, black and brown bars, respectively, within the ^{14}C-based endmember ranges for non-fossil (dark green rectangle, bottom) and fossil fuel combustion (grey rectangle, top). The $\delta^{13}C$ signatures of C3 plants (green rectangle), liquid fossil (e.g., oil, diesel, and gasoline, black rectangle), and coal (brown rectangle) are indicated as mean ± standard deviation in Table S1. The $\delta^{13}C$ signatures of C4 plants burning is -16.45 ± 1.4 ‰ is not shown on x-axis.

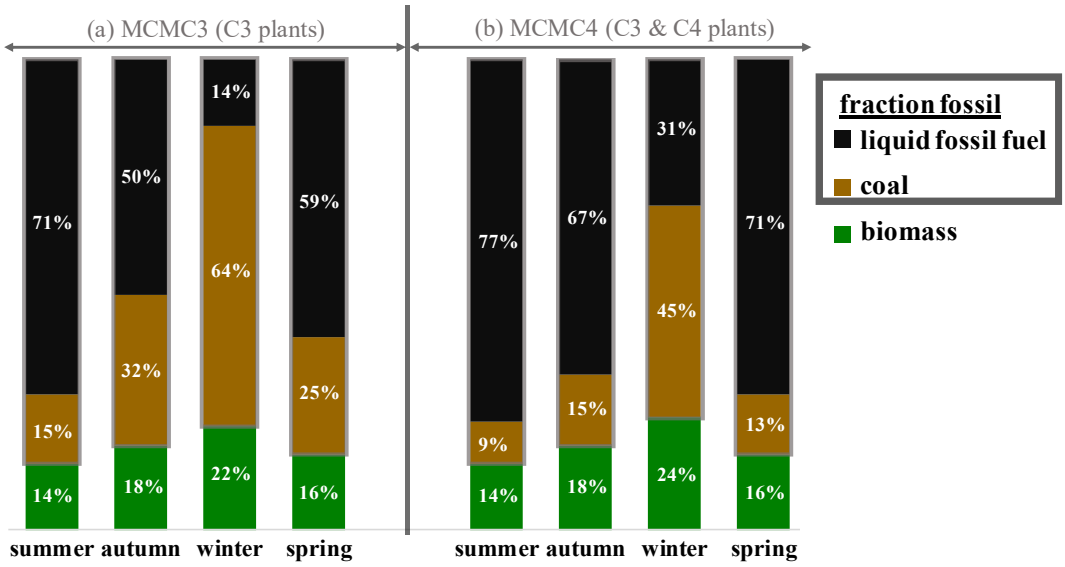

Figure 45. Sources of EC in different seasons. Results from the $F^{14}C$ and $\delta^{13}C$ based Bayesian source apportionment calculations of EC. The numbers in the bars represent the median contribution of liquid fossil fuel, coal and biomass burning. (a) results from the MCMC3 model, including C3 plants as biomass, coal and liquid fossil fuel; (b) Impact of C4 plants burning on EC source apportionment is tested by including C4 biomass into the calculations (MCMC4). Including C4 plants in calculation does not affect the contribution of biomass burning to EC. The relative fraction of C3 and C4 plants in biomass burning is shown in Fig. ~~S8~~S10. In winter, the sample taken on Chinese New Year eve (25 January 2009) was excluded.

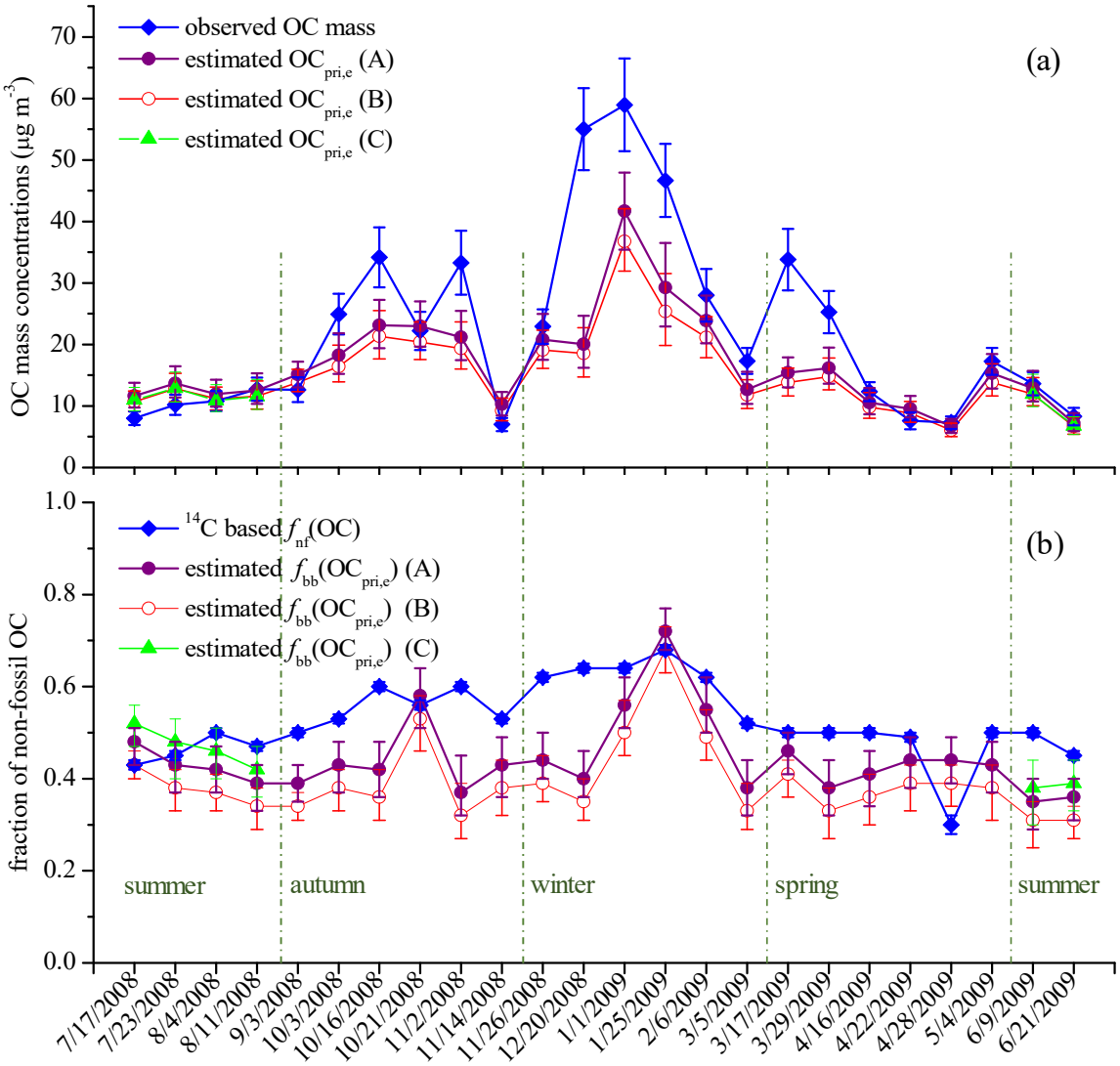

Figure 56. Estimated primary OC based on MCMC4 results. (a) measured OC concentrations (blue line and diamond symbols) with observational uncertainties (vertical bar) and estimated OC mass ($OC_{pri,e,}$ circle and triangular symbols) from apportioned EC and OC/EC ratios for different sources (Eq. (10)). (b) ^{14}C-based fraction of non-fossil OC ($f_{nf}(OC)$) and modelled non-fossil fraction in $OC_{pri,e}$ ($f_{bb}(OC_{pri,e})$) derived from Eq. (11). Interquartile range (25th-75th percentile) of the median $OC_{pri,e}$ and $f_{bb}(OC_{pri,e})$ are shown in purple (A), red (B) and green (C) vertical bars. "A" and "B" denotes different OC/EC ratios applied to primary biomass burning emissions (r_{bb}): A. r_{bb} = 5 (3–7, minimum-maximum); B. r_{bb} = 4 (3–5); "C" denotes 80 % $r_{liq.fossil}$ applied in summer with r_{bb}= 5. $f_{nf}(OC)$ uncertainties are shown but not visible.

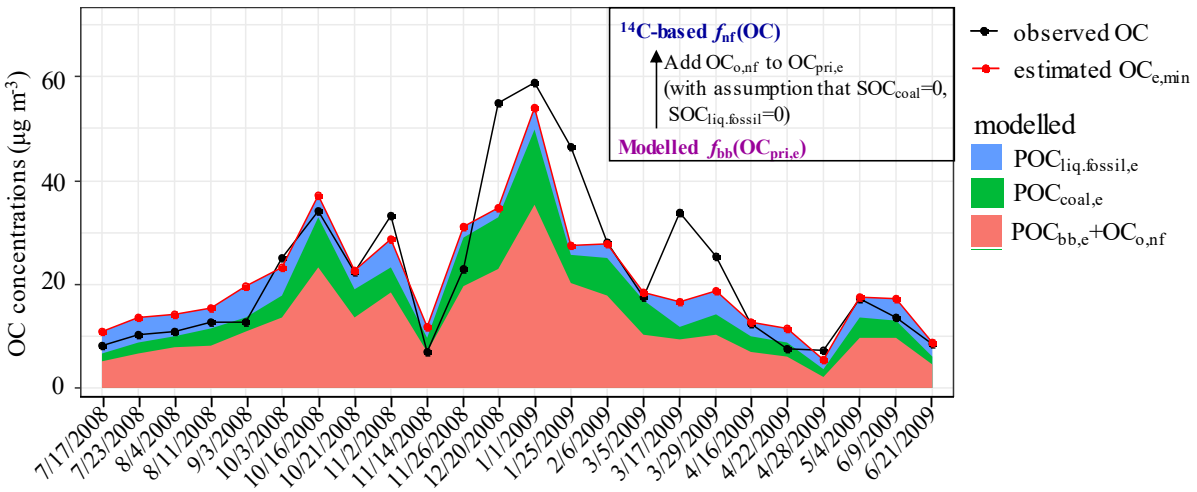

Figure 87. Observed and estimated OC concentrations. Modelled $OC_{e,min}$ is the sum of $OC_{pri,e}$ and $OC_{o,nf}$. $OC_{o,nf}$ accounts for the differences between $f_{nf}(OC)$ and $f_{bb}(OC_{pri,e})$, with an unrealistic assumption of no secondary fossil OC, leading to minimum addition to $OC_{pri,e}$. Coral area shows the $POC_{bb,e}$ and $OC_{o,nf}$, green area the $POC_{coal,e}$ and blue area the $POC_{liq.fossil,e}$. Estimation is based on MCMC4 results for EC source apportionment and primary OC/EC ratios corresponding to case (A) in Fig. 56.

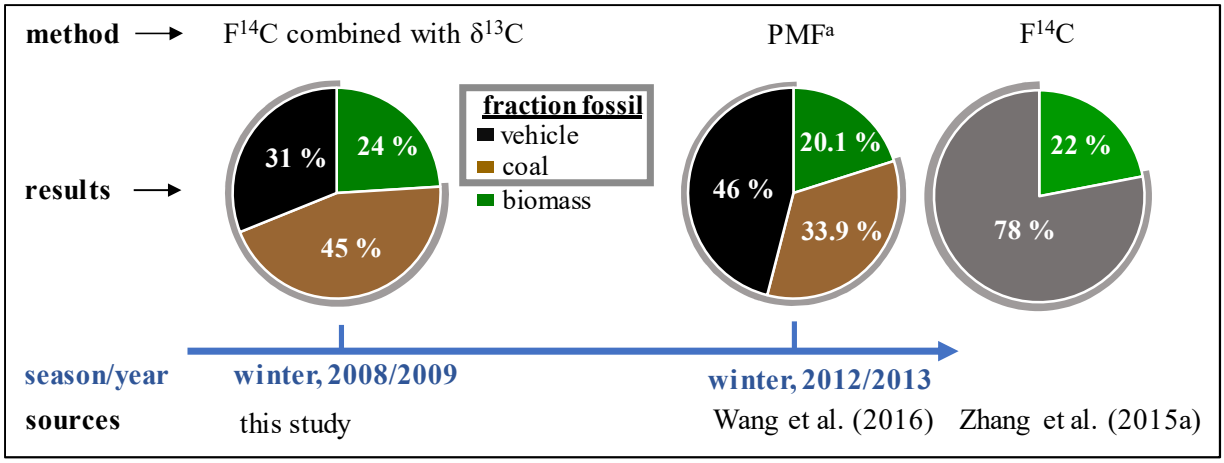

Figure 78. Comparison of EC source apportionment in winter 2008/2009 with two other studies in winter 2012/2013 at the same sampling site. [a]positive matrix factorization (PMF) receptor model simulation.

Supplement of

Source apportionment of carbonaceous aerosols in Xi'an, China: insights from a full year of measurements of radiocarbon and the stable isotope ^{13}C

Haiyan Ni[1,2,3,4], Ru-Jin Huang[2,3*], Junji Cao[3,5*], Weiguo Liu[2], Ting Zhang[3], Meng Wang[3], Harro A.J. Meijer[1], Ulrike Dusek[1]

[1]Centre for Isotope Research (CIO), Energy and Sustainability Research Institute Groningen (ESRIG), University of Groningen, Groningen, 9747 AG, the Netherlands

[2]State Key Laboratory of Loess and Quaternary Geology (SKLLQG), Institute of Earth Environment, Chinese Academy of Sciences, Xi'an, 710061, China

[3]Key Laboratory of Aerosol Chemistry & Physics (KLACP), Institute of Earth Environment, Chinese Academy of Sciences, Xi'an, 710061, China

[4]University of Chinese Academy of Sciences, Beijing, 100049, China

[5]Institute of Global Environmental Change, Xi'an Jiaotong University, Xi'an 710049, China

Correspondence to: Ru-Jin Huang (rujin.huang@ieecas.cn); Junji Cao (cao@loess.llqg.ac.cn)

S1 Sample selection for radiocarbon (^{14}C) measurements

There are 58 $PM_{2.5}$ samples in total, with 13 collected in spring, 15 in summer, 12 in autumn, and 18 in winter. Six samples with varying $PM_{2.5}$ mass and carbonaceous aerosols loading were selected per season for ^{14}C analysis. Air mass back trajectories (for identifying the probable sources and transport pathways of air pollutions) are also considered when selecting samples for ^{14}C analysis. 72h air mass back trajectories starting 150 m above ground level at 2:00 UTC (10:00 a.m., local standard time) were calculated using NOAA HYSPLIT trajectory model. The best situation is that the back trajectories were similar between days with high $PM_{2.5}$ loading and low-to-mediuman $PM_{2.5}$ loading, in which case, the influence of air pollution transport to the sampling site could be minimized. Back trajectories of selected samples are presented in Fig. S2.

S2 Measurement of source markers (levoglucosan, hopanes, picene and water-soluble potassium)

Organic makers including levoglucosan, picene and hopanes were quantified using the Gas chromatography–mass spectrometry (GC/MS) instrumentation. Filter pieces were extracted with a mixture of dichloromethane and methanol (2:1, v/v) under ultrasonication. The extracts were concentrated using a rotary evaporator in vacuum and then blown down to dryness using a pure nitrogen stream. After reaction with N,O-bis-(trimethylsilyl) trifluoroacetamide (BSTFA) at 70 °C for 3 h, the derivatives were determined using a GC/MS technique. GC/MS analysis of the derivatized fraction was performed using an Agilent 7890A GC coupled with an Agilent 5975 CMSD. The GC separation was carried out on a HP-5MS fused silica capillary column with the GC oven temperature programmed from 50 °C (2 min) to 120 °C at 15 °C min^{-1} and then to 300 °C at 5 °C min^{-1} with a final isothermal hold at 300 °C for 16 min. The sample was injected in a splitless mode at an injector temperature of 280 °C, and scanned from 50 to 650 Daltons using electron impact (EI) mode at 70 eV. GC/MS response factors were determined using authentic standards. We use the sum of measured hopanes (Σhopanes) in this study, including 17α(H),22,29,30-Trisnorhopane, 17α(H),21β(H)-30-Norhopane, 17β(H),21α(H)-30-Norhopane, 17α(H),21β(H)-Hopane, 17α(H),21α(H)-Hopane, 17β(H),21α(H)-Hopane, 17α(H),21β(H)-(22S)-Homohopane, and 17α(H),21β(H)-(22R)-Homohopane.

Water-soluble potassium (K^+) was measured in water extracts using Ion Chromatography (Dionex 600, Thermal Scientific-Dionex, Sunnyvale, CA, USA). IonPac CS12A column was used for the separation of cations. 20mM methanesulfonic acid with a flow rate of 1 mL min^{-1} was utilized as eluent for cation separation. The MDLs for K^+ was 0.001 μg mL^{-1}. Details of these measurements are described in Li et al. (2016a) and Zhang et al. (2011).

S3 Determination of modern and fossil contamination for radiocarbon measurement

$F^{14}C$ of aerosols samples was corrected for contamination that occurred during graphitization and AMS measurement. For AMS measurements, samples are usually analysed together with varying amounts of reference material covering the range of sample mass. Two such materials with known ^{14}C content are used: the oxalic acid OXII calibration material ($F^{14}C$ = 1.3406) and a ^{14}C-free CO_2 gas ($F^{14}C$ = 0).

Contamination during the graphitization and AMS measurement results into the differences between measured and nominal $F^{14}C$ values. The magnitude of these deviations can be used to quantify the contamination with fossil carbon ($F^{14}C_F = 0$) and modern carbon ($F^{14}C_M = 1$), which in turn are used for correcting the sample values (de Rooi et al., 2010).

The contamination with fossil carbon and modern carbon is quantified using isotope mass balance (Dusek et al., 2014):

$$F^{14}C_m \cdot M_m = F^{14}C_{st} \cdot M_{st} + F^{14}C_F \cdot M_F + F^{14}C_M \cdot M_M. \quad (S1)$$

M_m and M_{st} stand for the experimentally determined mass and the mass of reference materials either the oxalic acid OXII calibration material ($F^{14}C = 1.3406$) or a ^{14}C-free CO_2 gas ($F^{14}C = 0$) with a unit of μgC, respectively. $F^{14}C_m$ and $F^{14}C_{st}$ represent the experimentally determined $F^{14}C$ measured by AMS and nominal $F^{14}C$ of reference materials (Table S9).

The relationships among all masses are described as Eq. (S2):

$$M_m = M_{st} + M_F + M_M, \quad (S2)$$

where M_M is calculated using Eq. (S1) by substituting $F^{14}C_{st} = 0$ for a ^{14}C-free CO_2 gas as:

$$M_M = F^{14}C_m \cdot M_m. \quad (S3)$$

Substitute $F^{14}C_{st} = 1.3406$ for OXII and the derived M_M from Eq. (S3), M_F is derived by combining Eq. (S1) and Eq. (S2) as:

$$M_F = ((1.3406 - F^{14}C_m) \cdot M_m - (1.3406 - 1) \cdot M_M)/1.3406. \quad (S4)$$

M_M and M_F is calculated by applying Eq. (S3) and Eq. (S4), and they are mass dependent. The modern carbon contamination (M_M) is between 0.35 and 0.50 μg C, and the fossil carbon contamination (M_F) is typically around 2 μg C for sample bigger than 100 μgC.

~~S3~~ S4 Primary OC/EC ratios from biomass burning (r_{bb}), coal combustion (r_{coal}), and liquid fossil fuel combustion ($r_{liq.fossil}$)

There is considerable variability in the published OC/EC ratios for biomass burning (Fig. ~~S14~~S16), coal combustion (Fig. ~~S15~~S17) and liquid fossil fuel combustion (e.g., vehicle emissions; Table S10~~9~~). OC/EC ratios differ due to variabilities in experimental factors, such as fuel types and properties, combustion conditions (e.g., smoldering vs. flaming), sampling and analysis methods (e.g., different protocols for OCEC measurements) etc.

When selecting OC/EC ratios for each source, we applied the following rules: first, we prioritize localized measurements of fresh emissions and estimations specific to China; second, OCEC measured by IMPROVE_A (Chow et al., 2007), the same protocol applied in this study, have higher priorities than those measured by other protocols. This is because different protocols (e.g., IMPROVE_A, IMPROVE and NIOSH) can lead to differences in OC/EC ratios up to over 3 times (Chow et al., 2001). The difference in OC/EC ratios between IMPROVE and IMPROVE_A can be up to a factor of 2 (Chow et al., 2007); third, for sources with limited data, average of the available data is used.

Biomass burning emissions are mixtures of emissions from crop residues open burning, crop residues

burning in household stove, and wood burning in household stove etc. Higher OC/EC ratios are reported for crop residues open burning than those reported for similar fuels burned in household stove (Ni et al., 2015), perhaps due to a more complete combustion of household biofuels leading to higher EC emission. As it is difficult to estimate the distribution among different biomass burning subtype, here we take OC/EC ratios from emission inventories, where major types of biomass burning are included. OC and EC emission amounts from previously reported emission inventories are summarized and their ratios are presented in Fig. ~~S14~~S16. OC/EC ratios ranged from 3 to 7, with the mean of 4.4. This range covers the OC/EC ratios from fresh emissions of wood combustion (e.g., 4.67 for wood burning in rural China by Shen et al. (2015) and crop residues burning (e.g., 7 for mixture of wheat straw, rice straw and corn stalk by Han et al. (2016). We took $\boldsymbol{r_{bb} = 5\ (3–7)}$ to account for the variabilities of biomass burning emissions. A bit lower central value of 4.5 was used in previous ^{14}C-based source apportionments (Zhang et al., 2014, 2015b).

OC/EC ratios for fresh emissions from **coal combustion** are summarized in Fig. ~~S15~~S17. A relatively wide range of OC/EC ratios is found, partially can be explained by different protocol applied to OC/EC measurements (Chow et al., 2001, 2004; Han et al., 2016). We took OC/EC ratios in the literature measured by IMPROVE_A protocol when available, to be consistent with our OCEC measurements. 1.4 ± 1.3 and 6.3 ± 1.3 (average ± 1 standard deviation) are used as OC/EC ratios from bituminous and anthracite coal combustion, respectively. They are quantified from typical used coals in residential sector in China (Tian et al., 2017), and measured by IMPROVE_A protocol (Chow et al., 2007). The selected OC/EC ratios of 1.4 ± 1.3 and 6.3 ± 1.3 for bituminous and anthracite coal, respectively overlaps most of data in literatures (Fig. ~~S15~~S17). The final OC/EC ratios for coal combustion (r_{coal}) depends on the share of bituminous coal and anthracite coal. Bituminous and anthracite coal are apportioned 80% and 20% respectively, according to raw coal production data (Chen et al., 2005; Zhi et al., 2008), leading to $r_{coal} = 2.38 \pm 0.44$ derived from Monte Carlo Simulation with assumption of triangular distribution. This ratio is similar to 2.25 derived from OC and EC emission amounts from emission inventories of coal combustion for 2000, and 2.26 for the year 2005 estimated by Zhi et al. (2008).

Vehicle emissions can be influenced by vehicle type, fuel quality, speed of the vehicle, as well as the features of the road (He et al., 2008; Cheng et al., 2010; Cui et al., 2016). Literature searches were conducted (Table ~~S9~~S10) to establish OC/EC ratios for vehicle emissions. Due to the limitation of published data, the lower/upper bonds were estimated as the mean of all lower/upper bounds from different datasets. The mean was then calculated as the average of the lower and upper bounds. The established $r_{liq.fossil}$ ranged from 0.69 to 1.01 with the mean of 0.85.

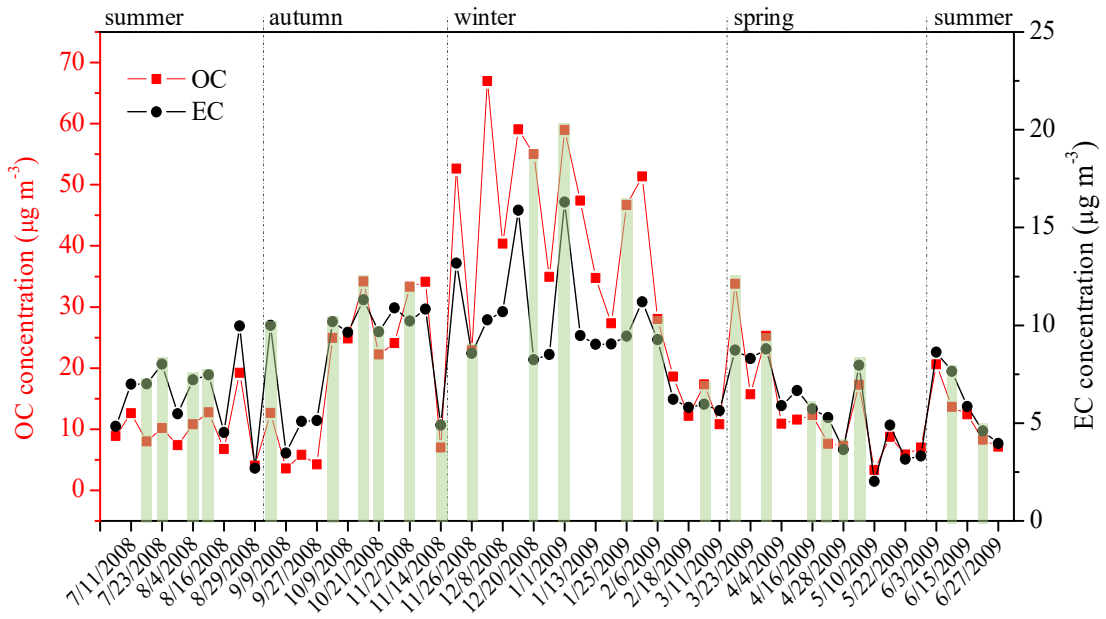

Figure S1. Temporal variability of OC and EC mass concentrations in $PM_{2.5}$ in Xi'an, China, during July 2008 to June 2009 (n=58)**.** Twenty-four samples were selected for ^{14}C analysis and highlighted in light green. Details on sample selection are presented in Supplemental S1.

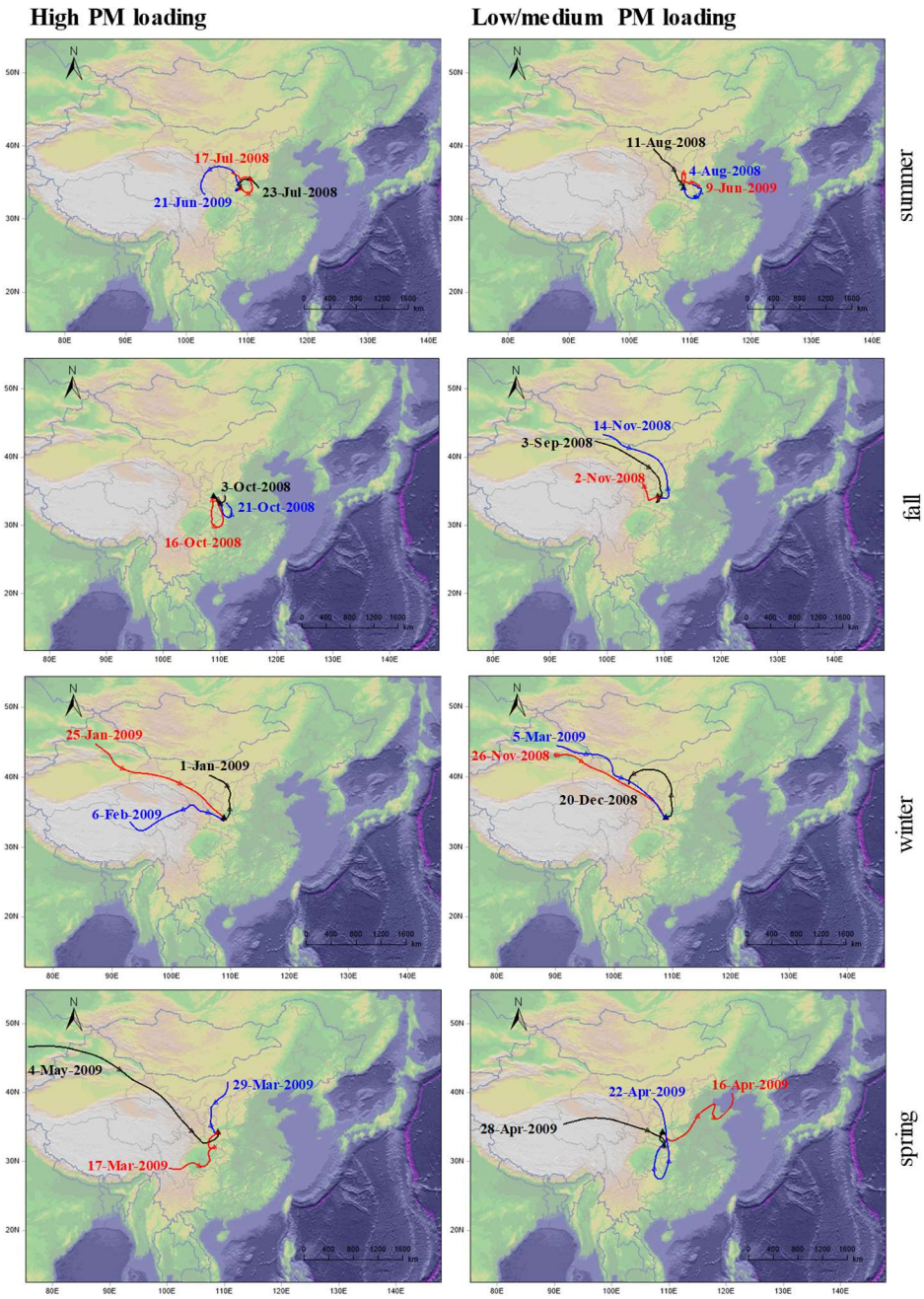

Figure S2. Three-day air backward-in-time air mass trajectory analysis of selected samples for radiocarbon measurements.

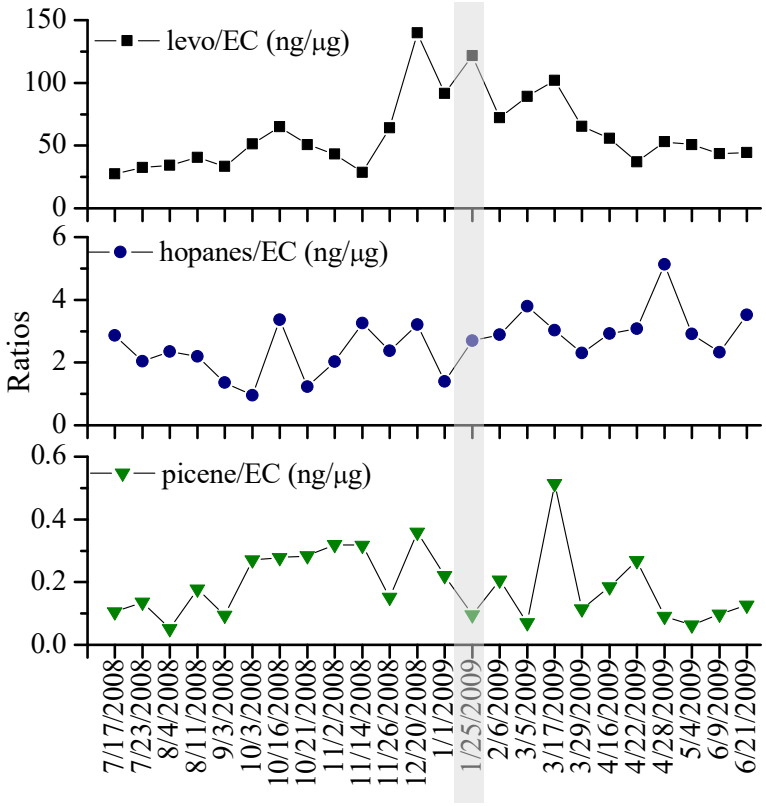

Figure S3. Temporal variation of levoglucosan to EC mass ratios (levo/EC), Σhopanes to EC ratios (Σhopanes/EC), picene to EC ratios (picene/EC) for samples selected for radiocarbon measurements. Details of measurements are in Supplemental S2.

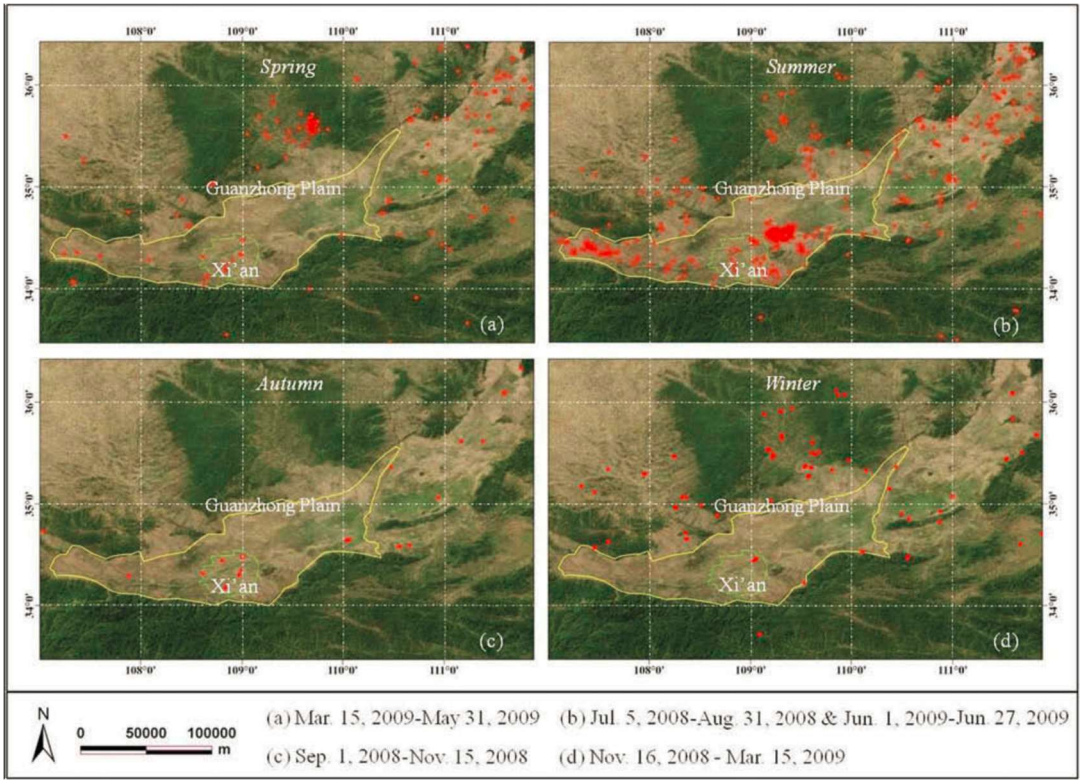

Figure ~~S10~~S4. Fire counts (red points) monitored by MODIS in different seasons during the sampling period (https://firms.modaps.eosdis.nasa.gov/firemap/). The sampling site is Xi'an. Xi'an is located in the Guanzhong Plain, one of the major agricultural production areas.

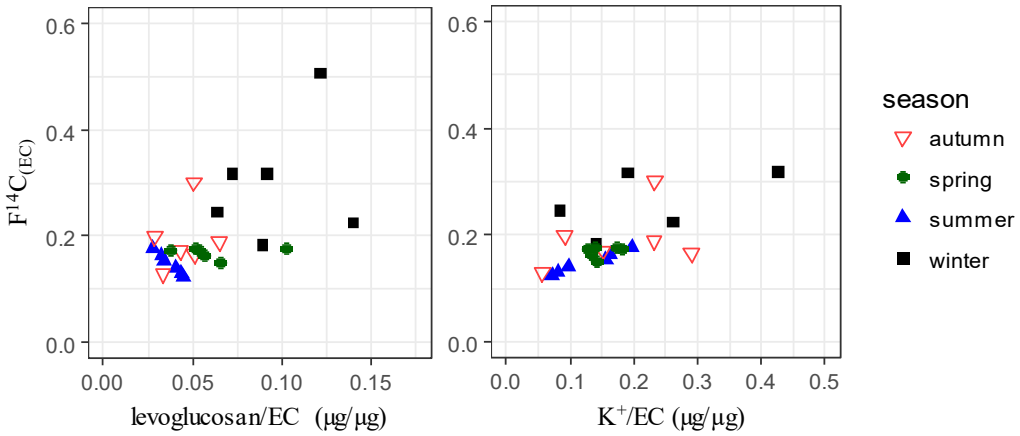

Figure ~~S11~~S5. Correlation between $F^{14}C_{(EC)}$ and levoglucosan/EC ratios, K^+/EC ratios in different seasons (red: autumn; dark green: spring; blue: summer; winter: black). One data point with extremely high K^+ concentration on Chinese New Year is removed.

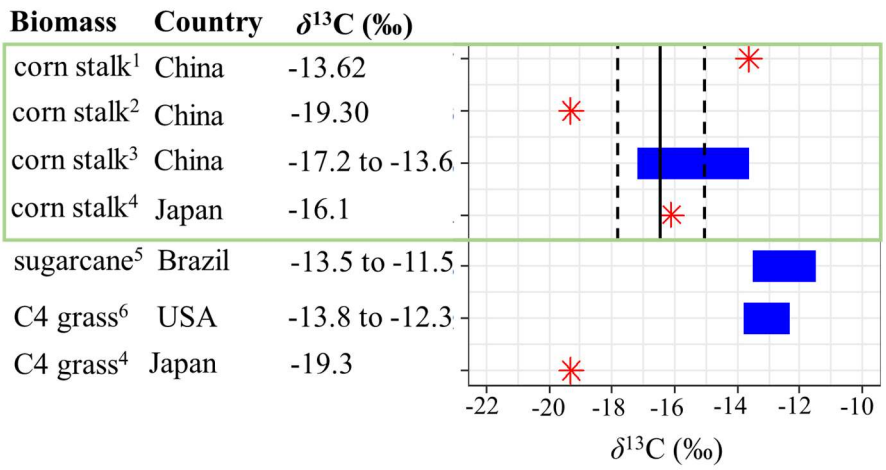

Figure ~~S4~~S6. The $\delta^{13}C$ variability for EC from burning C4 plants ~~endmembers~~. In this study, $\delta^{13}C$ for corn stalk is used as it is the dominant C4 plant in Xi'an and its surrounding areas (Guanzhong Plain). The range used as $\delta^{13}C$ of burning corn stalk is indicated as dashed vertical lines, and the mean is shown by a solid vertical line. Sources: [1]Chen et al. (2012), [2]Guo et al. (2016), [3]Liu et al. (2014), [4]Kawashima and Haneishi (2012), [5]Martinelli et al. (2002), [6]Das et al. (2010).

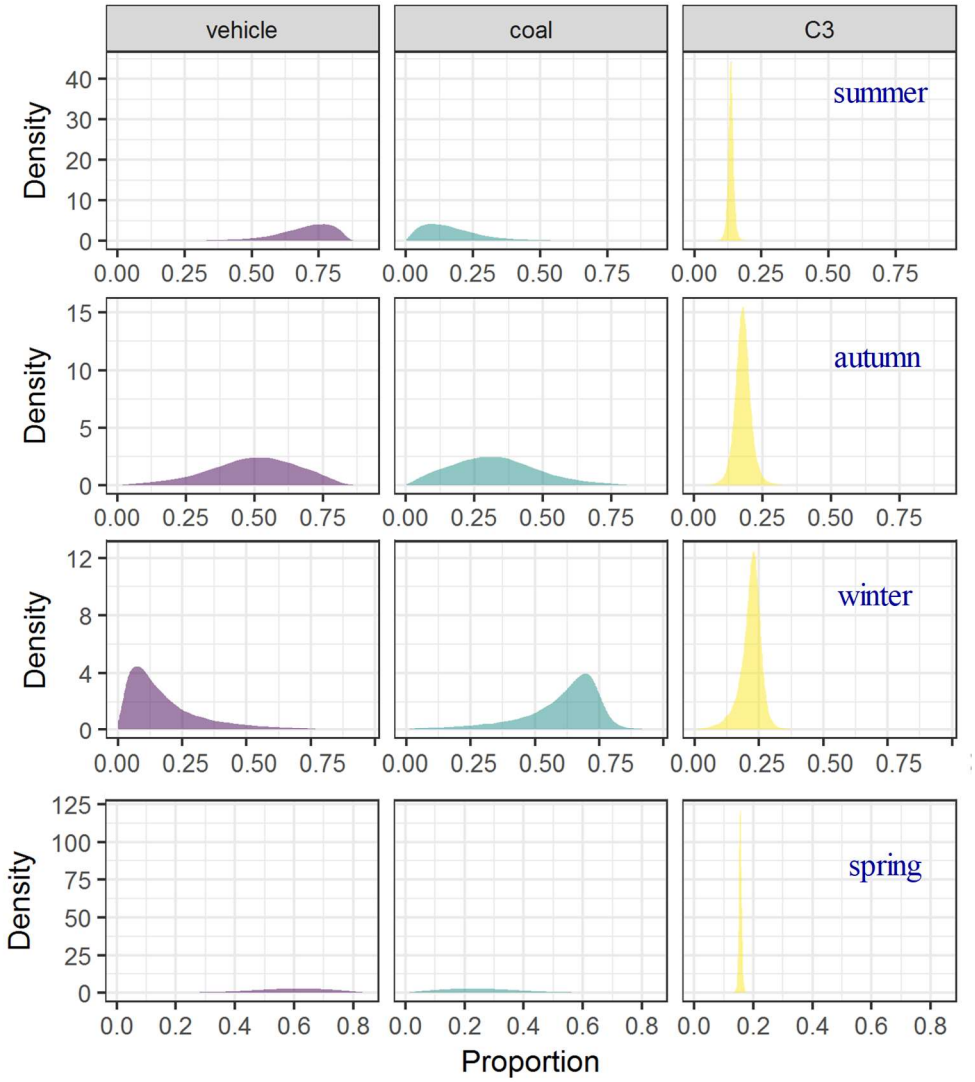

Figure S5S7. MCMC3-derived posterior probability density functions (PDF) of the relative source contributions of C3 plants (denoted as C3), coal and liquid fossil fuel combustion (vehicle) to EC in different seasons, calculated using the Bayesian Markov chain Monte Carlo approach.

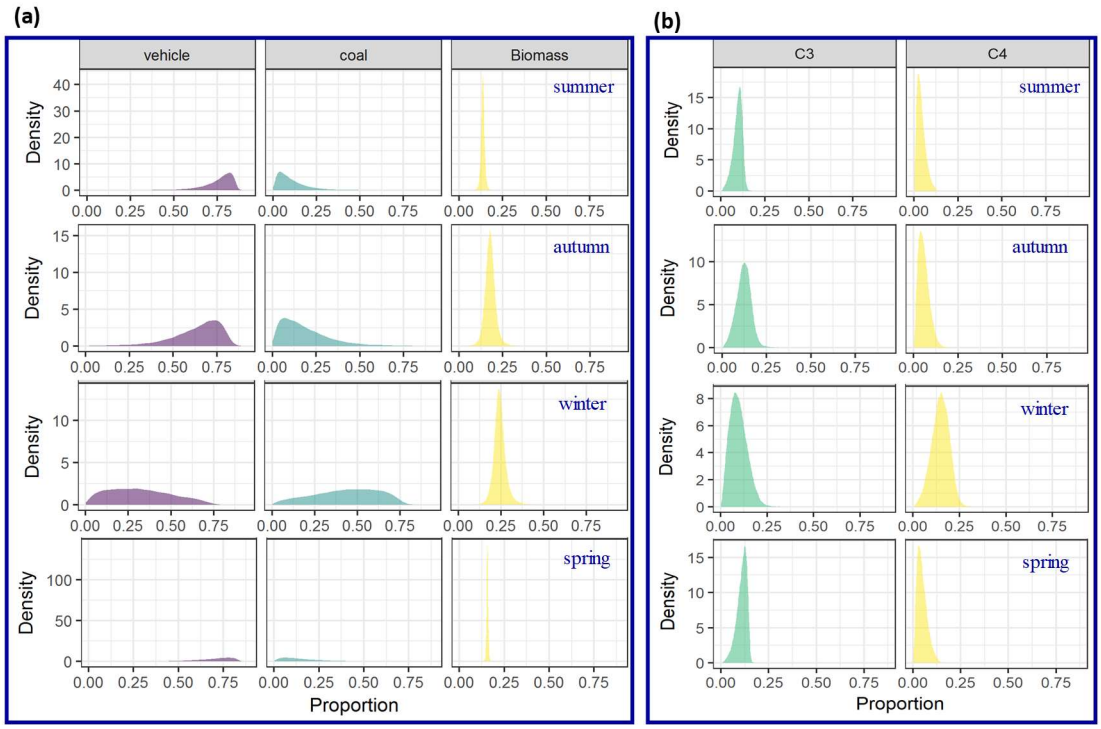

Figure ~~S6~~S8. MCMC4-derived posterior probability density functions (PDF) of the relative source contributions of liquid fossil fuel combustion (vehicle), coal and biomass burning (C3 and C4 plants, denoted as biomass) to EC in different seasons (a), calculated using the Bayesian Markov chain Monte Carlo approach. The PDF of the relative source contributions of biomass burning (a) is a posteriori combination of PDF for C3 plants and C4 plants, as shown in panel (b).

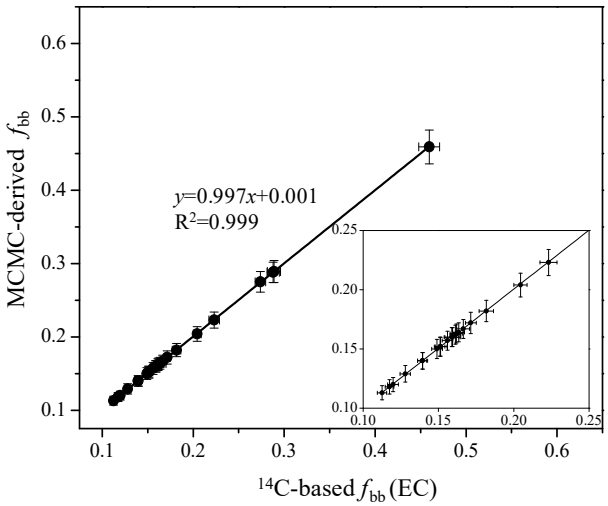

Figure ~~S7~~S9. Comparison between the MCMC-derived fraction of biomass burning EC (~~MCMC-derived~~ f_{bb} derived from MCMC4) and that obtained from radiocarbon data (^{14}C-based f_{bb}(EC)). Average and ~~Error bars represent~~ one standard deviation is shown for f_{bb}(EC), median with interquartile range is shown for f_{bb} . f_{bb} derived from MCMC3 is also very similar to f_{bb}(EC).

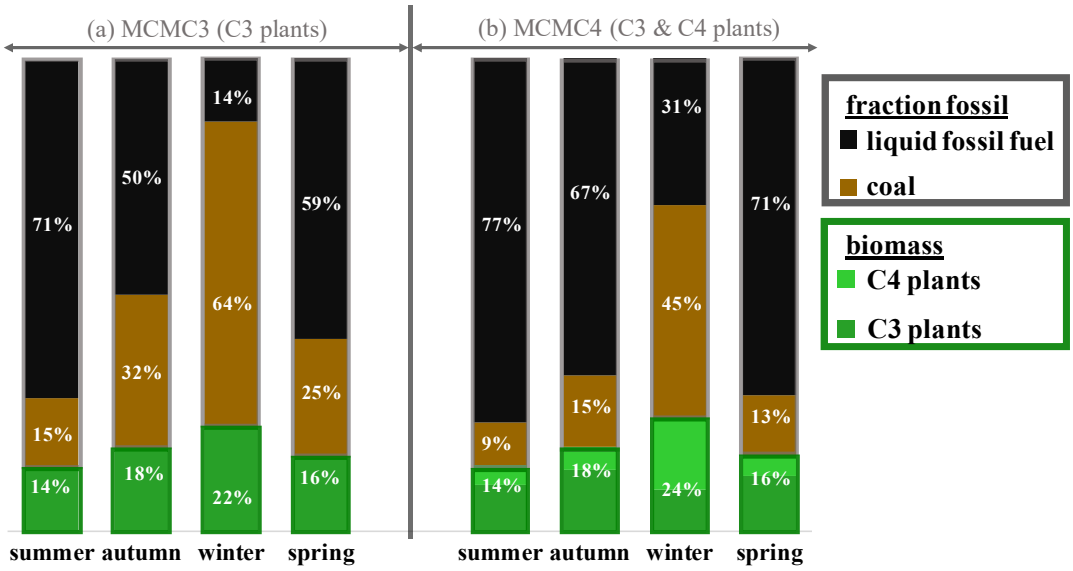

Figure S8S10. Sources of EC in different seasons. Results from the $F^{14}C$ and $\delta^{13}C$ based Bayesian source apportionment calculations of EC. The numbers in the bars represent the median contribution of liquid fossil fuel, coal and biomass burning. (a) results from the MCMC3 model, including C3 plants as biomass, coal and liquid fossil fuel; (b) Impact of C4 plants burning on EC source apportionment is tested by including C4 biomass into the calculations (MCMC4). For MCMC4, the PDF for C3 and C4 plants is combined and named as biomass burning. Bars filled with green colour indicate the relative contribution of biomass burning, including C3 plants (light green) and C4 plants (dark green). In winter, the sample taken on Chinese New Year eve (25 January 2009) was excluded.

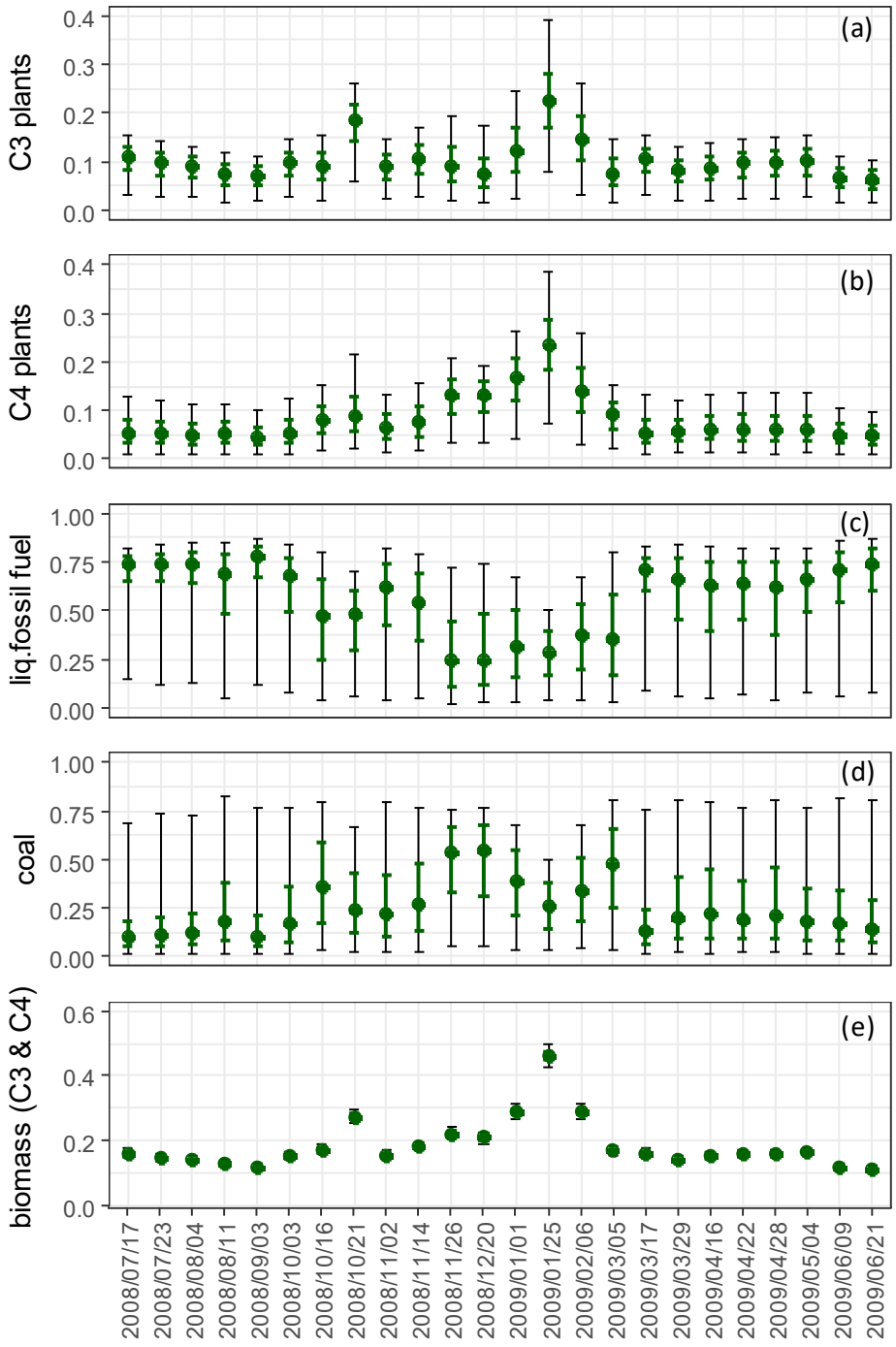

Figure S9S11. MCMC4-derived source contributions to EC for each data point computed using the Bayesian Markov chain Monte Carlo approach. (a). biomass burning from C3 plants; (b). biomass burning from C4 plants; (c). liquid fossil fuel combustion; (d). coal combustion. Range of 95 % credible intervals (Bayesian analogue of confidence intervals) and interquartile range (25^{th}-75^{th} percentile) from the computed probability density functions (PDF) and shown in black and green error bars, respectively. To better compare results with MCMC3, we did a posteriori combination of PDF for C3 biomass (a) and C4 biomass (b) and named the combined PDF as biomass burning (e).

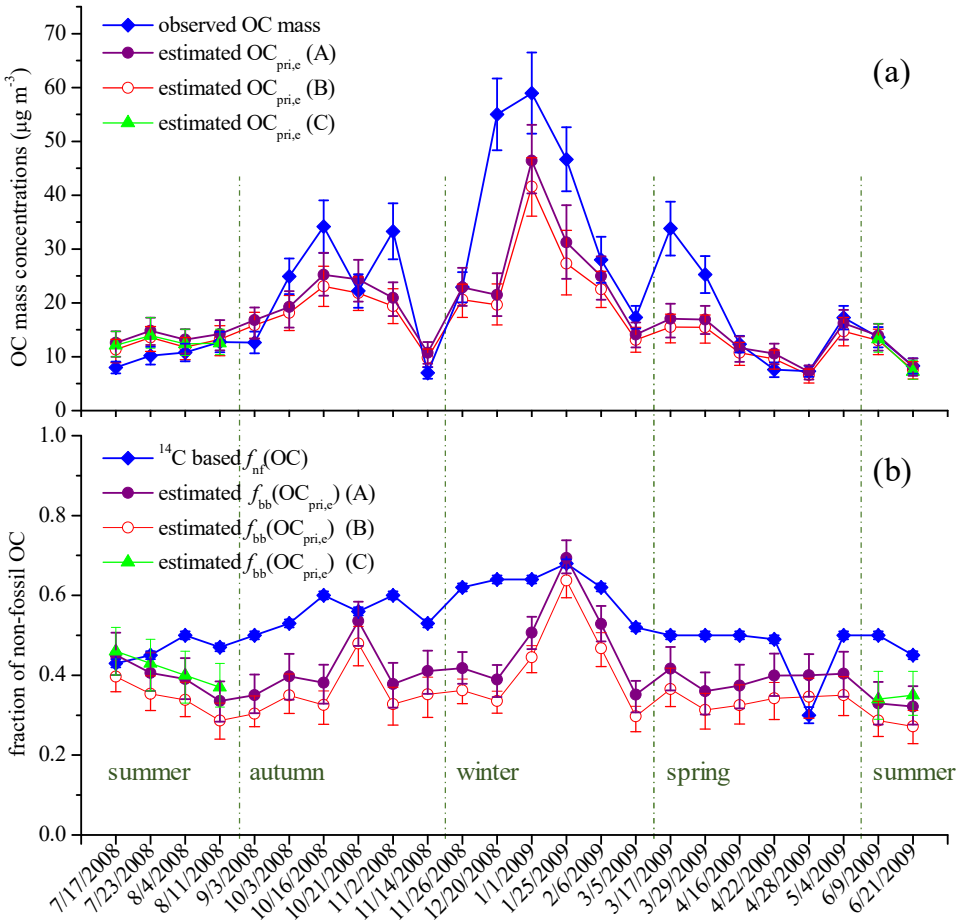

Figure S12. Estimated primary OC based on MCMC3 results. (a) measured OC concentrations (blue line and diamond symbols) with observational uncertainties (vertical bar) and estimated OC mass ($OC_{pri,e}$, circle and triangular symbols) from apportioned EC and OC/EC ratios for different sources (Eq. (10)). (b) ^{14}C-based fraction of non-fossil OC ($f_{nf}(OC)$) and modelled non-fossil fraction in $OC_{pri,e}$ ($f_{bb}(OC_{pri,e})$) derived from Eq. (11). Interquartile range (25^{th}-75^{th} percentile) of the median $OC_{pri,e}$ and $f_{bb}(OC_{pri,e})$ are shown in purple (A), red (B) and green (C) vertical bars. "A" and "B" denotes different OC/EC ratios applied to primary biomass burning emissions (r_{bb}): A. $r_{bb} = 5$ (3–7, minimum-maximum), B. $r_{bb} = 4$ (3–5). "C" denotes 80 % $r_{liq.fossil}$ applied in summer with $r_{bb} = 5$. $f_{nf}(OC)$ uncertainties are shown but not visible.

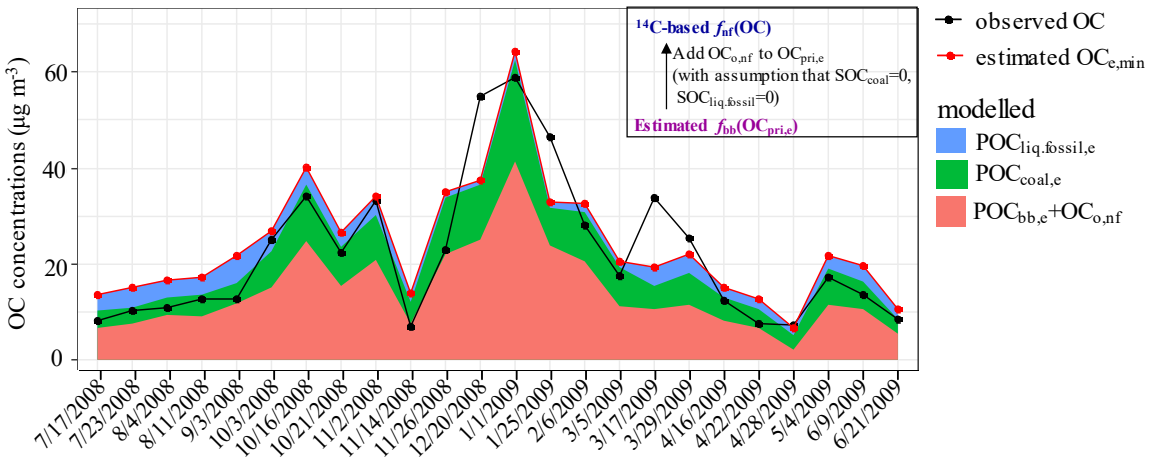

Figure S13. Observed and estimated OC concentrations. Modelled $OC_{e,min}$ is the sum of $OC_{pri,e}$ and $OC_{o,nf}$. $OC_{o,nf}$ accounts for the differences between $f_{nf}(OC)$ and $f_{bb}(OC_{pri,e})$, with an unrealistic assumption of no secondary fossil OC, leading to minimum addition to $OC_{pri,e}$. Coral area shows the $POC_{bb,e}$ and $OC_{o,nf}$, green area the $POC_{coal,e}$ and blue area the $POC_{liq.fossil,e}$. Estimation is based on MCMC3 results for EC source apportionment and primary OC/EC ratios corresponding to case (A) in Fig. S12.

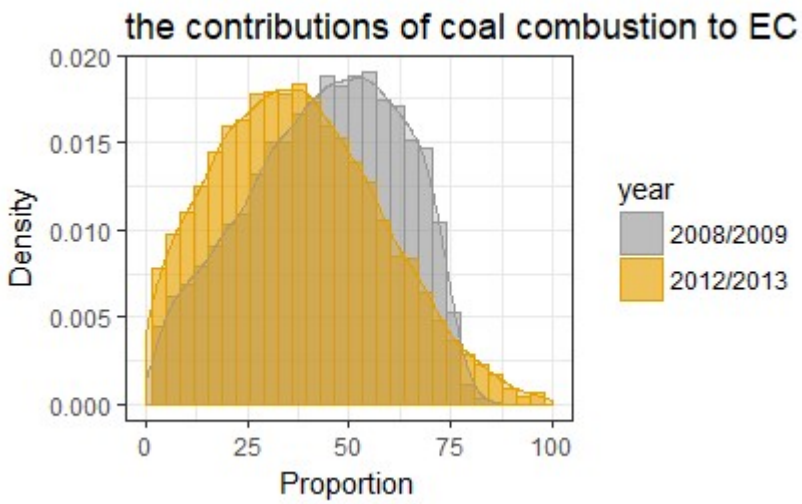

Figure S14. Probability density functions (PDF) of the relative source contributions of coal combustion to EC in winter in the year 2008/2009 (this study, shown in grey; this is also shown in Fig. S8) and 2012/2013 by Wang et al. (2016), shown in yellow.

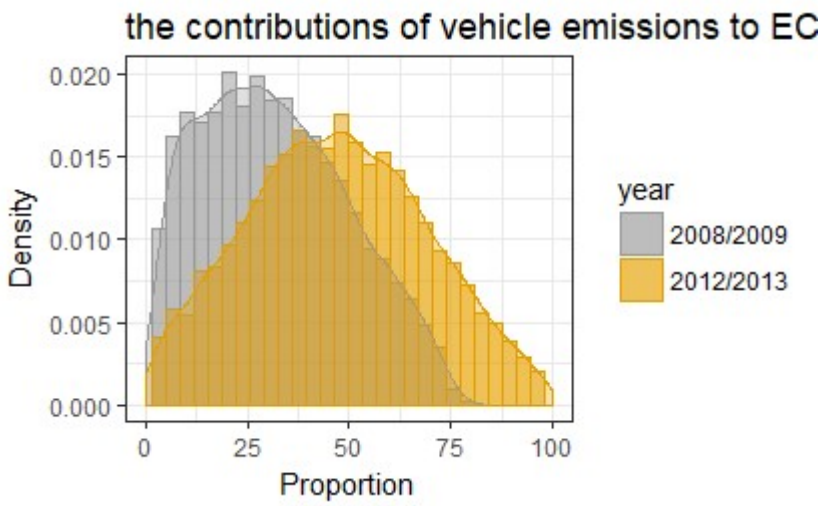

Figure S15. Probability density functions (PDF) of the relative source contributions of vehicle emissions to EC in winter in the year 2008/2009 (this study, shown in grey; this is also shown in Fig. S8) and 2012/2013 by Wang et al. (2016), shown in yellow.

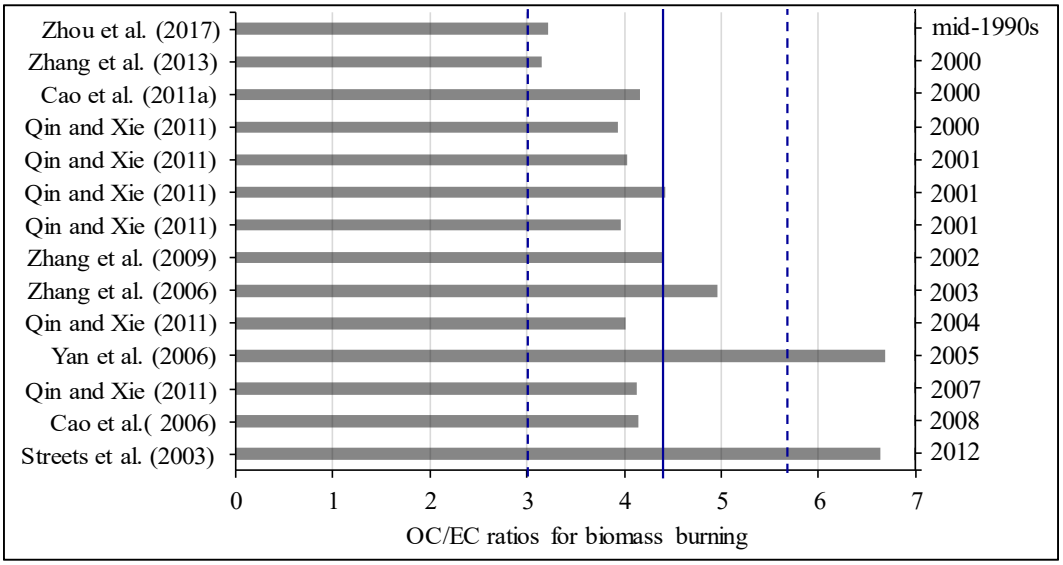

Figure ~~S14~~S16. OC/EC ratios estimated from OC and EC emission amounts from biomass burning emission inventories specific to China. y-axis on the right side indicates the year of estimation. The range applied in OC estimation (Sect. ~~3.5~~4.4 in main text) is shown by dashed vertical lines, and the mean is indicated by a full vertical line. Data sources: Streets et al. (2003); Yan et al. (2006); Zhang et al. (2006, 2009); Cao et al. (2006, 2011a), Qin and Xie (2011), Zhang et al. (2013), Zhou et al. (2017).

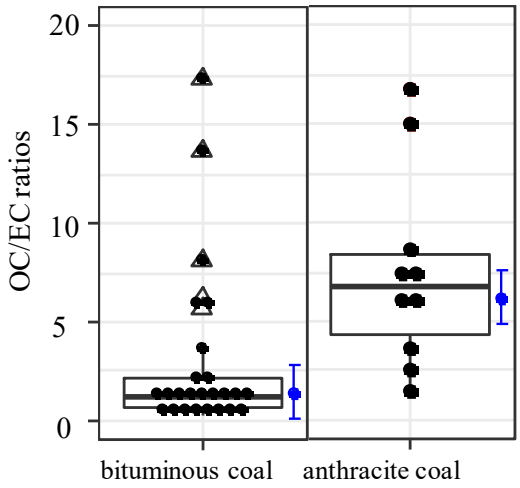

Figure ~~S15~~S17. Literature reported OC/EC ratios for combustion of bituminous coal and anthracite coal. Boxplots show the median (thick line across the box), interquartile range (25^{th}-75^{th} percentile, vertical ends of the box). Outliers are shown as triangles. Blue dots (averages) with error bars (one standard deviation) represents OC/EC ratios measured by IMPROVE_A protocol reported by Tian et al. (2017). Data sources: Chen et al. (2005, 2006, 2015), Zhang et al., (2008, 2012), Zhi et al. (2008), Shen et al. (2010, 2015), Li et al. (2016b).

Table S1. Range of $\delta^{13}C$ values for each source reported in previous studies

Sources	$\delta^{13}C$ ~~(‰)~~ of emissions from sources (ranges)	Source signatures of $\delta^{13}C$ used in the source apportionment calculations of EC (mean ± standard deviation)	Reference
Corn stalk~~C4 plants (corn, sugar cane, grass)~~	-19.30 ‰ to -~~11.5~~13.6 ‰[a]	-16.4 ± 1.4 ‰[a]	(Martinelli et al., 2002; Das et al., 2010; Chen et al., 2012; Kawashima and Haneishi, 2012; Liu et al., 2014; Guo et al., 2016)
C3 plants (wood, wheat straw, etc.)	-35 ‰ to -24 ‰ ~~-26.7 ± 1.8 ‰~~	-26.7 ± 1.8 ‰	Andersson et al. (2015) and references therein
coal	-25 ‰ to -21 ‰ ~~-23.38 ± 1.3 ‰~~	-23.4 ± 1.3 ‰	Andersson et al. (2015) and references therein
liquid fuel (e.g., gasoline, diesel, and oil)	-28 ‰ to -24 ‰ ~~-25.5 ± 1.3 ‰~~	-25.5 ± 1.3 ‰	Andersson et al. (2015) and references therein

[a] $\delta^{13}C$ source signatures for ~~emissions~~ EC from burning corn stalk (C4 plant) of -16.4~~5~~ ± 1.4 ‰ (mean ± standard deviation) are applied in MCMC4 calculations. In this study, $\delta^{13}C$ for corn stalk is used as it is the dominant C4 plant in Xi'an and its surrounding areas (Sun et al., 2017; Zhu et al., 2017), with little sugarcane and other C4 plants. See details on selection of $\delta^{13}C$ signature for C4 plants in the study area (corn stalk) in Sect.~~3.4.1~~4.3.1 and Fig. S6..

Table S2. Mass concentrations of $PM_{2.5}$, OC and EC in Xi'an, China from July 2008 to June 2009.

	$PM_{2.5}$ (μg m^{-3})	OC (μg m^{-3})	EC (μg m^{-3})
Spring (n=~~12~~13)	124.0 ± 40.4 *(55.9–193.4)*[a]	14.4 ± 9.6 *(3.3–33.8)*	5.7 ± 2.3 *(2.0–8.8)*
Summer (n=~~22~~15)	83.0 ± 30.7 *(31.8–139.2)*	12.7 ± 4.5 *(4.0–20.6)*	6.3 ± 2.0 *(2.7–10.0)*
Autumn (n=12)	125.1 ± 69.3 *(41.0–212.6)*	22.2 ± 13.6 *(3.6–34.2)*	8.4 ± 2.9 *(3.5–11.3)*
Winter (n=~~19~~18)	213.4 ± 91.8 *(73.1–408.5)*	39.0 ±17.8 *(10.8–67.0)*	9.1 ± 3.1 *(5.6–16.3)*
Annual	142.0 ± 82.4 *(31.8–408.5)*	21.5 ± 16.6 *(3.3–67.0)*	7.6 ± 3.0 *(2.0–16.3)*

[a] average ± standard deviation, the number in the parentheses is the range of each dataset.

Table S3. Average fraction modern ($F^{14}C$) and stable carbon signature ($\delta^{13}C$, ‰) of OC and EC for selected samples.

Date	$F^{14}C_{(OC)}$	$F^{14}C_{(EC)}$	$\delta^{13}C_{OC}$	$\delta^{13}C_{EC}$	Season
7/17/2008[a]	0.466 ± 0.010	0.178 ± 0.003	-26.80	-26.50	summer
7/23/2008	0.489 ± 0.008	0.164 ± 0.003	-25.94	-26.33	summer
8/4/2008	0.546 ± 0.007	0.153 ± 0.002	-25.86	-26.16	summer
8/11/2008	0.512 ± 0.008	0.141 ± 0.003	-25.21	-25.53	summer
9/3/2008	0.549 ± 0.006	0.129 ± 0.002	-25.94	-26.23	autumn
10/3/2008	0.581 ± 0.006	0.166 ± 0.002	-24.55	-25.51	autumn
10/16/2008	0.659 ± 0.007	0.188 ± 0.002	-23.70	-24.31	autumn
10/21/2008	0.610 ± 0.005	0.301 ± 0.003	-24.51	-24.92	autumn
11/2/2008	0.651 ± 0.006	0.172 ± 0.002	-24.94	-25.10	autumn
11/14/2008	0.579 ± 0.007	0.200 ± 0.004	-25.48	-24.79	autumn
11/26/2008	0.671 ± 0.009	0.245 ± 0.004	-24.71	-22.93	winter
12/20/2008	0.696 ± 0.008	0.225 ± 0.002	-24.06	-22.81	winter
1/1/2009	0.693 ± 0.007	0.317 ± 0.004	-23.23	-23.12	winter
1/25/2009	0.745 ± 0.005	0.505 ± 0.008	-23.39	-23.07	winter
2/6/2009	0.671 ± 0.007	0.318 ± 0.005	-23.92	-23.72	winter
3/5/2009	0.572 ± 0.006	0.183 ± 0.003	-25.44	-23.53	winter
3/17/2009	0.545 ± 0.004	0.177 ± 0.002	-25.72	-26.03	spring
3/29/2009	0.547 ± 0.006	0.153 ± 0.002	-26.91	-25.38	spring
4/16/2009	0.545 ± 0.007	0.166 ± 0.003	-27.42	-25.05	spring
4/22/2009	0.535 ± 0.006	0.175 ± 0.004	-26.33	-25.27	spring
4/28/2009	0.330 ± 0.021	0.175 ± 0.005	-26.41	-25.33	spring
5/4/2009	0.544 ± 0.004	0.180 ± 0.003	-26.66	-25.35	spring
6/9/2009	0.549 ± 0.006	0.132 ± 0.003	-24.24	-25.37	summer
6/21/2009	0.489 ± 0.006	0.124 ± 0.002	-26.30	-25.73	summer
summer[b]	0.509 ± 0.033	0.149 ± 0.020	-25.73 ± 0.90	-25.94 ± 0.465	
autumn	0.605 ± 0.044	0.193 ± 0.058	-24.859 ± 0.798	-25.14 ± 0.667	
winter	0.675 ± 0.057	0.299 ± 0.114	-24.13 ± 0.83	-23.20 ± 0.354	
spring	0.508 ± 0.087	0.171 ± 0.010	-26.586 ± 0.576	-25.40 ± 0.334	

[a] Daily $F^{14}C$ values are given in average ± measurement uncertainties;

[b] Seasonal averaged $F^{14}C$ and $\delta^{13}C$ values are given in average ± standard deviation.

Table S4. Average OC and EC concentrations from non-fossil sources (OC_{nf}, EC_{bb}) and fossil sources (OC_{fossil}, EC_{fossil}), relative non-fossil sources contribution to OC and EC (f_{nf}(OC), f_{bb}(EC)), and relative fossil sources contribution to OC and EC (f_{fossil}(OC), f_{fossil}(EC)).

Date	OC_{nf}	OC_{fossil}	EC_{bb}	EC_{fossil}	f_{nf}(OC)	f_{fossil}(OC)	f_{bb}(EC)	f_{fossil}(EC)	Season
7/17/2008	3.53 ± 0.50	4.48 ± 0.63	1.13 ± 0.26	5.87 ± 1.29	0.440 ± 0.010	0.560 ± 0.010	0.162 ± 0.004	0.838 ± 0.004	summer
7/23/2008	4.70 ± 0.75	5.49 ± 0.89	1.20 ± 0.24	6.84 ± 1.41	0.461 ± 0.009	0.539 ± 0.009	0.149 ± 0.004	0.851 ± 0.004	summer
8/4/2008	5.56 ± 0.85	5.22 ± 0.80	1.01 ± 0.21	6.21 ± 1.26	0.515 ± 0.008	0.485 ± 0.008	0.139 ± 0.003	0.861 ± 0.003	summer
8/11/2008	6.16 ± 0.93	6.59 ± 0.99	0.96 ± 0.21	6.51 ± 1.41	0.483 ± 0.009	0.517 ± 0.009	0.128 ± 0.003	0.872 ± 0.003	summer
9/3/2008	6.54 ± 1.05	6.09 ± 0.98	1.17 ± 0.18	8.81 ± 1.32	0.518 ± 0.007	0.482 ± 0.007	0.117 ± 0.003	0.883 ± 0.003	autumn
10/3/2008	13.65 ± 1.80	11.26 ± 1.50	1.54 ± 0.31	8.64 ± 1.75	0.548 ± 0.007	0.452 ± 0.007	0.151 ± 0.003	0.849 ± 0.003	autumn
10/16/2008	21.23 ± 3.11	12.95 ± 1.86	1.94 ± 0.32	9.40 ± 1.57	0.622 ± 0.008	0.378 ± 0.008	0.171 ± 0.004	0.829 ± 0.004	autumn
10/21/2008	12.82 ± 1.78	9.41 ± 1.32	2.65 ± 0.44	7.03 ± 1.13	0.576 ± 0.007	0.424 ± 0.007	0.274 ± 0.006	0.726 ± 0.006	autumn
11/2/2008	20.42 ± 3.22	12.82 ± 2.03	1.60 ± 0.22	8.62 ± 1.20	0.614 ± 0.008	0.386 ± 0.008	0.156 ± 0.003	0.844 ± 0.003	autumn
11/14/2008	3.83 ± 0.60	3.16 ± 0.50	0.89 ± 0.18	4.00 ± 0.78	0.546 ± 0.008	0.454 ± 0.008	0.182 ± 0.005	0.818 ± 0.005	autumn
11/26/2008	14.49 ± 1.80	8.41 ± 1.05	1.91 ± 0.36	6.66 ± 1.25	0.634 ± 0.010	0.366 ± 0.010	0.223 ± 0.006	0.777 ± 0.006	winter
12/20/2008	36.16 ± 4.43	18.83 ± 2.37	1.69 ± 0.43	6.56 ± 1.69	0.657 ± 0.009	0.343 ± 0.009	0.204 ± 0.004	0.796 ± 0.004	winter
1/1/2009	38.59 ± 4.92	20.39 ± 2.65	4.69 ± 0.71	11.62 ± 1.72	0.654 ± 0.008	0.346 ± 0.008	0.288 ± 0.007	0.712 ± 0.007	winter
1/25/2009	32.79 ± 4.19	13.86 ± 1.78	4.34 ± 1.34	5.10 ± 1.58	0.703 ± 0.007	0.297 ± 0.007	0.459 ± 0.011	0.541 ± 0.011	winter
2/6/2009	17.71 ± 2.74	10.27 ± 1.61	2.68 ± 0.50	6.58 ± 1.19	0.633 ± 0.008	0.367 ± 0.008	0.289 ± 0.007	0.711 ± 0.007	winter
3/5/2009	9.36 ± 1.15	7.98 ± 0.98	0.99 ± 0.22	4.97 ± 1.08	0.540 ± 0.007	0.460 ± 0.007	0.166 ± 0.004	0.834 ± 0.004	winter
3/17/2009	17.38 ± 2.58	16.39 ± 2.47	1.41 ± 0.27	7.33 ± 1.37	0.514 ± 0.006	0.486 ± 0.006	0.161 ± 0.003	0.839 ± 0.003	spring
3/29/2009	13.05 ± 1.77	12.21 ± 1.67	1.22 ± 0.19	7.56 ± 1.15	0.517 ± 0.007	0.483 ± 0.007	0.139 ± 0.003	0.861 ± 0.003	spring
4/16/2009	6.33 ± 0.80	5.98 ± 0.76	0.87 ± 0.19	4.87 ± 1.07	0.515 ± 0.008	0.485 ± 0.008	0.151 ± 0.004	0.849 ± 0.004	spring
4/22/2009	3.84 ± 0.68	3.77 ± 0.68	0.84 ± 0.17	4.43 ± 0.89	0.505 ± 0.007	0.495 ± 0.007	0.159 ± 0.005	0.841 ± 0.005	spring
4/28/2009	2.28 ± 0.35	5.03 ± 0.72	0.58 ± 0.12	3.08 ± 0.63	0.311 ± 0.019	0.689 ± 0.019	0.159 ± 0.005	0.841 ± 0.005	spring
5/4/2009	8.86 ± 1.12	8.41 ± 1.08	1.30 ± 0.25	6.65 ± 1.30	0.513 ± 0.006	0.487 ± 0.006	0.163 ± 0.004	0.837 ± 0.004	spring
6/9/2009	7.07 ± 0.98	6.57 ± 0.92	0.91 ± 0.17	6.72 ± 1.23	0.518 ± 0.007	0.482 ± 0.007	0.120 ± 0.004	0.880 ± 0.004	summer
6/21/2009	3.81 ± 0.66	4.47 ± 0.78	0.52 ± 0.13	4.07 ± 1.02	0.462 ± 0.006	0.538 ± 0.006	0.113 ± 0.003	0.887 ± 0.003	summer

Table S5. OC and EC concentrations from non-fossil sources (OC_{nf}, EC_{bb}) and fossil sources (OC_{fossil}, EC_{fossil}), relative non-fossil sources contribution to OC and EC (f_{nf}(OC), f_{bb}(EC)), and relative fossil sources contribution to OC and EC (f_{fossil}(OC), f_{fossil}(EC)) in different seasons.

Season	OC_{nf}	OC_{fossil}	EC_{bb}	EC_{fossil}	f_{nf}(OC)	f_{fossil}(OC)	f_{bb}(EC)	f_{fossil}(EC)
summer	5.14 ± 1.38[a]	5.47 ± 0.95	0.95 ± 0.24	6.03 ± 1.02	0.480 ± 0.032	0.520 ± 0.032	0.135 ± 0.018	0.865 ± 0.018
	(3.53 ~ 7.07)	*(4.47 ~ 6.59)*	*(0.52 ~ 1.20)*	*(4.07 ~ 6.84)*	*(0.440 ~ 0.518)*	*(0.482 ~ 0.560)*	*(0.113 ~ 0.162)*	*(0.838 ~ 0.887)*
autumn	13.08 ± 7.06	9.28 ± 3.94	1.63 ± 0.62	7.75 ± 2.00	0.571 ± 0.041	0.429 ± 0.041	0.175 ± 0.053	0.825 ± 0.053
	(3.83 ~ 21.23)	*(3.16 ~ 12.95)*	*(0.89 ~ 2.65)*	*(4.00 ~ 9.40)*	*(0.518 ~ 0.622)*	*(0.378 ~ 0.482)*	*(0.117 ~ 0.274)*	*(0.726 ~ 0.883)*
winter[b]	23.26 ± 13.25	13.18 ± 5.96	2.39 ± 1.42	7.28 ± 2.53	0.624 ± 0.048	0.376 ± 0.048	0.234 ± 0.054	0.766 ± 0.054
	(9.36 ~ 38.59)	*(7.98 ~ 20.39)*	*(0.99 ~ 4.69)*	*(4.97 ~ 11.62)*	*(0.540 ~ 0.657)*	*(0.343 ~ 0.460)*	*(0.166 ~ 0.289)*	*(0.711 ~ 0.834)*
spring	8.62 ± 5.74	8.63 ± 4.83	1.04 ± 0.32	5.65 ± 1.80	0.479 ± 0.082	0.521 ± 0.082	0.155 ± 0.009	0.845 ± 0.009
	(2.28 ~ 17.38)	*(3.77 ~ 16.39)*	*(0.58 ~ 1.41)*	*(3.08 ~ 7.56)*	*(0.311 ~ 0.517)*	*(0.483 ~ 0.689)*	*(0.139 ~ 0.163)*	*(0.837 ~ 0.861)*
overall[b]	12.06 ± 9.81	8.96 ± 4.79	1.46 ± 0.90	6.65 ± 1.96	0.535 ± 0.080	0.465 ± 0.080	0.172 ± 0.051	0.828 ± 0.051
	(2.28 ~ 38.59)	*(3.16 ~ 20.39)*	*(0.52 ~ 4.69)*	*(3.08 ~ 11.62)*	*(0.311 ~ 0.657)*	*(0.343 ~ 0.689)*	*(0.113 ~ 0.289)*	*(0.711 ~ 0.887)*

[a] data is given in average ± standard deviation, minimum and maximum are shown in parentheses

[b] the sample taken on Chinese New Year eve (25 January 2009) was excluded.

Table ~~S8~~S6. Stable carbon isotopes for aerosols in China.

Location		Site type	Sampling period	Seasons	PM fraction	$\delta^{13}C_{OC}$ (‰)	$\delta^{13}C_{EC}$ (‰)	References
North China	Beijing, China	urban	Jan, 2013	winter	$PM_{2.5}$	-24.26 ± 0.29		Yan et al. (2017)
	Beijing, China	urban	Feb, 2010	winter	$PM_{2.5}$		-25.1 to -24.2	Chen et al. (2013)
	North China Plain	urban	Jan, 2013	winter	$PM_{2.5}$		-24.3 to -23.3	Andersson et al. (2015)
	7 cities in North China	urban	Jan 6–20, 2003	winter	$PM_{2.5}$	-25.54 to -23.08	-25.02 to -23.27	Cao et al. (2011b)
	Beijing, China	urban	June, 2013	summer	$PM_{2.5}$	-26.74 ± 0.65		Yan et al. (2017)
	7 cities in North China	urban	June 3–July 30, 2003	summer	$PM_{2.5}$	-26.90 to -26.33	-26.62 to -25.27	Cao et al. (2011b)
South China	Hong Kong	urban	Nov 2000–Feb 2001	winter	$PM_{2.5}$	-26.9 ± 0.6	-25.6 ± 0.1	Ho et al. (2006)
	Shanghai, China	urban	Jan, 2010	winter	$PM_{2.5}$		-25.8 to -24.7	Chen et al. (2013)
	Xiamen, China	urban	Dec, 2009	winter	$PM_{2.5}$		-25.3 to -24.9	Chen et al. (2013)
	Pearl River Delta	urban	Jan, 2013	winter	$PM_{2.5}$		-26.7 to -25.7	Andersson et al. (2015)
	Yangtze River Delta	urban	Jan, 2013	winter	$PM_{2.5}$		-27.7 to -25	Andersson et al. (2015)
	7 cities in South China	urban	Jan 6–20, 2003	winter	$PM_{2.5}$	-26.62 to -25.79	-26.10 to -25.33	Cao et al. (2011b)
	Shanghai, China	urban	Sept 1–20, 2009	Autumn	$PM_{2.5}$	-24.5 ± 0.8	-25.1 ± 0.6	Cao et al. (2013)
	Hong Kong	urban	June–August, 2001	summer	$PM_{2.5}$	-26.9 ± 0.5	-25.6 ± 0.1	Ho et al. (2006)
	7 cities in South China	urban	June 3–July 30, 2003	summer	$PM_{2.5}$	-26.74 to -25.29	-26.63 to -25.41	Cao et al. (2011b)
North China	Xi'an China	urban		winter	$PM_{2.5}$	-24.1~~3~~ ± 0.8~~3~~	-23.2~~0~~ ± 0.~~35~~4	This study
				autumn	$PM_{2.5}$	-24.9~~85~~ ± 0.~~87~~9	-25.1~~4~~ ± 0.~~66~~7	
				summer	$PM_{2.5}$	-25.7~~3~~ ± 0.9~~0~~	-25.9~~4~~ ± 0.~~46~~5	
				spring	$PM_{2.5}$	-26.~~58~~ 6 ± 0.~~57~~6	-25.4~~0~~ ± 0.3~~3~~	
				annual	$PM_{2.5}$	-25.3~~2~~ ± 1.~~19~~2	-24.9~~2~~ ± 1.1~~4~~	

Table ~~S6~~S7. MCMC3 results[a] from the $F^{14}C$- and $\delta^{13}C$-based Bayesian Source Apportionment Calculations of EC (Median, interquartile range (25^{th}-75^{th} percentile), and 95 % Credible Intervals).

	Seasons	summer	autumn	winter[b]	spring	annual[b]
Biomass burning	median	0.136	0.177	0.221	0.156	0.173
(C3 plants)	25^{th}-75^{th} percentile	(0.129–0.142)	(0.16–0.197)	(0.196–0.242)	(0.153–0.159)	(0.166–0.18)
	95% credible intervals	(0.113–0.159)	(0.117–0.245)	(0.106–0.288)	(0.145–0.167)	(0.15–0.196)
coal combustion	median	0.147	0.323	0.644	0.251	0.328
	25^{th}-75^{th} percentile	(0.086–0.23)	(0.221–0.436)	(0.534–0.709)	(0.167–0.346)	(0.25–0.403)
	95% credible intervals	(0.025–0.494)	(0.061–0.673)	(0.165–0.805)	(0.055–0.56)	(0.117–0.557)
liquid fossil	median	0.717	0.497	0.136	0.594	0.499
	25^{th}-75^{th} percentile	(0.633–0.778)	(0.383–0.607)	(0.076–0.245)	(0.498–0.677)	(0.423–0.578)
	95% credible intervals	(0.365–0.842)	(0.147–0.774)	(0.022–0.61)	(0.282–0.79)	(0.269–0.712)

[a] Three main source categories were differentiated using this technique: C3 plants (e.g., wood and crop residue), coal and liquid fossil fuel (e.g., oil, diesel, and gasoline) combustion.

[b] the sample taken on Chinese New Year eve (25 January 2009) was excluded.

Table ~~S7~~S8. The contribution of C3 and C4 plants burning to EC from the MCMC4 results[a] (Median, interquartile range (25^{th}-75^{th} percentile), and 95% Credible Intervals).

	Seasons	summer	autumn	winter[c]	spring	annual[c]
Biomass burning[b]	median	0.099	0.123	0.088	0.113	0.123
from C3 plants	25^{th}-75^{th} percentile	(0.080–0.114)	(0.094–0.149)	(0.058–0.122)	(0.092–0.129)	(0.105–0.139)
	95% credible intervals	(0.037–0.137)	(0.041–0.199)	(0.019–0.196)	(0.045–0.149)	(0.07–0.165)
Biomass burning	median	0.035	0.051	0.152	0.042	0.05
from C4 plants	25^{th}-75^{th} percentile	(0.022–0.054)	(0.033–0.074)	(0.119–0.182)	(0.027–0.063)	(0.034–0.066)
	95% credible intervals	(0.007–0.097)	(0.012–0.128)	(0.052–0.240)	(0.010–0.11)	(0.013–0.097)

[a]Results from the four-sources (C3 biomass, C4 biomass, coal and liquid fossil fuel) MCMC4 model.

[b]Contribution of biomass burning is shown in Table 2 and done by a posteriori combination of PDF for C3 plants and that for C4 plants.

[c]Sample taken from Chinese New Year eve (25 January 2009) was excluded.

Table S9. The measured $F^{14}C$ values and masses of the standards with their nominal $F^{14}C$ values.

Standards		nominal $F^{14}C$	measured $F^{14}C$ ($F^{14}C_m$)	measured mass (M_m, μgC)
Combustion processes[a]	OXII	1.3406	1.327 ± 0.022	65
	OXII	1.3406	1.321 ± 0.012	117
	anthracite	0	0.020 ± 0.001	51
	anthracite	0	0.002 ± 0.001	75
	anthracite	0	0.004 ± 0.001	219
	anthracite	0	0.005 ± 0.001	254
Graphitization and ^{14}C measurements[b]	^{14}C-free CO_2 gas	0	0.008 ± 0.001	42
	^{14}C-free CO_2 gas	0	0.004 ± 0.000	81
	^{14}C-free CO_2 gas	0	0.005 ± 0.000	91
	^{14}C-free CO_2 gas	0	0.004 ± 0.000	123
	^{14}C-free CO_2 gas	0	0.003 ± 0.000	162
	^{14}C-free CO_2 gas	0	0.002 ± 0.000	186
	^{14}C-free CO_2 gas	0	0.003 ± 0.000	287
	OXII	1.3406	1.268 ± 0.013	45
	OXII	1.3406	1.270 ± 0.012	81
	OXII	1.3406	1.280 ± 0.011	96
	OXII	1.3406	1.305 ± 0.010	128
	OXII	1.3406	1.337 ± 0.010	162
	OXII	1.3406	1.306 ± 0.006	214
	OXII	1.3406	1.311 ± 0.005	321

[a] For combustion processes, two sets of standard material: the oxalic acid HOxII and anthracite with known ^{14}C contents ($F^{14}C$ = 1.3406 and $F^{14}C$ = 0, respectively) were combusted using ACS and used for quality control;

[b] Varying amounts of reference materials covering the range of sample mass are graphitized and analyzed together with samples in the same wheel of AMS, to correct contamination during graphitization and AMS measurement.

Table S9S10. Published OC/EC ratios for vehicle emissions specific to China.

OC/EC ratios	Sampling site	Measurement protocol	References
0.6 ± 0.2	Shing Mun tunnel (Hongkong, China)	IMPROVE[a]	Cheng et al. (2010)
0.8 ± 0.1	roadside sites (Hongkong, China)	IMPROVE[a]	Cheng et al. (2010)
0.86* (0.48–1.45)**	Wuzushan tunnel (Yantai, China)	IMPROVE[a]	Cui et al. (2016)
1.03*(0.77–1.35)**	Zhujiang tunnel (Guangzhou, China)	NIOSH[b]	Dai et al. (2015)
0.49 ± 0.04 (0.44–0.57)**	Zhujiang tunnel (Guangzhou, China)	NIOSH[b]	He et al. (2008)
0.57	Zhujiang tunnel (Guangzhou, China)	NIOSH[b]	Huang et al. (2006)
1.45	Zhujiang tunnel (Guangzhou, China)	NIOSH[b]	Zhang et al. (2015a)

*represents averaged values;
** represents the range of values;
[a] Chow et al. (2004);
[b] Birch and Cary, (1996).

References

Andersson, A., Deng, J., Du, K., Zheng, M., Yan, C., Sköld, M., and Gustafsson, Ö.: Regionally-varying combustion sources of the January 2013 severe haze events over eastern China, Environ. Sci. Technol., 49, 2038–2043, 2015.

Birch, M. and Cary, R.: Elemental carbon-based method for monitoring occupational exposures to particulate diesel exhaust, Aerosol Sci. Technol., 25, 221–241, 1996.

Cao, G., Zhang, X., and Zheng, F.: Inventory of black carbon and organic carbon emissions from China, Atmos. Environ., 40, 6516–6527, 2006.

Cao, G., Zhang, X., Gong, S., An, X., and Wang, Y.: Emission inventories of primary particles and pollutant gases for China, Chin. Sci. Bull., 56, 781–788, 2011a.

Cao, J. J., Chow, J. C., Tao, J., Lee, S.C., Watson, J. G., Ho, K.F., Wang, G.H., Zhu, C.S., and Han, Y.M.: Stable carbon isotopes in aerosols from Chinese cities: influence of fossil fuels, Atmos. Environ., 45, 1359–1363, 2011b.

Cao, J. J., Zhu, C. S., Tie, X. X., Geng, F. H., Xu, H. M., Ho, S. S. H., Wang, G. H., Han, Y. M., and Ho, K. F.: Characteristics and sources of carbonaceous aerosols from Shanghai, China, Atmos. Chem. Phys., 13, 803–817, 2013.

Chen, B., Andersson, A., Lee, M., Kirillova, E. N., Xiao, Q., Kruså, M., Shi, M., Hu, K., Lu, Z., Streets, D. G., Du, K., and Gustafsson, Ö.: Source forensics of black carbon aerosols from China, Environ. Sci. Technol., 47, 9102–9108, 2013.

Chen, Y., Sheng, G., Bi, X., Feng, Y., Mai, B., and Fu, J.: Emission factors for carbonaceous particles and polycyclic aromatic hydrocarbons from residential coal combustion in China, Environ. Sci. Technol., 39, 1861–1867, 2005.

Chen, Y., Zhi, G., Feng, Y., Fu, J., Feng, J., Sheng, G., and Simoneit, B. R. T.: Measurements of emission factors for primary carbonaceous particles from residential raw-coal combustion in China, Geophys. Res. Lett., 33, 2006.

Chen, Y., Cai, W., Huang, G., Li, J., and Zhang, G.:Stable carbon isotope of black carbon from typical emission sources in China. Environ. Sci. 33, 673–678, 2012 (in Chinese).

Chen, Y., Tian, C., Feng, Y., Zhi, G., Li, J., and Zhang, G.: Measurements of emission factors of $PM_{2.5}$, OC, EC, and BC for household stoves of coal combustion in China, Atmos. Environ., 109, 190–196, 2015.

Cheng, Y., Lee, S. C., Ho, K. F., Chow, J. C., Watson, J. G., Louie, P. K. K., Cao, J. J., and Hai, X.: Chemically-speciated on-road $PM_{2.5}$ motor vehicle emission factors in Hong Kong, Sci. Total Environ., 408, 1621–1627, 2010.

Chow, J. C., Watson, J. G., Crow, D., Lowenthal, D. H., and Merrifield, T.: Comparison of IMPROVE and NIOSH carbon measurements, Aerosol Sci. Technol., 34, 23–34, 2001.

Chow, J. C., Watson, J. G., Chen, L.-W. A., Arnott, W. P., Moosmüller, H., and Fung, K. K.: Equivalence of elemental carbon by Thermal/Optical Reflectance and Transmittance with different temperature protocols, Environ. Sci. Technol., 38, 4414–4422, 2004.

Chow, J. C., Watson, J. G., Chen, L.-W. A., Chang, M. O., Robinson, N. F., Trimble, D., and Kohl, S.: The IMPROVE_A temperature protocol for thermal/optical carbon analysis: maintaining consistency with a long-term database, J. Air Waste Manage., 57, 1014–1023, 2007.

Cui, M., Chen, Y., Tian, C., Zhang, F., Yan, C., and Zheng, M.: Chemical composition of $PM_{2.5}$ from two tunnels with different vehicular fleet characteristics, Sci. Total Environ., 550, 123–132, 2016.

Dai, S., Bi, X., Chan, L., He, J., Wang, B., Wang, X., Peng, P., Sheng, G., and Fu, J.: Chemical and stable carbon isotopic composition of $PM_{2.5}$ from on-road vehicle emissions in the PRD region and implications for vehicle emission control policy, Atmos. Chem. Phys., 15, 3097–3108, 2015.

Das, O., Wang, Y., and Hsieh, Y.-P.: Chemical and carbon isotopic characteristics of ash and smoke derived from burning of C3 and C4 grasses, Org. Geochem., 41, 263–269, 2010.

Guo, Z., Jiang, W., Chen, S., Sun, D., Shi, L., Zeng, G., and Rui, M.: Stable isotopic compositions of elemental carbon in $PM_{1.1}$ in north suburb of Nanjing region, China, Atmos. Res., 168, 105–111, 2016.

Han, Y., Chen, L.-W., Huang, R.-J., Chow, J., Watson, J., Ni, H., Liu, S., Fung, K., Shen, Z., and Wei, C.: Carbonaceous aerosols in megacity Xi'an, China: Implications of thermal/optical protocols comparison, Atmos. Environ., 132, 58–68, 2016.

He, L.-Y., Hu, M., Zhang, Y.-H., Huang, X.-F., and Yao, T.-T.: Fine particle emissions from on-road vehicles in the Zhujiang Tunnel, China, Environ. Sci. Technol., 42, 4461–4466, 2008.

Ho, K., Lee, S., Cao, J., Li, Y., Chow, J. C., Watson, J. G., and Fung, K.: Variability of organic and elemental carbon, water soluble organic carbon, and isotopes in Hong Kong, Atmos. Chem. Phys., 6, 4569–4576, 2006.

Huang, X. F., Yu, J. Z., He, L. Y., and Hu, M.: Size distribution characteristics of elemental carbon emitted from Chinese vehicles: Results of a tunnel study and atmospheric implications, Environ. Sci. Technol., 40, 5355–5360, 2006.

Kawashima, H. and Haneishi, Y.: Effects of combustion emissions from the Eurasian continent in winter on seasonal $\delta^{13}C$ of elemental carbon in aerosols in Japan, Atmos. Environ., 46, 568–579, 2012.

Li, J., Wang, G., Ren, Y., Wang, J., Wu, C., Han, Y., Zhang, L., Cheng, C., and Meng, J.: Identification of chemical compositions and sources of atmospheric aerosols in Xi'an, inland China during two types of haze events, Sci. Total Environ., 566, 230–237, 2016a.

Li, Q., Li, X., Jiang, J., Duan, L., Ge, S., Zhang, Q., Deng, J., Wang, S., and Hao, J.: Semi-coke briquettes: towards reducing emissions of primary $PM_{2.5}$, particulate carbon, and carbon monoxide from household coal combustion in China, Sci. Rep., 6, 2016b.

Liu, G., Li, J., Xu, H., Wu, D., Liu, Y., and Yang, H.: Isotopic compositions of elemental carbon in smoke and ash derived from crop straw combustion, Atmos. Environ., 92, 303–308, 2014.

Martinelli, L., Camargo, P., Lara, L., Victoria, R., and Artaxo, P.: Stable carbon and nitrogen isotopic composition of bulk aerosol particles in a C4 plant landscape of southeast Brazil, Atmos. Environ., 36, 2427–2432, 2002.

Ni, H. Y., Han, Y. M., Cao, J. J., Chen, L.-W. A., Tian, J., Wang, X. L., Chow, J. C., Watson, J. G., Wang, Q. Y., Wang, P., Li, H., and Huang, R. J.: Emission characteristics of carbonaceous particles and trace gases from open burning of crop residue in China, Atmos. Environ., 123, 399–406, 2015.

Qin, Y. and Xie, S.: Historical estimation of carbonaceous aerosol emissions from biomass open burning in China for the period 1990-2005, Environ. Pollut., 159, 3323, 2011.

Shen, G., Yang, Y., Wang, W., Tao, S., Zhu, C., Min, Y., Xue, M., Ding, J., Wang, B., Wang, R., Shen, H., Li, W., Wang, X., and Russell, A. G.: Emission factors of particulate matter and elemental carbon for crop residues and coals burned in typical household stoves in China, Environ. Sci. Technol., 44, 7157–7162, 2010.

Shen, G., Chen, Y., Xue, C., Lin, N., Huang, Y., Shen, H., wang, Y., Li, T., Zhang, Y., and Su, S.: Pollutant emissions from improved coal-and wood-fuelled cookstoves in rural households, Environ. Sci. Technol., 49, 6590–6598, 2015.

Streets, D., Yarber, K., Woo, J. H., and Carmichael, G.: Biomass burning in Asia: Annual and seasonal estimates and atmospheric emissions, Global Biogeochem. Cy., 17, 2003.

Sun, J., Shen, Z., Cao, J., Zhang, L., Wu, T., Zhang, Q., Yin, X., Lei, Y., Huang, Y., Huang, R., Liu, S., Han, Y., Xu, H., Zheng, C., and Liu, P.: Particulate matters emitted from maize straw burning for winter heating in rural areas in Guanzhong Plain, China: current emission and future reduction, Atmos. Res., 184, 66–76, 2017.

Tian, J., Ni, H., Cao, J., Han, Y., Wang, Q., Wang, X., Chen, L. W. A., Chow, J. C., Watson, J. G., Wei, C., Sun, J., Zhang, T., and Huang, R.: Characteristics of carbonaceous particles from residential coal combustion and agricultural biomass burning in China, Atmos. Pollut. Res., 8, 521–527, 2017.

Yan, C., Zheng, M., Bosch, C., Andersson, A., Desyaterik, Y., Sullivan, A. P., Collett, J. L., Zhao, B., Wang, S., and He, K.: Important fossil source contribution to brown carbon in Beijing during winter, Sci. Rep., 7, 2017.

Yan, X., Ohara, T., and Akimoto, H.: Bottom-up estimate of biomass burning in mainland China, Atmos. Environ., 40, 5262-5273, 2006.

Zhang, H., Wang, S., Hao, J., Wan, L., Jiang, J., Zhang, M., Mestl, H. E. S., Alnes, L. W. H., Aunan, K., and Mellouki, A. W.: Chemical and size characterization of particles emitted from the burning of coal and wood in rural households in Guizhou, China, Atmos. Environ., 51, 94–99, 2012.

Zhang, Q., Klimont, Z., Streets, D. G., Huo, H., and He, K. B.: An anthropogenic PM emission model for China and emission inventory for the year 2001, Prog. Nat. Sci., 16, 223–231, 2006 (in Chinese).

Zhang, Q., Streets, D. G., Carmichael, G. R., He, K., Huo, H., Kannari, A., Klimont, Z., Park, I., Reddy, S., and Fu, J.: Asian emissions in 2006 for the NASA INTEX-B mission, Atmos. Chem. Phys., 9, 5131–5153, 2009.

Zhang, T., Cao, J. J., Tie, X. X., Shen, Z. X., Liu, S. X., Ding, H., Han, Y. M., Wang, G. H., Ho, K. F., Qiang, J., and Li, W. T.: Water-soluble ions in atmospheric aerosols measured in Xi'an, China: seasonal variations and sources, Atmos. Res., 102, 110-119, 2011.

Zhang, Y. L., Li, J., Zhang, G., Zotter, P., Huang, R.-J., Tang, J.-H., Wacker, L., Prévôt, A. S. H., and Szidat, S.: Radiocarbon-based source apportionment of carbonaceous aerosols at a regional background site on Hainan island, South China, Environ. Sci. Technol., 48, 2651–2659, 2014.

Zhang, Y. L., Wang, X., Li, G., Yang, W., Huang, Z., Zhang, Z., Huang, X., Deng, W., Liu, T., Huang, Z., and Zhang, Z.: Emission factors of fine particles, carbonaceous aerosols and traces gases from road vehicles: Recent tests in an urban tunnel in the Pearl River Delta, China, Atmos. Environ., 122, 876–884, 2015a.

Zhang, Y. L., Huang, R. J., El Haddad, I., Ho, K. F., Cao, J. J., Han, Y., Zotter, P., Bozzetti, C., Daellenbach, K. R., Canonaco, F., Slowik, J. G., Salazar, G., Schwikowski, M., Schnelle-Kreis, J., Abbaszade, G., Zimmermann, R., Baltensperger, U., Prévôt, A. S. H., and Szidat, S.: Fossil vs. non-fossil sources of fine carbonaceous aerosols in four Chinese cities during the extreme winter haze episode of 2013, Atmos. Chem. Phys., 15, 1299-1312, 2015b.

Zhang, Y. X., Schauer, J. J., Zhang, Y., Zeng, L., Wei, Y., Liu, Y., and Shao, M.: Characteristics of particulate carbon emissions from real-world Chinese coal combustion, Environ. Sci. Technol., 42, 5068–5073, 2008.

Zhang, Y. S., Shao, M., Lin, Y., Luan, S., Mao, N., Chen, W., and Wang, M.: Emission inventory of carbonaceous pollutants from biomass burning in the Pearl River Delta Region, China, Atmos. Environ., 76, 189–199, 2013.

Zhi, G., Chen, Y., Feng, Y., Xiong, S., Li, J., Zhang, G., Sheng, G., and Fu, J.: Emission characteristics of carbonaceous particles from various residential coal-stoves in China, Environ. Sci. Technol., 42, 3310–3315, 2008.

Zhou, Y., Xing, X., Lang, J., Chen, D., Cheng, S., Wei, L., Wei, X., and Liu, C.: A comprehensive biomass burning emission inventory with high spatial and temporal resolution in China, Atmos. Chem. Phys., 17, 2839–2864, 2017.

Zhu, C. S., Cao, J. J., Tsai, C. J., Zhang, Z. S., and Tao, J.: Biomass burning tracers in rural and urban ultrafine particles in Xi'an, China, Atmos. Pollut. Res., 8, 614–618, http://dx.doi.org/10.1016/j.apr.2016.12.011, 2017.